Coupled land surface and radiative transfer models for the analysis of passive microwave satellite observations

Florian Schlenz

Dissertation
an der Fakultät für Geowissenschaften
der Ludwig-Maximilians-Universität
München

vorgelegt von
Florian Schlenz
aus Forchheim

eingereicht am 19.4.2012

1. Gutachter: Prof. Dr. Wolfram Mauser
2. Gutachter: Dr. habil. Alexander Löw
Tag der Disputation: 13.7.2012

Preface

At first I would like to thank my doctoral advisor Prof. Wolfram Mauser for the support he gave me throughout the years. It was great to have such an interesting job with so much freedom and responsibility. Thank you very much.

Special thanks go to Dr. Alexander Löw, my second supervisor. It was great to work with you, Alex. You were always open minded for my ideas and discussions. Thanks for all your support and assurance.

Thank you, Johanna. It was great to have you as a teammate on this project.

I would like to thank my colleagues and friends for supporting me throughout the work that led to this thesis. Thanks Thomas, Flo, Andrea, Toni, Matthias, Caro, Susan, Philip, Swen, Markus, Daniel, Tobi, Moni, Timo and the others.

Furthermore I would like to thank all students I have been working with in the frame of our field campaigns, it was a pleasure. Special thanks go to Joachim, Malin, Philip, Katja and Inga.

I would like to thank Yann Kerr and his team at CESBIO, Toulouse including Philippe, Simone and Arnaud for supporting me and enabling a very motivating stay in Toulouse.

I would like to thank Mr. Kerscher from the Bavarian State Research Center for Agriculture, Department Meteorology and Mr. Heiles from the research farm Puch. The technical and logistical support you provided is gratefully acknowledged!

Special thanks go to my family for making all this possible!

Zusammenfassung

Die Bodenfeuchte ist eine der wichtigsten Variablen zur Steuerung der Energie- und Wasseraustauschprozesse zwischen Erdoberfläche und Atmosphäre. Deshalb haben Fernerkundungsprodukte der Bodenfeuchte potentielle Anwendungen in vielen Disziplinen. Dazu zählen neben Wettervorhersage und Klimaforschung auch die Landwirtschaft und hydrologische Anwendungen wie Hochwasser- oder Dürrevorhersagen.

Der erste speziell für die Lieferung operationeller Bodenfeuchteprodukte konzipierte Satellit, SMOS (Soil Moisture and Ocean Salinity), wurde 2009 von der europäischen Weltraumorganisation (ESA) gestartet. SMOS arbeitet mit einem passiven Mikrowellenradiometer im L-band des Mikrowellenbereichs, das einer Frequenz von ca. 1.4 GHz entspricht, und beruht auf einem neuartigen Konzept. Die von der Erde emittierte Strahlung wird als Strahlungstemperatur in verschiedenen Einfallswinkeln gemessen. Daraus werden die Bodenfeuchte und die optische Dicke der Vegetation in einer Invertierung mittels eines Strahlungstransfermodells abgeleitet. Die optische Dicke der Vegetation ist ein Maß für die Abschwächung der Mikrowellenemission des Bodens durch die Vegetation.

Für die Anwendung von Fernerkundungsprodukten passiver Mikrowellensensoren wie SMOS, ist es entscheidend, dass diese Daten gründlich validiert werden, und die Unsicherheiten bekannt sind. Da diese Sensoren eine räumliche Auflösung in der Größenordnung von 40 – 50 km haben, ist eine umfangreiche Validierung, die ausschließlich auf Messdaten beruht, teuer und arbeitsintensiv. Hier können Umweltmodelle einen wertvollen Beitrag leisten.

Die vorliegende Arbeit befasst sich daher mit der Frage, welchen Beitrag gekoppelte Landoberflächenprozess- und Strahlungstransfermodelle zur Validierung und Analyse von Fernerkundungsdaten passiver Mikrowellensensoren leisten können. Es soll geklärt werden, ob es möglich ist, bekannte Probleme in den SMOS Bodenfeuchteprodukten zu erklären und mögliche Ansätze zur Verbesserung aufzuzeigen.

Dafür werden das Landoberflächenprozessmodell PROMET (PRocesses Of Mass and Energy Transfer) und das Strahlungstransfermodell L-MEB (L-band Microwave Emission of the Biosphere) gekoppelt, um die Beschaffenheit der Landoberfläche, wie z.B. die Temperatur und die Bodenfeuchte, und die resultierende Mikrowellenemission simulieren zu können. L-MEB wird ebenfalls im SMOS-Bodenfeuchteprozessor verwendet, um aus der gemessenen Mikrowellenemission der Erdoberfläche die Bodenfeuchte simultan mit der optischen Dicke abzuleiten. Das Untersuchungsgebiet dieser Arbeit ist das obere Donaueinzugsgebiet, das sich größtenteils in Süddeutschland befindet.

Da Modellvalidierung unerlässlich ist, wenn Modelldaten als Referenz verwendet werden sollen, werden beide Modelle auf verschiedenen räumlichen Skalen mit Messdaten validiert und die Unsicherheiten der Modelle quantifiziert. So beträgt die mittlere quadratische Abweichung zwischen modellierter und gemessener Bodenfeuchte mehrerer Messstationen auf der Punktskala 0.065 m^3/m^3, auf der SMOS Skala 0.039 m^3/m^3. Der Korrelationskoeffizient auf der Punktskala beträgt 0.84.

Da es entscheidend für die Bodenfeuchteableitung aus passiven Mikrowellendaten ist, ob die Strahlungstransfermodellierung unter lokalen Bedingungen funktioniert, werden die gekoppelten Modelle verwendet, um auf der Punktskala und der SMOS-Skala im oberen Donaueinzugsgebiet die Strahlungstransfermodellierung mit L-MEB zu überprüfen. Dabei wird zum ersten Mal die Emissionscharakteristik von Raps im Mikrowellenbereich beschrieben und die Bodenfeuchteableitungsfähigkeit von L-MEB mit einer neuentwickelten L-MEB-Parametrisierung für diese Landnutzung untersucht. Die Ergebnisse zeigen, dass die Strahlungstransfermodellierung im Untersuchungsgebiet unter den meisten Bedingungen gut funktioniert. Die mittlere quadratische Abweichung der modellierten von der mit einem

Flugzeug gemessenen Strahlungstemperatur auf SMOS-Skala beträgt weniger als 6 – 9 K für die verschiedenen Aufnahmewinkel.

Die gekoppelten Modelle werden verwendet um SMOS-Strahlungstemperaturen und die optische Dicke in den SMOS Produkten aus dem Bereich des oberen Donaueinzugsgebietes in Süddeutschland zu analysieren. Da die SMOS-Bodenfeuchteprodukte in Süddeutschland und verschiedenen anderen Teilen der Welt eine verminderte Qualität zeigen, wird mit Hilfe dieser Analysen versucht einzugrenzen, was mögliche Ursachen sind.

Die ausführliche Analyse der SMOS-Strahlungstemperaturen für das Jahr 2011 zeigt, dass die Qualität der Messdaten, ebenso wie die der SMOS-Bodenfeuchteprodukte, vermindert ist. Dies deutet auf Probleme durch Hochfrequenzstörungen (engl.:, Radio Frequency Interference, RFI) hin, die bekannt sind, aber noch nicht detailliert untersucht wurden. Dies ist konsistent mit den Charakteristika der beobachteten Probleme in den SMOS-Bodenfeuchteprodukten. Außerdem wird festgestellt, dass die SMOS-Strahlungstemperaturen in niedrigen Aufnahmewinkeln eine verminderte Qualität zeigen. Diese Erkenntnis könnte verwendet werden, um die Filterung der Strahlungstemperatur-Messdaten zu verbessern bevor die Bodenfeuchte abgeleitet wird.

Eine Analyse der optischen Dicke in den SMOS-Produkten 2011 ergibt, dass dieser Parameter keine sinnvolle Information über die Vegetation enthält. Stattdessen wird eine Korrelation mit den SMOS-Bodenfeuchteprodukten gefunden, die nicht erwartet wurde. Dies deutet auf Probleme bei der SMOS-Bodenfeuchteableitung hin, die möglicherweise von RFI beeinflusst werden.

Die vorliegende Arbeit zeigt, dass gekoppelte Landoberflächenprozess- und Strahlungstransfermodelle einen wichtigen Beitrag zur Validierung und Analyse von Fernerkundungsdaten passiver Mikrowellensensoren leisten können. Der einzigartige Ansatz dieser Arbeit, der Modellierungen mit hoher räumlicher und zeitlicher Auflösung auf verschiedenen Skalen umfasst, erlaubt es, sowohl detaillierte Prozessstudien auf der Punktskala, als auch Analysen von Satellitendaten auf der SMOS-Skala durchzuführen. Dies könnte bei der Validierung zukünftiger Satellitenmissionen genutzt werden. Beispielsweise bei SMAP (Soil Moisture Active Passive), die gerade von der NASA (National Aeronautics and Space Administration) vorbereitet wird. Da RFI auf Grund der gewonnenen Erkenntnisse einen großen Einfluss auf die SMOS-Produkte zu haben scheint, und die Qualität der SMOS-Produkte in anderen Teilen der Welt sehr gut ist, sollten die RFI-Eindämmungs- und Vermeidungsbemühungen fortgesetzt werden, die seit dem Start von SMOS durchgeführt werden.

Summary

Soil moisture is one of the key variables controlling the water and energy exchanges between Earth's surface and the atmosphere. Therefore, remote sensing based soil moisture information has potential applications in many disciplines. Besides numerical weather forecasting and climate research these include agriculture and hydrologic applications like flood and drought forecasting.

The first satellite specifically designed to deliver operational soil moisture products, SMOS (Soil Moisture and Ocean Salinity), was launched 2009 by the European Space Agency (ESA). SMOS is a passive microwave radiometer working in the L-band of the microwave domain, corresponding to a frequency of roughly 1.4 GHz and relies on a new concept. The microwave radiation emitted by the Earth's surface is measured as brightness temperatures in several look angles. A radiative transfer model is used in an inversion algorithm to retrieve soil moisture and vegetation optical depth, a measure for the vegetation attenuation of the soil's microwave emission.

For the application of passive microwave remote sensing products a proper validation and uncertainty assessment is essential. As these sensors have typical spatial resolutions in the order of $40 - 50$ km, a validation that relies solely on ground measurements is costly and labour intensive. Here, environmental modelling can make a valuable contribution.

Therefore the present thesis concentrates on the question which contribution coupled land surface and radiative transfer models can make to the validation and analysis of passive microwave remote sensing products. The objective is to study whether it is possible to explain known problems in the SMOS soil moisture products and to identify potential approaches to improve the data quality.

The land surface model PROMET (PRocesses Of Mass and Energy Transfer) and the radiative transfer model L-MEB (L-band microwave emission of the Biosphere) are coupled to simulate land surface states, e.g. temperatures and soil moisture, and the resulting microwave emission. L-MEB is also used in the SMOS soil moisture processor to retrieve soil moisture and vegetation optical depth simultaneously from the measured microwave emission. The study area of this work is the Upper Danube Catchment, located mostly in Southern Germany.

Since model validation is essential if model data are to be used as reference, both models are validated on different spatial scales with measurements. The uncertainties of the models are quantified. The root mean squared error between modelled and measured soil moisture at several measuring stations on the point scale is 0.065 m^3/m^3. On the SMOS scale it is 0.039 m^3/m^3. The correlation coefficient on the point scale is 0.84.

As it is essential for the soil moisture retrieval from passive microwave data that the radiative transfer modelling works under local conditions, the coupled models are used to assess the radiative transfer modelling with L-MEB on the local and SMOS scales in the Upper Danube Catchment. In doing so, the emission characteristics of rape are described for the first time and the soil moisture retrieval abilities of L-MEB are assessed with a newly developed L-MEB parameterization. The results show that the radiative transfer modelling works well under most conditions in the study area. The root mean squared error between modelled and airborne measured brightness temperatures on the SMOS scale is less than $6 - 9$ K for the different look angles.

The coupled models are used to analyse SMOS brightness temperatures and vegetation optical depth data in the Upper Danube Catchment in Southern Germany. Since the SMOS soil moisture products are degraded in Southern Germany and in different other parts of the world these analyses are used to narrow down possible reasons for this.

The thorough analysis of SMOS brightness temperatures for the year 2011 reveals that the quality of the measurements is degraded like in the SMOS soil moisture product. This points

towards radio frequency interference problems (RFI), that are known, but have not yet been studied thoroughly. This is consistent with the characteristics of the problems observed in the SMOS soil moisture products. In addition to that it is observed that the brightness temperatures in the lower look angles are less reliable. This finding could be used to improve the brightness temperature filtering before the soil moisture retrieval.

An analysis of SMOS optical depth data in 2011 reveals that this parameter does not contain valuable information about vegetation. Instead, an unexpected correlation with SMOS soil moisture is found. This points towards problems with the SMOS soil moisture retrieval, possibly under the influence of RFI.

The present thesis demonstrates that coupled land surface and radiative transfer models can make a valuable contribution to the validation and analysis of passive microwave remote sensing products. The unique approach of this work incorporates modelling with a high spatial and temporal resolution on different scales. This makes detailed process studies on the local scale as well as analyses of satellite data on the SMOS scale possible. This could be exploited for the validation of future satellite missions, e.g. SMAP (Soil Moisture Active and Passive) which is currently being prepared by NASA (National Aeronautics and Space Administration). Since RFI seems to have a considerable influence on the SMOS data due to the gained insights and the quality of the SMOS products is very good in other parts of the world, the RFI containment and mitigation efforts carried out since the launch of SMOS should be continued.

Contents

1   Introduction

1.1   Passive microwave remote sensing of soil moisture

Soil moisture is one of the key variables controlling the energy and water exchange processes between the Earth's surface and the atmosphere and therefore plays an important role in the local, regional and global water cycle and the global climate system (Jung et al., 2010). It controls evaporation rates, surface runoff and infiltration as well as plant growth (Jung et al., 2010). Therefore, observations of soil moisture have potential applications in numerical weather forecasting and climate research, hydrologic applications like flood and drought modelling and agriculture (Entekhabi et al., 1999;Wagner et al., 2007b;Seneviratne et al., 2006;Dirmeyer, 2000;Schumann et al., 2009). For example, it has been shown that soil moisture played an important role in recent summer droughts in Europe and that soil moisture estimates could have the potential to improve the prediction ability of numerical weather forecast models for events like these (Loew et al., 2009;Fischer et al., 2007). Therefore, there is a need for reliable soil moisture data (Seneviratne 2006).

Monitoring soil moisture from space is very important because ground measurements of soil moisture are typically only valid for very small volumes due to the high spatial variability of soil moisture that is influenced by weather, terrain, soil and vegetation characteristics. This makes distributed soil moisture measurements very costly and labour intensive.

Different remote sensing approaches have been proposed to measure soil moisture from satellites (Wagner et al., 2007b;Aires et al., 2005;Loew et al., 2006;Mauser et al., 1994). Passive microwave remote sensing in the L-band (i.e. the frequency band between 1400 and 1427 MHz) is a promising technique as it can provide soil moisture information on large scales in a timely fashion while being almost independent from weather conditions and solar illumination (Aires et al., 2005;Wigneron et al., 2003;Wagner et al., 2007a). Compared to higher frequencies, the sensitivity to vegetation is reduced in the L-band (Wagner et al., 2007a).

The microwave emission of the Earth's surface shows a direct relationship to soil moisture through the soil's dielectric constant but is also influenced by land surface roughness, vegetation characteristics and temperature (Wagner et al., 2007a). At L-band the sensitivity of emitted radiation over bare soil to the soil moisture in the first centimetres of the soil is around 2 K per 0.01 m^3/m^3 (Kerr et al., 2001). It is measured in brightness temperatures. Typically soil moisture is inverted from the measured brightness temperatures through an inversion algorithm using a radiative transfer model as forward model (Kerr et al., 2010). Due to technical limitations related to the antenna size, the spatial resolution for this technique is rather low, in the order of 40-50 km.

In 2009 the Soil Moisture and Ocean Salinity (SMOS) mission was launched by the European Space Agency (ESA) to monitor soil moisture and ocean salinity globally (Kerr et al., 2010). SMOS is the first spaceborne sensor in the L-band dedicated especially to operational soil moisture measurements. It utilizes a novel sensing technique based on passive microwave remote sensing with a frequency of 1.4 GHz (Kerr et al., 2010). Another satellite mission focusing on soil moisture observation is momentarily being prepared by the United States' National Aeronautics and Space Administration (NASA): the Soil Moisture Active and Passive (SMAP) mission. It also incorporates a passive microwave remote sensing system and is planned to be launched in 2014 (Das et al., 2011).

Other applications of passive microwave remote sensing are for example ocean salinity measurements, frost detection and monitoring of sea ice.

1.2 The SMOS mission

The SMOS mission works with the unique 2-D interferometric L-band radiometer MIRAS (Microwave Imaging Radiometer with Aperture Synthesis), that observes the Earth's surface from multiple look angles between 0° and 55° (Kerr et al., 2010). Using these multiangular brightness temperature observations in an iterative inversion algorithm allows to disentangle vegetation and soil moisture dynamics. In the SMOS retrieval, soil moisture and vegetation optical depth, that is a measure for the vegetation attenuation of the soil's microwave emission, are retrieved simultaneously. This inversion relies on minimizing a cost function between measured and forward modelled multiangular brightness temperatures. The forward model used in this algorithm is the L-band Microwave Emission of the Biosphere (L-MEB) model (Wigneron et al., 2007). In order to model the influence of temperatures and vegetation characteristics on the brightness temperatures realistically, it relies heavily on auxiliary data. SMOS brightness temperature measurements are delivered as Level 1c (L1c) data, while soil moisture and vegetation optical depth are contained in the Level 2 (L2) data sets. The vegetation optical depth could be a valuable source of information about vegetation characteristics. Global near-surface soil moisture maps are delivered every 2-3 days with an accuracy target of 0.04 m^3/m^3 random error (Kerr et al., 2010;ESA, 2002). The data products have a mean spatial resolution of 43 km and are delivered on an ISEA (icosahedral Snyder equal area projection) grid that has a spacing of 12.5 km between grid points (Kerr et al., 2010).

The L-MEB model is based on the Tau (τ)-Omega (ω) model that simulates the overall (top of atmosphere) brightness temperature of a vegetated surface T_{TOA} [K]. It uses the two parameters vegetation optical depth (τ) and single scattering albedo (ω) to characterize the vegetation attenuation and scattering effects of the land surface. In L-MEB the overall microwave emission from soil and vegetation is for horizontal and vertical polarization the sum of the three terms (illustrated in Figure 1):

- direct vegetation emission (T_V)
- vegetation emission reflected by the soil and attenuated again by the vegetation ($T_V\, r\, \gamma_V$)
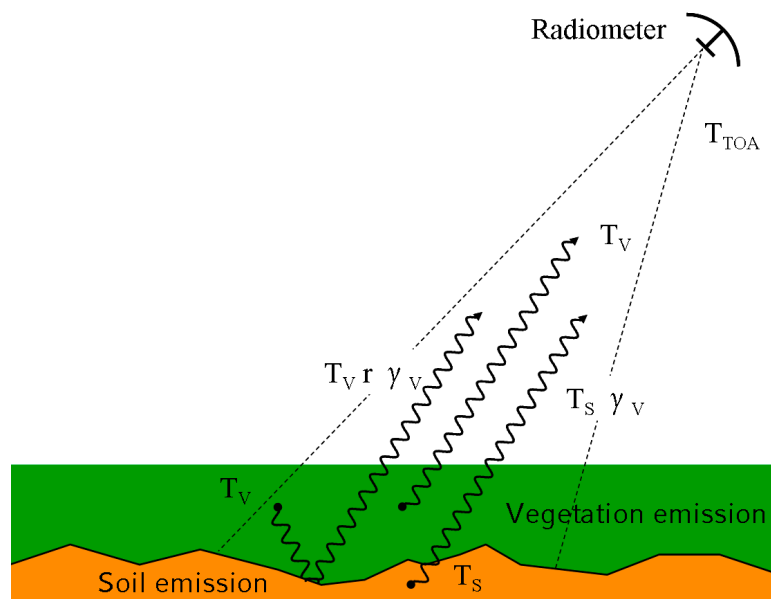- soil emission attenuated (scattered and absorbed) by the vegetation layer ($T_S\, \gamma_V$).

Figure 1. The simplified main principle of the Tau-Omega model. The top of atmosphere brightness temperature (T_{TOA}) is the sum of the three terms direct vegetation emission (T_V), vegetation emission reflected by the soil and attenuated again by the vegetation ($T_V\, r\, \gamma_V$) and the soil emission attenuated by the vegetation ($T_S\, \gamma_V$).

The reflectivity at the soil/atmosphere interface (r) plays an important role and is dependent on the dielectric properties of the soil that depend on soil moisture, temperature, salinity, roughness and soil texture (Woodhouse, 2006). The transmissivity of the vegetation (γ_V) is a function of the vegetation optical depth at nadir (τ) and the observation angle. τ can be related to the vegetation parameters vegetation water content or leaf area index with linear functions. A more detailed description of the Tau-Omega model can be found in (Wigneron et al., 2007) and (Schlenz et al., 2012) in the Appendix I.

L-MEB has been parameterised for different land surfaces through the use of ground and airborne L-band radiometer experiment data sets (Wigneron et al., 2007;Grant et al., 2007;Saleh et al., 2007). As L-MEB forms the core of the SMOS soil moisture retrieval, it is important that the radiative transfer modelling with L-MEB works properly because radiative transfer uncertainties could lead to problems in the SMOS soil moisture retrieval.

For calibration and validation (cal/val) of SMOS, ESA relies on a number of cal/val test sites around the world. One of the major SMOS cal/val test sites in Europe is the Upper Danube Catchment in Southern Germany (Delwart et al., 2008) that has been at the focus of a number of hydrological, remote sensing and global change studies, e.g. (Mauser and Schädlich, 1998;Ludwig and Mauser, 2000;Probeck et al., 2005;Loew et al., 2006;Mauser and Bach, 2009;Ludwig et al., 2003;Bach et al., 2003;Schlenz et al., 2008;Loew and Mauser, 2008;Loew, 2008;Loew et al., 2009;Loew and Schlenz, 2011). Extensive field campaigns have taken place here that delivered data sets of distributed soil moisture and vegetation measurements as well as airborne and ground based L-band radiometer data (dall'Amico et al., 2011;Schlenz et al., 2012;Schlenz et al., 2009). Focus of the campaigns has been the Vils test site in the Northeast of the Upper Danube Catchment which is about the size of a SMOS footprint. Figure 2 illustrates the location of the Vils test site in the Upper Danube Catchment and the location of permanent soil moisture and L-band radiometer measurement stations.
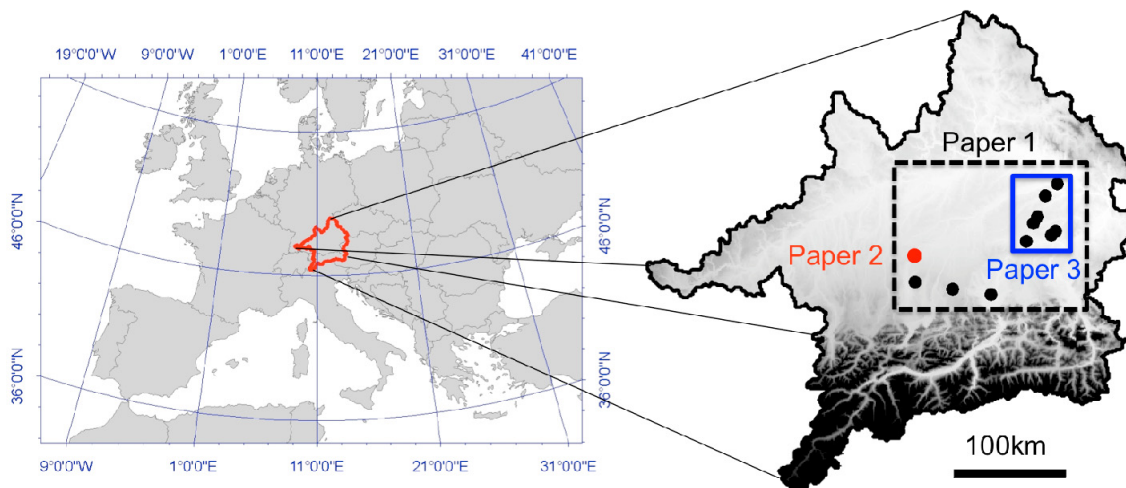
Figure 2. The Upper Danube Catchment and its location in Central Europe. The size of the Catchment is 77 000 km^2. Indicated are the Vils test site (blue box), the soil moisture measuring stations (black dots) and the L-band radiometer test site Puch (red dot). The background of the catchment is a digital elevation model with 1 km resolution (white: 312 m.a.s.l.; black: 3630 m.a.s.l.). The study areas of the three papers summarized in this thesis are indicated.

In several parts of the world, e.g. in Central Europe, the performance of SMOS L2 soil moisture data has been reported to be degraded and does not yet meet the mission target (Parrens et al., 2012;Albergel et al., 2012;dall'Amico et al., 2011;dall'Amico, 2012). In Southern Germany SMOS L2 soil moisture shows a considerable dry bias in the order of 0.1 - 0.3 m³/m³ and correlation coefficients below 0.53 for comparisons with in situ data in the Upper Danube Catchment (Albergel et al., 2012;dall'Amico et al., 2011;dall'Amico, 2012).

Parts of these problems have been attributed to radio frequency interference (RFI) which has affected SMOS data in Europe and certain other parts of the world since the launch (Oliva et al., 2012), but this has never been studied explicitly. RFI is caused by man-made emitters on the ground, on aircraft or other spaceborne systems that emit radiation in the 1400 – 1427 – MHz passive frequency band (L-band), in which SMOS is operating. This frequency band is protected by international regulations, which should have guaranteed the observation of radiation emitted only by natural sources (Oliva et al., 2012). The emitting sources are for example air surveillance radar systems and television or other radio links working in adjacent frequency bands spilling into the protected band or unauthorized transmissions within this frequency band (Oliva et al., 2012). The potential impact of RFI on SMOS data was underestimated before launch. Since 2010 ESA is working together with the national authorities to track down and switch off RFI sources (Oliva et al., 2012). Since 2010 a considerable amount of RFI sources could be identified and switched off, but much work remains to be done (Oliva et al., 2012). RFI is flagged in the SMOS data, but this method does not yet work reliably.

In addition to soil moisture, the SMOS L2 product contains the variable vegetation optical depth that is retrieved simultaneously from the L1c brightness temperatures in the SMOS L2 processor. This could prove a valuable source of information about vegetation characteristics for different applications but it is not clear yet whether it is reliable. In addition to that the vegetation optical depth could provide insights into the functioning of the SMOS soil moisture retrieval because the retrieval can compensate problems with one variable into other, simultaneously retrieved, variables. As, (Jackson et al., 2011) state that the vegetation optical depth does not contain reliable information about vegetation in the US, it is necessary to study this variable in other parts of the world to clarify this issue. There has been no thorough analysis of vegetation optical depth reported in literature so far.

1.3   The role of models for the validation and analysis of SMOS data

A proper validation of remotely sensed soil moisture products is important to ensure good product quality which is a prerequisite for the application of the data. In the SMOS case this is especially important as a new technology is being used. Due to the mismatch in scale between satellite products and in situ measurements, the validation of passive microwave soil moisture products is challenging (Bartalis et al., 2008). Typically point measurements of soil moisture are used for validation purposes (Prigent et al., 2005;Wagner et al., 2007b;Sahoo et al., 2008;Albergel et al., 2012;Jackson et al., 2011). As dense soil moisture sampling is very costly and labour intensive it can only be carried out during short term field campaigns, often in conjunction with airborne campaigns, e.g. SMEX02 and SMEX03 (Famiglietti et al., 2008) or the SMOS validation campaigns in Europe (Delwart et al., 2008;Bircher et al., 2011;dall'Amico et al., 2011;Albergel et al., 2011) and Australia (Panciera et al., 2008). To overcome this limitation for long term satellite soil moisture validation activities, different approaches have been proposed. Concepts for upscaling soil moisture measurements to larger scales comprise the use of temporally persistent soil moisture fields (e.g. (Cosh et al., 2006)), additional remote sensing data products (e.g. (Parrens et al., 2012)) and distributed land surface modelling (e.g. (Crow et al., 2005;Albergel et al., 2010;Juglea et al., 2010;Rüdiger et al., 2009)). The triple collocation approach can also be used to quantify the uncertainties related to satellite soil moisture products. It uses three independent data sets and calculates relative error estimates for each data set (Miralles et al., 2010). Loew and Schlenz (2011) have adopted this technique to compare coarse scale satellite soil moisture products with modelled soil moisture fields and soil moisture measurements in a temporally dynamic way. They also worked with data from the land surface model used in this thesis and the soil moisture stations in the Upper Danube Catchment.

As the L-MEB model plays a central part in the SMOS L2 soil moisture retrieval it is necessary to ensure that the radiative transfer modelling with L-MEB works properly and globally for the SMOS case. This is especially critical as most experiments carried out to validate and parameterise the model have been performed with ground based or airborne L-band data in a limited number of locations on a different scale than the SMOS observations (Wigneron et al., 2007). A proper knowledge about the microwave emission characteristics of different land surfaces is necessary to ensure that the soil moisture retrievals from passive microwave remote sensing data work reliably in different parts of the world. Until now, very few studies have thoroughly analysed the radiative transfer modelling abilities of L-MEB over vegetated surfaces on the SMOS scale with real SMOS data. Bircher et al. (2011) have performed such an analysis on one day during the SMOS validation campaign in Denmark with airborne brightness temperatures. Parrens et al. (2012) and (Albergel et al., 2011) have used calibrated statistical relationships to derive soil moisture estimates from SMOS L1c brightness temperature data. Montzka et al. (2011) have compared SMOS L1c with measured brightness temperatures on five days during the SMOS validation campaign in western Germany. There have been no long-term validation or analysis activities for SMOS L1c data over vegetated surfaces that are reported in literature so far.

1.4 Scope of this thesis

This thesis concentrates on the question whether coupled land surface and radiative transfer models can make a valuable contribution to the validation and analysis of passive microwave remote sensing data sets. More specifically, the question is, whether it is possible to find explanations for the apparent problems in the SMOS data sets and identify potential approaches to improve the data quality. For this, it is necessary to study whether the radiative transfer modelling in the L-band works reliably under local conditions.

To address these issues, the PROMET land surface model (Mauser and Bach, 2009) has been coupled with the radiative transfer model L-MEB (Wigneron et al., 2007). The coupled models are used as a tool for the analysis of SMOS data products in the highly instrumented Upper Danube Catchment. The coupled models allow simulating land surface states in a high temporal and spatial resolution as well as the resulting microwave emissions. The models are validated with in situ and airborne data on different scales in the Upper Danube Catchment. The uncertainties of the two models under local conditions are thoroughly investigated as this is a prerequisite if modelled data are to be used as reference in such an analysis.

Possible explanations for the obvious problems in the SMOS L2 soil moisture products are analysed with the coupled models. The radiative transfer modelling abilities of L-MEB are assessed under local conditions over a rape field at the radiometer test site Puch and on the SMOS scale in the Vils test site, as it has been stated by different authors that a local optimisation of the L-MEB parameterizations may be necessary (Bircher et al., 2011;Panciera et al., 2009). The emission characteristics of winter oilseed rape are described for the first time and the soil moisture retrieval abilities of L-MEB over rape are tested with a newly developed parameterization.

The coupled models are used to analyse SMOS L1c brightness temperature data and L2 optical depth data thoroughly in the Vils test site. SMOS soil moisture data analysis are not subject of this work as this issue is addressed thoroughly by (dall'Amico et al., 2011) and (dall'Amico, 2012). The published manuscript by (dall'Amico et al., 2011) is added to this work for reference in the Appendix II as it contains background information that is related to the work summarized in this thesis. The next section summarizes the manuscripts that are subject of this thesis, which is followed by the Conclusions and an Outlook.

2   Overview of the Publications

This thesis summarizes the following three manuscripts:

- Schlenz, F., dall'Amico, J. T., Loew, A., and Mauser, W.: Uncertainty Assessment of the SMOS Validation in the Upper Danube Catchment, Geoscience and Remote Sensing, IEEE Transactions on, PP, 1-13, 2011. (in print, published online: http://ieeexplore.ieee.org/Xplore/guesthome.jsp)
- Schlenz, F., Fallmann, J., Marzahn, P., Loew, A., and Mauser, W.: Characterization of Rape Field Microwave Emission and Implications to Surface Soil Moisture Retrievals, Remote Sensing, 4, 247-270, 2012. (published online: http://www.mdpi.com/2072-4292/4/1/247/)
- Schlenz, F., dall'Amico, J. T., Mauser, W., and Loew, A.: Analysis of SMOS brightness temperature and vegetation optical depth data with coupled land surface and radiative transfer models in Southern Germany, Hydrol. Earth Syst. Sci. Discuss., 9, 1-48, 2012. (accepted; doi: 10.5194/hessd-9-1-2012)

Figure 3 illustrates the subjects of the three papers and how they interact, while the study areas of the papers are indicated in Figure 2.
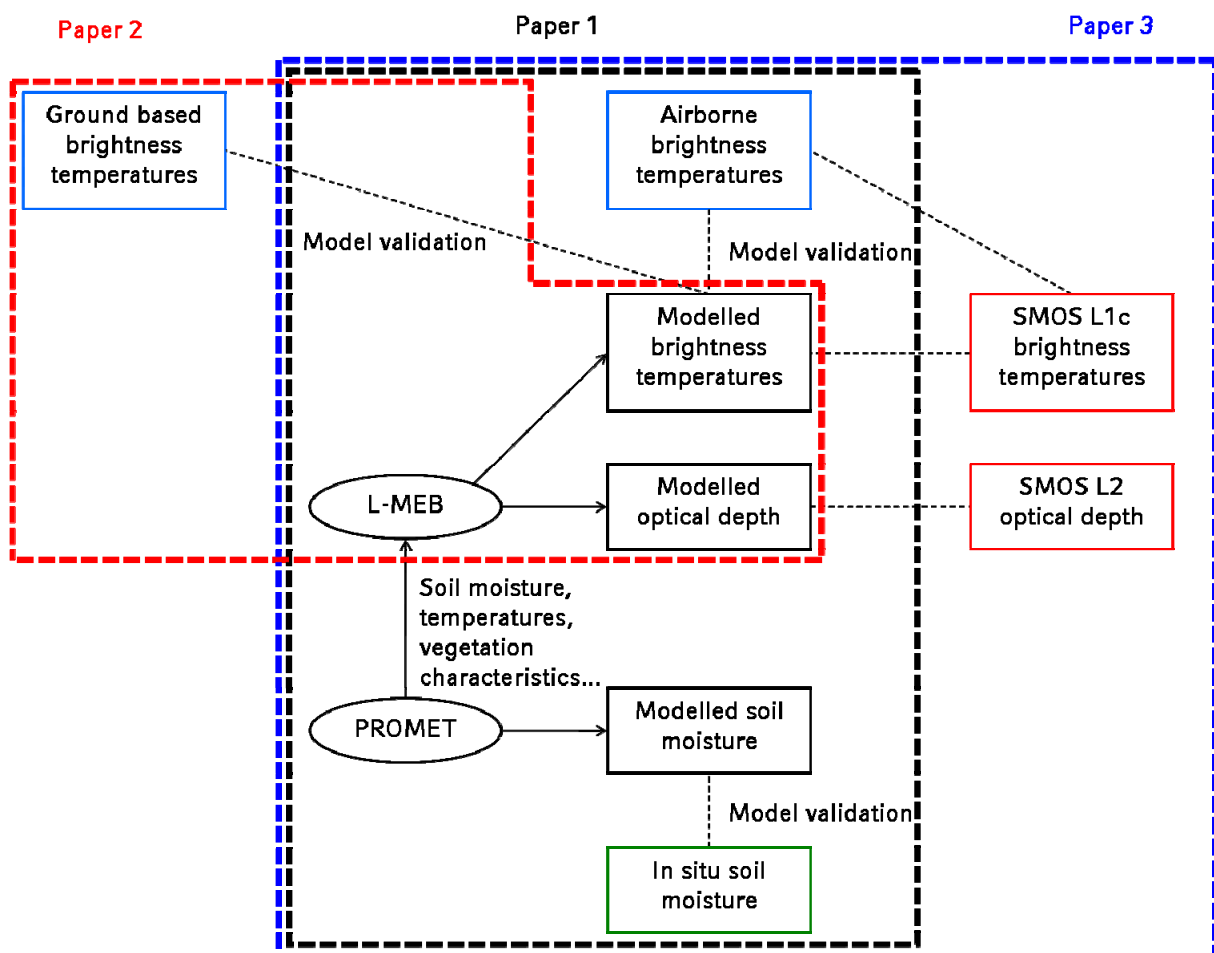

Figure 3. An overview of the different data sets (boxes) and comparisons (slim dashed lines) in this thesis. Black boxes depict modelled data sets provided by the models PROMET and L-MEB, red boxes represent SMOS data, the blue box brightness temperature data and the green box in situ data. The subjects of the three papers summarized in this thesis are indicated with the big dashed boxes.

The first manuscript outlines the approach of the coupling of the land surface model PROMET and the radiative transfer model L-MEB. It describes all data sets acquired during field and airborne campaigns in the frame of SMOS cal/val activities in the Upper Danube Catchment in Southern Germany (see Figure 2), that are used for model validation. The uncertainties that are related to the different measurements and the modelling of the land surface and the radiative transfer are analysed. The models are thoroughly validated from the point scale to the SMOS scale. The soil moisture and brightness temperature modelling uncertainties are quantified and considered small enough to allow for a valuable contribution to SMOS validation activities.

The second publication concentrates on the radiative transfer model L-MEB that is used in the SMOS L2 soil moisture retrieval algorithm as forward model. The abilities of the model to simulate the L-band emission of a winter rape canopy under local conditions are tested on the experimental farm Puch in the Upper Danube Catchment (see Figure 2) that had been equipped with a ground based L-band radiometer delivering reference measurements. As there are no L-band microwave emission measurements over a rape canopy reported in literature, the emission characteristics of a winter rape field are characterized for the first time and a new L-MEB parameterization for that land use is developed. The soil moisture retrieval abilities of the model with the new parameterization are assessed. This study contributes to the knowledge about the microwave emission characteristics of different land surface types which is important for global soil moisture retrievals from satellite data. Rape was one of the three most important crops grown in Germany in 2010 (FNR, 2010). It is concluded that the model performs reliably under local conditions but that a proper vegetation and roughness parameterization are crucial for the radiative transfer modelling.

The last manuscript uses the coupled land surface and radiative transfer models already described in the first publication to analyse SMOS data in the highly instrumented Vils test site in the Upper Danube Catchment (see Figure 2). The model validation with ground and airborne data from the first two manuscripts is summarized incorporating model improvements that were based on the findings in the first manuscript. The newly developed L-MEB parameterization for rape is used in addition to other parameterizations from literature. The radiative transfer modelling abilities of the coupled models are assessed under local conditions. Then SMOS L1c brightness temperature and L2 optical depth data are analysed with the coupled models in 2010 and 2011 to study possible explanations for the observed problems in the SMOS L2 soil moisture product. The coupled models make these long-term analyses possible.

In the following the abstracts of these publications give an overview about the manuscripts.

2.1 Uncertainty Assessment of the SMOS Validation in the Upper Danube Catchment (Paper 1)

The validation of coarse-scale remote sensing products like SMOS (ESA's Soil Moisture and Ocean Salinity mission) L2 soil moisture or L1c brightness temperature data requires the maintenance of long-term soil moisture monitoring sites like the Upper Danube Catchment SMOS validation site situated in Southern Germany. An automatic framework has been built up to compare SMOS data against in situ measurements, land surface model simulations, and ancillary satellite data. The uncertainties of the different data sets used for SMOS validation are being assessed in this paper by comparing different microwave radiative transfer and land surface model results to measured soil moisture and brightness temperature data from local scale to SMOS scale. The mean observed uncertainties of the modelled soil moisture decrease from 0.094 m^3 m^{-3} on the local scale to 0.040 m³/m³ root mean squared error (RMSE) on the large scale. The RMSE of anomalies is 0.023 m³/m³ on the large scale. The mean R^2 increases from 0.6 on the local scale to 0.75 on the medium scale. The land surface model tends to underestimate soil moisture under wet conditions and has a smaller dynamical range than the

measurements. The brightness temperature comparison leads to a RMSE around 12–16 K between microwave radiative transfer model and airborne measurements under varying soil moisture and vegetation conditions. The assessed data sets are considered reliable and robust enough to be able to provide a valuable contribution to SMOS validation activities.

2.2 Characterization of Rape Field Microwave Emission and Implications to Surface Soil Moisture Retrievals (Paper 2)

In the course of Soil Moisture and Ocean Salinity (SMOS) mission calibration and validation activities, a ground based L-band radiometer ELBARA II was situated at the test site Puch in Southern Germany in the Upper Danube Catchment. The experiment is described and the different data sets acquired are presented. The L-band microwave emission of the biosphere (L-MEB) model that is also used in the SMOS L2 soil moisture algorithm is used to simulate the microwave emission of a winter oilseed rape field in Puch that was also observed by the radiometer. As there is a lack of a rape parameterization for L-MEB the SMOS default parameters for crops are used in a first step which does not lead to satisfying modelling results. Therefore, a new parameterization for L-MEB is developed that allows us to model the microwave emission of a winter oilseed rape field at the test site with better results. The soil moisture retrieval performance of the new parameterization is assessed in different retrieval configurations and the results are discussed. To allow satisfying results, the periods before and after winter have to be modelled with different parameter sets as the vegetation behavior is very different during these two development stages. With the new parameterization it is possible to retrieve soil moisture from multiangular brightness temperature data with a root mean squared error around 0.045–0.051 m³/m³ in a two parameter retrieval with soil moisture and roughness parameter Hr as free parameters.

2.3 Analysis of SMOS brightness temperature and vegetation optical depth data with coupled land surface and radiative transfer models in Southern Germany (Paper 3)

Soil Moisture and Ocean Salinity (SMOS) L1c brightness temperature and L2 optical depth data are analysed with a coupled land surface (PROMET) and radiative transfer model (L-MEB) that are used as tool for the analysis and validation of passive microwave satellite observations. The coupled models are validated with ground and airborne measurements under contrasting soil moisture, vegetation and temperature conditions during the SMOS Validation Campaign in May and June 2010 in the SMOS test site Upper Danube Catchment in Southern Germany with good results. The brightness temperature root-mean-squared errors are between 6 K and 9 K and can partly be attributed to a known bias in the airborne L-band measurements. The L-MEB parameterization is considered appropriate under local conditions even though it might possibly further be optimised. SMOS L1c brightness temperature data are processed and analysed in the Upper Danube Catchment using the coupled models in 2011 and during the SMOS Validation Campaign 2010 together with airborne L-band brightness temperature data. Only low to fair correlations are found for this comparison (R < 0.5). SMOS L1c brightness temperature data do not show the expected seasonal behaviour and are positively biased. It is concluded that RFI is responsible for most of the observed problems in the SMOS data products in the Upper Danube Catchment. This is consistent with the observed dry bias in the SMOS L2 soil moisture products which can also be related to RFI. It is confirmed that the brightness temperature data from the lower SMOS look angles are less reliable. This information could be used to improve the brightness temperature data filtering before the soil moisture retrieval. SMOS L2 optical depth values have been compared to modelled data and are not considered a reliable source of information about vegetation due to missing seasonal behaviour and a very high mean value. A fairly strong correlation between

SMOS L2 soil moisture and optical depth was found (R = 0.65) even though the two variables are considered independent in the study area. The value of coupled models for the analysis of passive microwave remote sensing data is demonstrated by extending this SMOS data analysis from a few days during a field campaign to a long term comparison.

3　　Conclusion and Outlook

It is demonstrated in this thesis that coupled land surface and radiative transfer models can make a valuable contribution to the validation and analysis of passive microwave remote sensing products. The coupled models made an extensive analysis of SMOS L1c and L2 optical depth data possible, that would have been limited to a few days of distributed ground measurements during a field campaign otherwise. A comparable analysis over vegetated surfaces has not been reported in literature before. The unique approach of this work that incorporated land surface and radiative transfer modelling with high temporal and spatial resolution on different scales made a variety of studies possible. These ranged from detailed process studies on the point scale to satellite product analysis and validation on the SMOS scale. Soil moisture is an important environmental variable and therefore remote sensing soil moisture products have many potential applications. Since there are considerable problems with the SMOS L2 soil moisture products in the study area, it is important to analyse where these problems originate from, and if the radiative transfer modelling works reliably under local conditions.

Since a proper model validation is essential if model data are to be used as reference data sets, the uncertainties of the coupled models have thoroughly been assessed. The soil moisture modelling abilities of the land surface model PROMET have been analysed from the point to the SMOS scale and are considered to be reliable. The overall root mean squared error between modelled and measured soil moisture at all stations in the Upper Danube Catchment for the period 2008 - 2010 is 0.065 m^3/m^3 and the correlation coefficient is 0.84. On the SMOS scale this RMSE decreases to 0.039 m^3/m^3 in the Vils test site.

The radiative transfer modelling abilities of L-MEB, that is also in the core of the SMOS L2 soil moisture processor, have been tested under local conditions. This is important as the parameterizations used for the SMOS soil moisture retrieval have only been derived from experiments that were carried out in a limited number of locations. Different authors have reported that it might be necessary to optimise L-MEB parameterizations under local conditions. On the local scale the soil moisture retrieval uncertainties from passive microwave emissions were assessed for different retrieval configurations over a rape field in the Upper Danube Catchment with data from a ground based L-band radiometer. As there are no L-band radiometer experiments over rape fields reported in literature, the L-band emission characteristics of rape have been described for the first time, and a new L-MEB parameterization for rape has been derived. The new parameterization allows soil moisture retrievals from multiangular brightness temperature data with a root mean squared error of 0.045–0.051 m³/m³ in a two parameter retrieval. This is relevant because rape was one of the three most important crops grown in Germany in 2010 (FNR, 2010). It plays an important role in the renewable energy sector. This study contributes to the knowledge about the L-band microwave emission characteristics of different land surfaces. A proper knowledge about the microwave emission characteristics of land surfaces in different regions and climates is necessary to be able to refine the soil moisture retrievals from passive microwave remote sensing data in different parts of the world. On the SMOS scale, the brightness temperature modelling abilities of L-MEB have been found to be reliable under most conditions in the Vils test site. The root mean squared error between modelled and airborne measured brightness temperatures in the Vils test site is less than 6 – 9 K for the two look angles 0° and 40°.

An extensive analysis of SMOS L1c brightness temperature data with the coupled models was carried out in the Vils test site in 2011. It was concluded that RFI is the most probable explanation for the degraded L2 soil moisture product as it degrades the SMOS L1c data despite filtering. This is consistent with the observed dry bias in the SMOS L2 soil moisture that can also be attributed to RFI. This result is interesting as RFI has been discussed to be one of the reasons for the degraded SMOS L2 soil moisture product but this had never been

investigated explicitly. An analysis of the SMOS L2 optical depth data with the coupled models revealed that this data product does not contain reliable information about vegetation characteristics due to missing seasonal behaviour and a very high mean value. A clear correlation with the SMOS L2 soil moisture product was also found, even though these two variables are considered independent in the study area. This finding is interesting as it has not been reported before and points towards problems in the SMOS L2 soil moisture retrieval, possibly under the influence of RFI. Also, it was found that SMOS brightness temperature data in the lower look angles are less reliable. This could be exploited in a refined brightness temperature data filtering before the SMOS soil moisture retrieval.

As RFI was identified as one of the major factors degrading the SMOS L2 soil moisture product, the RFI mitigation efforts that are already being carried out (Oliva et al., 2012) should be continued to enable an improvement of the SMOS data products in Southern Germany.

In other parts of the world, the SMOS L2 data products are also degraded and show similar characteristics like in the Upper Danube Catchment (Albergel et al., 2012). Coupled land surface and radiative transfer models could prove valuable to assess possible explanations for this behaviour. Even though RFI seems to be a major problem, other factors, e.g. inappropriate radiative transfer modelling, could also play a role. In the frame of the preparations for the upcoming SMAP mission, that incorporates a similar approach as SMOS, such findings could prove valuable.

As the quality of the SMOS L2 soil moisture products is very good in certain regions without RFI (e.g. the US and Australia (Albergel et al., 2012;Jackson et al., 2011)), it may also become a very valuable data product in Central Europe when the RFI influence can be successfully narrowed down.

In a next step, some of the analysis performed in this thesis could be extended to larger areas. For example the analysis of the SMOS L2 optical depth data could be carried out in RFI-free areas to check whether RFI influences the correlation between soil moisture and Tau.

The coupled models could also be used to assess the potential of different soil moisture retrieval algorithms to improve the SMOS soil moisture retrieval. For example model data could be used to improve the SMOS brightness temperature data filtering before the soil moisture retrieval.

References

Aires, F., Prigent, C., and Rossow, W. B.: Sensitivity of satellite microwave and infrared observations to soil moisture at a global scale: 2. Global statistical relationships, J. Geophys. Res., 110, D11103, 10.1029/2004jd005094, 2005.

Albergel, C., Calvet, J. C., de Rosnay, P., Balsamo, G., Wagner, W., Hasenauer, S., Naeimi, V., Martin, E., Bazile, E., Bouyssel, F., and Mahfouf, J. F.: Cross-evaluation of modelled and remotely sensed surface soil moisture with in situ data in southwestern France, Hydrol. Earth Syst. Sci., 14, 2177-2191, 10.5194/hess-14-2177-2010, 2010.

Albergel, C., Zakharova, E., Calvet, J.-C., Zribi, M., Pardé, M., Wigneron, J.-P., Novello, N., Kerr, Y., Mialon, A., and Fritz, N.-e.-D.: A first assessment of the SMOS data in southwestern France using in situ and airborne soil moisture estimates: The CAROLS airborne campaign, REMOTE SENSING OF ENVIRONMENT, 115, 2718-2728, 10.1016/j.rse.2011.06.012, 2011.

Albergel, C., de Rosnay, P., Gruhier, C., Muñoz-Sabater, J., Hasenauer, S., Isaksen, L., Kerr, Y., and Wagner, W.: Evaluation of remotely sensed and modelled soil moisture products using global ground-based in situ observations, REMOTE SENSING OF ENVIRONMENT, 118, 215-226, 10.1016/j.rse.2011.11.017, 2012.

Bach, H., Braun, M., Lampart, G., and Mauser, W.: Use of remote sensing for hydrological parameterisation of Alpine catchments, Hydrol. Earth Syst. Sci., 7, 862-876, 10.5194/hess-7-862-2003, 2003.

Bartalis, Z., Wagner, W., Anderson, C., Bonekamp, H., Naeimi, V., and Hasenauer, S.: Validation of Coarse Resolution Microwave Soil Moisture Products, Geoscience and Remote Sensing Symposium (IGARSS), 2008 IEEE International, 2008, II-173-II-176,

Bircher, S., Balling, J. E., Skou, N., and Kerr, Y.: SMOS Validation by means of an airborne campaign in the Skjern River Catchment, Western Denmark, IEEE Transactions on Geoscience and Remote Sensing, accepted, 2011., DOI: 10.1109/TGRS.2011.2170177, 2011.

Cosh, M. H., Jackson, T. J., Starks, P., and Heathman, G.: Temporal stability of surface soil moisture in the Little Washita River watershed and its applications in satellite soil moisture product validation, Journal of Hydrology, 323, 168-177, DOI: 10.1016/j.jhydrol.2005.08.020, 2006.

Crow, W. T., Ryu, D., and Famiglietti, J. S.: Upscaling of field-scale soil moisture measurements using distributed land surface modeling, Advances in Water Resources, 28, 1-14, DOI: 10.1016/j.advwatres.2004.10.004, 2005.

dall'Amico, J.: Multiscale analysis of soil moisture using satellite and aircraft microwave remote sensing, in situ measurements and numerical modeling, Phd, Department for Geography, Ludwig Maximilians University, Munich, Germany, 2012.

dall'Amico, J. T., Schlenz, F., Loew, A., and Mauser, W.: First Results of SMOS Soil Moisture Validation in the Upper Danube Catchment, Geoscience and Remote Sensing, IEEE Transactions on, PP, 1-10, 2011.

dall'Amico, J. T., Schlenz, F., Loew, A., Mauser, W., Kainulainen, J., Balling, J., and Bouzinac, C.: The SMOS Validation Campaign 2010 in the Upper Danube Catchment: A Data Set for Studies of Soil Moisture, Brightness Temperature and their Spatial Variability over a Heterogeneous Land Surface, IEEE Transactions on Geoscience and Remote Sensing, accepted, 2011.

Das, N. N., Entekhabi, D., and Njoku, E. G.: An Algorithm for Merging SMAP Radiometer and Radar Data for High-Resolution Soil-Moisture Retrieval, Geoscience and Remote Sensing, IEEE Transactions on, 49, 1504-1512, 2011.

Delwart, S., Bouzinac, C., Wursteisen, P., Berger, M., Drinkwater, M., Martin-Neira, M., and Kerr, Y. H.: SMOS Validation and the COSMOS Campaigns, Geoscience and Remote Sensing, IEEE Transactions on, 46, 695-704, 2008.

Dirmeyer, P. A.: Using a Global Soil Wetness Dataset to Improve Seasonal Climate Simulation, Journal of Climate, 13, 2900-2922, doi:10.1175/1520-0442(2000)013<2900:UAGSWD>2.0.CO;2, 2000.

Entekhabi, D., Asrar, G. R., Betts, A. K., Beven, K. J., Bras, R. L., Duffy, C. J., Dunne, T., Koster, R. D., Lettenmaier, D. P., Mclaughlin, D. B., Shuttleworth, W. J., Van Genuchten, M. T., Wei, M.-Y., and Wood, E. F.: An agenda for land-surface hydrology research and a call for the second international hydrological decade, Bulletin of the American Meteorological Society, 80, 2043-2057, 1999.

ESA: Mission Objectives and Scientific Requirements of the Soil Moisture and Ocean Salinity (SMOS) Mission, Version 5, European Space Agency (ESA), 2002.

Famiglietti, J. S., Ryu, D., Berg, A. A., Rodell, M., and Jackson, T. J.: Field observations of soil moisture variability across scales, Water Resour. Res., 44, W01423, 10.1029/2006wr005804, 2008.

Fischer, E. M., Seneviratne, S. I., Vidale, P. L., Lüthi, D., and Schär, C.: Soil Moisture–Atmosphere Interactions during the 2003 European Summer Heat Wave, Journal of Climate, 20, 5081-5099, doi:10.1175/JCLI4288.1, 2007.

FNR: Jahresbericht 2009/2010, Fachagentur Nachwachsende Rohstoffe e.V. (FNR), Gülzow-Prüzen, 2010.

Grant, J. P., Wigneron, J. P., Van de Griend, A. A., Kruszewski, A., Søbjærg, S. S., and Skou, N.: A field experiment on microwave forest radiometry: L-band signal behaviour for varying conditions of surface wetness, Remote Sensing of Environment, 109, 10-19, 10.1016/j.rse.2006.12.001, 2007.

Jackson, T. J., Bindlish, R., Cosh, M. H., Zhao, T., Starks, P. J., Bosch, D. D., Seyfried, M., Moran, M. S., Goodrich, D. C., Kerr, Y. H., and Leroux, D.: Validation of Soil Moisture and Ocean Salinity (SMOS) Soil Moisture Over Watershed Networks in the U.S, Geoscience and Remote Sensing, IEEE Transactions on, PP, 1-14, 2011.

Juglea, S., Kerr, Y., Mialon, A., Wigneron, J. P., Lopez-Baeza, E., Cano, A., Albitar, A., Millan-Scheiding, C., Carmen Antolin, M., and Delwart, S.: Modelling soil moisture at SMOS scale by use of a SVAT model over the Valencia Anchor Station, Hydrol. Earth Syst. Sci., 14, 831-846, 10.5194/hess-14-831-2010, 2010.

Jung, M., Reichstein, M., Ciais, P., Seneviratne, S. I., Sheffield, J., Goulden, M. L., Bonan, G., Cescatti, A., Chen, J., de Jeu, R., Dolman, A. J., Eugster, W., Gerten, D., Gianelle, D., Gobron, N., Heinke, J., Kimball, J., Law, B. E., Montagnani, L., Mu, Q., Mueller, B., Oleson, K., Papale, D., Richardson, A. D., Roupsard, O., Running, S., Tomelleri, E., Viovy, N., Weber, U., Williams, C., Wood, E., Zaehle, S., and Zhang, K.: Recent decline in the global land evapotranspiration trend due to limited moisture supply, Nature, 467, 951-954, 2010.

Kerr, Y. H., Waldteufel, P., Wigneron, J.-P., Martinuzzi, J.-M., Font, J., and Berger, M.: Soil Moisture Retrieval from Space: The Soil Moisture and Ocean Salinity (SMOS) Mission, IEEE Transactions on Geoscience and Remote Sensing, VOL. 39, NO. 8, 1729-1735, 2001.

Kerr, Y. H., Waldteufel, P., Wigneron, J. P., Delwart, S., Cabot, F., Boutin, J., Escorihuela, M. J., Font, J., Reul, N., Gruhier, C., Juglea, S. E., Drinkwater, M. R., Hahne, A., Marti, x, n-Neira, M., and Mecklenburg, S.: The SMOS Mission: New Tool for Monitoring Key Elements ofthe Global Water Cycle, Proceedings of the IEEE, 98, 666-687, 2010.

Loew, A., Ludwig, R., and Mauser, W.: Derivation of surface soil moisture from ENVISAT ASAR wide swath and image mode data in agricultural areas, Geoscience and Remote Sensing, IEEE Transactions on, 44, 889-899, 2006.

Loew, A.: Impact of surface heterogeneity on surface soil moisture retrievals from passive microwave data at the regional scale: The Upper Danube case, Remote Sensing of Environment, 112, 231-248, DOI: 10.1016/j.rse.2007.04.009, 2008.

Loew, A., and Mauser, W.: On the Disaggregation of Passive Microwave Soil Moisture Data Using A Priori Knowledge of Temporally Persistent Soil Moisture Fields, Geoscience and Remote Sensing, IEEE Transactions on, 46, 819-834, 2008.

Loew, A., Holmes, T., and de Jeu, R.: The European heat wave 2003: Early indicators from multisensoral microwave remote sensing?, J. Geophys. Res., 114, D05103, 10.1029/2008jd010533, 2009.

Loew, A., and Schlenz, F.: A dynamic approach for evaluating coarse scale satellite soil moisture products, Hydrol. Earth Syst. Sci., 15, 75-90, 10.5194/hess-15-75-2011, 2011.

Ludwig, R., and Mauser, W.: Modelling catchment hydrology within a GIS based SVAT-model framework, Hydrol. Earth Syst. Sci., 4, 239-249, 10.5194/hess-4-239-2000, 2000.

Ludwig, R., Mauser, W., Niemeyer, S., Colgan, A., Stolz, R., Escher-Vetter, H., Kuhn, M., Reichstein, M., Tenhunen, J., Kraus, A., Ludwig, M., Barth, M., and Hennicker, R.: Web-based modelling of energy, water and matter fluxes to support decision making in mesoscale catchments—the integrative perspective of GLOWA-Danube, Physics and Chemistry of the Earth, 28, 621-634, citeulike-article-id:2923875, 2003.

Mauser, W., Rombach, M., Bach, H., Demircan, A., and Kellndorfer, J.: Determination of spatial and temporal soil-moisture development using multitemporal ERS-1 data, European Symposium on Satellite Remote Sensing, SPIE 2314, 1994, 502-515,

Mauser, W., and Schädlich, S.: Modelling the spatial distribution of evapotranspiration on different scales using remote sensing data, Journal of Hydrology, 212-213, 250-267, Doi: 10.1016/s0022-1694(98)00228-5, 1998.

Mauser, W., and Bach, H.: PROMET – Large scale distributed hydrological modelling to study the impact of climate change on the water flows of mountain watersheds, Journal of Hydrology, 376, 362–377, 2009.

Miralles, D. G., Crow, W. T., and Cosh, M. H.: Estimating Spatial Sampling Errors in Coarse-Scale Soil Moisture Estimates Derived from Point-Scale Observations, Journal of Hydrometeorology, 11, 1423-1429, doi:10.1175/2010JHM1285.1, 2010.

Montzka, C., Bogena, H., Weihermueller, L., Jonard, F., Dimitrov, M., Bouzinac, C., Kainulainen, J., Balling, J. E., Vanderborght, J., and Vereecken, H.: Radio brightness validation on different spatial scales during the SMOS validation campaign 2010 in the Rur catchment, Germany, Geoscience and Remote Sensing Symposium (IGARSS), 2011 IEEE International, 2011, 3760-3763,

Oliva, R., Daganzo-Eusebio, E., Kerr, Y. H., Mecklenburg, S., Nieto, S., Richaume, P., and Gruhier, C.: SMOS Radio Frequency Interference Scenario: Status and Actions Taken to Improve the RFI Environment in the 1400–1427-MHz Passive Band, Geoscience and Remote Sensing, IEEE Transactions on, PP, 1-13, 2012.

Panciera, R., Walker, J. P., Kalma, J. D., Kim, E. J., Hacker, J. M., Merlin, O., Berger, M., and Skou, N.: The NAFE'05/CoSMOS Data Set: Toward SMOS Soil Moisture Retrieval, Downscaling, and Assimilation, Geoscience and Remote Sensing, IEEE Transactions on, 46, 736-745, 2008.

Panciera, R., Walker, J. P., and Merlin, O.: Improved Understanding of Soil Surface Roughness Parameterization for L-Band Passive Microwave Soil Moisture Retrieval, Geoscience and Remote Sensing Letters, IEEE, 6, 625-629, 2009.

Parrens, M., Zakharova, E., Lafont, S., Calvet, J. C., Kerr, Y., Wagner, W., and Wigneron, J. P.: Comparing soil moisture retrievals from SMOS and ASCAT over France, Hydrol. Earth Syst. Sci., 16, 423-440, 10.5194/hess-16-423-2012, 2012.

Prigent, C., Aires, F., Rossow, W. B., and Robock, A.: Sensitivity of satellite microwave and infrared observations to soil moisture at a global scale: Relationship of satellite observations to in situ soil moisture measurements, J. Geophys. Res., 110, D07110, 10.1029/2004jd005087, 2005.

Probeck, M., Ludwig, R., and Mauser, W.: Fusion of NOAA-AVHRR imagery and geographical information system techniques to derive subscale land cover information for the upper Danube watershed, Hydrological Processes, 19, 2407-2418, 10.1002/hyp.5892, 2005.

Rüdiger, C., Calvet, J.-C., Gruhier, C., Holmes, T. R. H., de Jeu, R. A. M., and Wagner, W.: An Intercomparison of ERS-Scat and AMSR-E Soil Moisture Observations with Model Simulations over France, Journal of Hydrometeorology, 10, 431-447, doi:10.1175/2008JHM997.1, 2009.

Sahoo, A. K., Houser, P. R., Ferguson, C., Wood, E. F., Dirmeyer, P. A., and Kafatos, M.: Evaluation of AMSR-E soil moisture results using the in-situ data over the Little River Experimental Watershed, Georgia, Remote Sensing of Environment, 112, 3142-3152, DOI: 10.1016/j.rse.2008.03.007, 2008.

Saleh, K., Wigneron, J. P., Waldteufel, P., de Rosnay, P., Schwank, M., Calvet, J. C., and Kerr, Y. H.: Estimates of surface soil moisture under grass covers using L-band radiometry, Remote Sensing of Environment, 109, 42-53, DOI: 10.1016/j.rse.2006.12.002, 2007.

Schlenz, F., Loew, A., and Mauser, W.: Soil Moisture Retrieval from Passive Microwave Data: A Sensitivity Study Using a Coupled Svat-Radiative Transfer Model at the Upper Danube Anchor Site, Geoscience and Remote Sensing Symposium (IGARSS), 2008 IEEE International, Boston, 2008, II-680-II-683, 2008.

Schlenz, F., Loew, A., Dall'Amico, J. T., and Mauser, W.: SMOS rehearsal campaign 2008: Data analysis and soil moisture retrieval at the Upper Danube test site, Earth Observation and Water Cycle conference, Frascati (Rome), 18 - 20 November 2009, 2009.

Schlenz, F., Fallmann, J., Marzahn, P., Loew, A., and Mauser, W.: Characterization of Rape Field Microwave Emission and Implications to Surface Soil Moisture Retrievals, Remote Sensing, 4, 247-270, 2012.

Schumann, G., Lunt, D. J., Valdes, P. J., de Jeu, R. A. M., Scipal, K., and Bates, P. D.: Assessment of soil moisture fields from imperfect climate models with uncertain satellite observations, Hydrol. Earth Syst. Sci., 13, 1545-1553, 10.5194/hess-13-1545-2009, 2009.

Seneviratne, S. I., Luthi, D., Litschi, M., and Schar, C.: Land-atmosphere coupling and climate change in Europe, Nature, 443, 205-209, 2006.

Wagner, W., Blöschl, G., Pampaloni, P., Calvet, J.-C., Bizzarri, B., Wigneron, J.-P., and Kerr, Y.: Operational readiness of microwave remote sensing of soil moisture for hydrologic applications, Nordic Hydrology, 38, 1–20, 2007a.

Wagner, W., Naeimi, V., Scipal, K., de Jeu, R., and Martínez-Fernández, J.: Soil moisture from operational meteorological satellites, Hydrogeology Journal, 15, 121-131, 10.1007/s10040-006-0104-6, 2007b.

Wigneron, J. P., Calvet, J. C., Pellarin, T., Van de Griend, A. A., Berger, M., and Ferrazzoli, P.: Retrieving near-surface soil moisture from microwave radiometric observations: current status and future plans, Remote Sensing of Environment, 85, 489-506, Doi: 10.1016/s0034-4257(03)00051-8, 2003.

Wigneron, J. P., Kerr, Y., Waldteufel, P., Saleh, K., Escorihuela, M. J., Richaume, P., Ferrazzoli, P., de Rosnay, P., Gurney, R., Calvet, J. C., Grant, J. P., Guglielmetti, M., Hornbuckle, B., Mätzler, C., Pellarin, T., and Schwank, M.: L-band Microwave Emission of the Biosphere (L-MEB) Model: Description and calibration against experimental data sets over crop fields, Remote Sensing of Environment, 107, 639-655, DOI: 10.1016/j.rse.2006.10.014, 2007.

Woodhouse, I. H.: Introduction to microwave remote sensing, Taylor and Francis, London, 2006.

Appendix I

Appendix I contains the three publications that are summarized in this thesis.

Publication 1

Schlenz, F., dall'Amico, J. T., Loew, A., and Mauser, W.: Uncertainty Assessment of the SMOS Validation in the Upper Danube Catchment, Geoscience and Remote Sensing, IEEE Transactions on, PP, 1-13, 2011. (in print, published online: http://ieeexplore.ieee.org/Xplore/guesthome.jsp)

Uncertainty Assessment of the SMOS Validation in the Upper Danube Catchment

Florian Schlenz, *Member, IEEE*, Johanna T. dall'Amico, Alexander Loew, *Member, IEEE*, and Wolfram Mauser, *Member, IEEE*

Abstract—The validation of coarse-scale remote sensing products like SMOS (ESA's Soil Moisture and Ocean Salinity mission) L2 soil moisture or L1c brightness temperature data requires the maintenance of long-term soil moisture monitoring sites like the Upper Danube Catchment SMOS validation site situated in Southern Germany. An automatic framework has been built up to compare SMOS data against *in situ* measurements, land surface model simulations, and ancillary satellite data. The uncertainties of the different data sets used for SMOS validation are being assessed in this paper by comparing different microwave radiative transfer and land surface model results to measured soil moisture and brightness temperature data from local scale to SMOS scale. The mean observed uncertainties of the modeled soil moisture decrease from 0.094 m^3 m^{-3} on the local scale to 0.040 m^3 m^{-3} root mean squared error (RMSE) on the large scale. The RMSE of anomalies is 0.023 m^3 m^{-3} on the large scale. The mean R^2 increases from 0.6 on the local scale to 0.75 on the medium scale. The land surface model tends to underestimate soil moisture under wet conditions and has a smaller dynamical range than the measurements. The brightness temperature comparison leads to a RMSE around 12–16 K between microwave radiative transfer model and airborne measurements under varying soil moisture and vegetation conditions. The assessed data sets are considered reliable and robust enough to be able to provide a valuable contribution to SMOS validation activities.

Index Terms—Brightness temperature, measurement, model, passive microwave remote sensing, soil moisture.

I. INTRODUCTION

THE WATER content of the soil layer is one of the key variables controlling the mass and energy exchanges between the Earth's surface and the atmosphere [1], [2]. It has an impact on the partitioning of rainfall into runoff and infiltration, affects the partitioning of available energy into sensible and latent heat flux by conditioning plant transpiration and soil evaporation, and can influence regional weather and vegetation development [2]. The development of extreme events like floods and droughts can be influenced considerably by soil moisture [3]–[6]. In this context, soil moisture plays an important role in numerical weather forecasting, land surface hydrology, agricultural applications, and in climate research [1], [7]. As soil moisture is very variable in time and space, it is complicated to measure over large areas and long time spans with appropriate spatial and temporal resolution. Therefore, the knowledge about soil moisture still needs considerable improvement [6]. Microwave remote sensing of soil moisture is a promising technique for that purpose as it can provide soil moisture information on large scales in a timely fashion [8]–[12]. The European Space Agency's (ESA) Soil Moisture and Ocean Salinity (SMOS) mission launched in November 2009 is designed to provide global near-surface soil moisture maps every 2–3 days with an accuracy target of 0.04 m^3 m^{-3} random error [13]–[15]. The unique SMOS 2-D interferometric L-band radiometer (1.4 GHz) allows to disentangle vegetation and soil moisture dynamics from multiangular (0° to 55°) brightness temperature measurements [13], [14]. The spatial resolution of the soil moisture data products is of the order of 40 km; they are delivered on the ISEA (icosahedral Snyder equal area projection) grid which has a spacing of 12.5 km between grid points [13], [14].

Validation of passive microwave remote sensing soil moisture products is difficult because a direct comparison with local soil moisture measurements, which serve as a reference, is hampered by the large size of the footprints [16]. Only if a large number of continuous soil moisture measurements were available, it would be possible to determine the soil moisture dynamics at the footprint scale with an accuracy better than 0.04 m^3 m^{-3} [17], which is the accuracy requirement for SMOS and other satellite soil moisture missions [14]. As dense sampling is very costly and labor intensive and therefore only possible during short-term field campaigns, often in conjunction with airborne measurements (e.g., SMEX02, SMEX03 [17], the SMOS validation campaigns in Europe [18]–[21] and Australia [22]), a lot of long-term satellite soil moisture validation activities rely on data of few point measurements or sparse networks scattered around the globe [9], [11], [23].

To avoid this problem, different approaches are proposed for validating satellite soil moisture products.

The analysis of temporally stable soil moisture patterns has been used to develop concepts for the upscaling of local soil moisture measurements to larger scales to be used for satellite soil moisture product validation [24]–[26].

The potential synergies of combining *in situ* soil moisture information with distributed land surface modeling for the
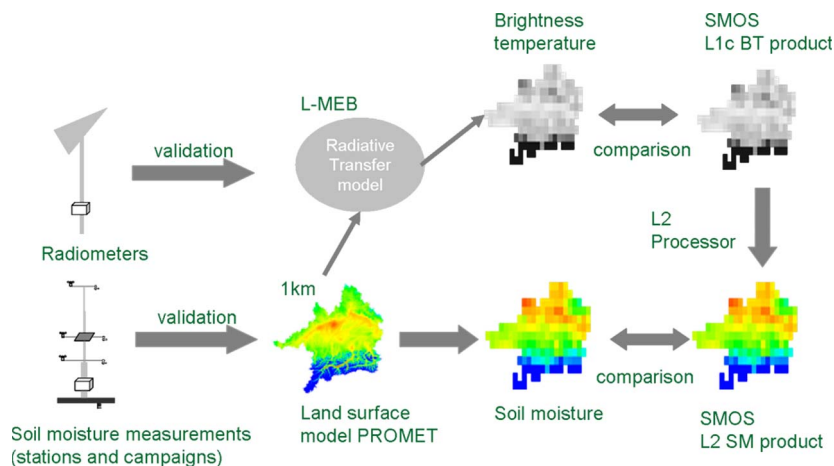
Fig. 1.   SMOS cal/val approach in the UDC.

validation of satellite products is a promising technique. It is being evaluated by [27]–[29] and is used for SMOS validation in the Valencia SMOS validation site [30] and in the Upper Danube Catchment (UDC), which is described in the present paper.

A new approach for the error estimation of satellite soil moisture products was investigated by [31]. They used the so-called triple collocation analysis, to quantify the uncertainty of three independent soil moisture data sets, namely a passive microwave soil moisture product, and data from a land surface model and sparse ground-based observations. Loew and Schlenz 2011 [32] adopted the triple collocation approach to compare coarse-scale satellite soil moisture products with modeled soil moisture fields and soil moisture measurements in a temporally dynamic way that applies the triple collocation method to monthly temporal slices. They used a similar data set in the same area as the present study to quantify the soil moisture anomalies related to the three different data sets. The soil moisture anomalies are computed by subtracting the mean value of each data set and calculating the root mean squared deviation of those two unbiased data sets afterward.

One of the long-term soil moisture monitoring test sites that are needed for calibration and validation purposes of a satellite like SMOS is situated in the UDC in Southern Germany [18], [33]. Since 2007, based on previous studies [34], [35], an automatic framework has been built up to compare SMOS products against *in situ* measurements, land surface model simulations, and ancillary satellite data. During the SMOS validation campaign that took place in the UDC in May and June 2010, airborne measurements with two L-band radiometers (EMIRAD and HUT-2D) were performed in five days together with extensive ground measurements. This data set forms an interesting extension to the other measurements and modeled data sets that are being used for SMOS validation in the UDC. Fig. 1 gives an overview about the SMOS cal/val approach in the UDC. As measurements and model results always have specific uncertainties that are related, e.g., to their scale, measurement principle or algorithm used, it is necessary to assess the accuracy of the data used for SMOS validation, which is the scope of this paper. No SMOS data are shown in this paper as this would require a detailed discussion of the

postprocessing that has been applied to the SMOS data which is beyond the scope of this paper. In addition, the SMOS L2 soil moisture products are not directly comparable to the data sets presented here as the SMOS L2 soil moisture product is valid only for low vegetation. A detailed comparison of SMOS data and the earlier mentioned validation data sets is performed in a companion paper [36] and discussed thoroughly. There, it is concluded that the SMOS soil moisture product exhibits a considerable dry bias in the order of -0.11 to 0.3 m^3/m^3 when compared to *in situ* measurements and land surface model simulations. A major issue hampering SMOS data analysis in the test site is radio-frequency interference (RFI) [36].

In Section II of this paper, the test site and the different data sets used in this study are introduced. They comprise different field measurements of soil moisture and other parameters as well as airborne data sets from the EMIRAD radiometer. The HUT-2D radiometer is not being used in this study. The following section gives an overview about the coupled land surface and radiative transfer models used. Section IV describes the model validation and uncertainty assessment. This is being done by comparing the model results on different scales to field measurements of soil moisture. Different field data sets of soil moisture are compared against each other to assess their specific uncertainties. After that, the brightness temperature simulations are being compared against airborne measurements from EMIRAD to assess the uncertainties related to the radiative transfer modeling. In Section V, the results from the previous sections are discussed considering scaling issues and the characteristics of the different measured and modeled data sets. In the following Section VI, conclusions are drawn to relate the results of this study to the SMOS validation being performed in the UDC.

II. TEST SITE AND DATA SETS

A. Cal/Val Approach

The SMOS validation in the UDC is being done by comparing the SMOS soil moisture products (Level 2 data) to land surface model simulations in the whole UDC. *In situ* measurements taken at soil moisture measuring stations and during
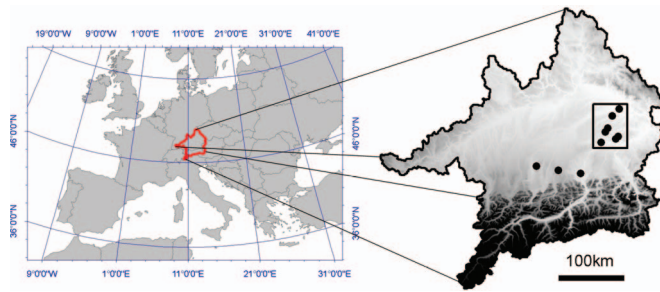
This article has been accepted for inclusion in a future issue of this journal. Content is final as presented, with the exception of pagination.

SCHLENZ *et al.*: UNCERTAINTY ASSESSMENT OF THE SMOS VALIDATION

3

Fig. 2. Upper Danube Catchment, located in Central Europe, with an area of 77 000 km^2 The black rectangle defines the Vils test site (approximately 50 × 60 km), the black dots represent the soil moisture stations. The background of the catchment is a digital elevation model with 1-km resolution (white: 312 m. a.s.l.; black: 3630 m.a.s.l.).

ground campaigns are used for model validation. In addition to that, SMOS L1c products (brightness temperatures) are being compared to modeled brightness temperatures obtained from a radiative transfer model coupled to the PROMET land surface model. The algorithms used in the radiative transfer model for retrieving soil moisture from SMOS observations are being validated with airborne radiometers during campaigns and the ground-based ETH L-Band Radiometer (ELBARA) 2 [37].

B. Upper Danube Catchment

The UDC is located mostly in Southern Germany and the Northern Alps (Fig. 2, [33]). It has been the focus of a wide range of hydrological, remote sensing, and global change studies for many years (e.g., [38]–[44]). Being situated in Central Europe, the climate is temperate and humid which is characteristic for many subcontinental regions in the midlatitudes. The average temperatures range from about -2 °C in January to about 17 °C in July, and the mean annual precipitation sum is about 900 mm in Munich, in the center of the catchment. Snow cover typically lasts for several weeks in winter. The test site is dominated by the alpine foreland with heterogeneous land cover and soil types, while the Alps form the southern border. The annual precipitation sum decreases from the Alps northwards, while the mean temperature increases.

Best soil moisture retrieval performance is expected in the Vils test site which is located in the catchment of the river Vils, situated in the Northeast of the city of Munich [45]. It has about the size of a SMOS footprint. The reason for expected good soil moisture retrieval performance is the lack of substantial open water bodies or large urban areas which could considerably affect the passive microwave signal in that area. The terrain is undulating with elevations varying between about 320 and 470 m a.s.l. The soils are fairly homogeneous and consist mainly of loam with high percentages of silt, particularly in areas where Loess can be found. The area is being used intensively by agriculture. The three most important agricultural land cover types in the Vils test site, grass, maize, and winter wheat, cover more than 60% of the area.

Since 2007, a total of ten soil moisture stations have been built up at different locations in and around the Vils Catchment.

For validation purposes, the study of scaling issues related to SMOS and the verification of model parameters, two airborne

TABLE I
OVERVIEW ABOUT THE SOIL MOISTURE STATIONS
IN THE UPPER DANUBE CATCHMENT

Station number	Name	Lat/lon [deg]	Elev. [m]	sand/clay content [%]	TDR / FD	Operation period	In Vils test site
14	Neusling	12.87/ 48.69	345	19.5/6.8	TDR	11/2007 -	X
16	Steinbeissen	12.73/ 48.60	380	30.5/5.5	TDR	3/2008 -	X
49	Frieding	12.83/ 48.33	480	36.6/5.1	TDR	3/2008 -	X
74	Lochheim	12.49/ 48.27	410	27.6/11.2	TDR	3/2008 -	X
80	Rothenfeld	11.22/ 47.97	690	67.1/3.1	FD	3/2008 – 3/2010	-
115	Wettlkam	11.64/ 47.91	675	65.4/3.5	FD	3/2008 – 10/2008	-
118	Engersdorf	12.63/ 48.45	460	40.3/6.4	TDR	11/2007 -	X
125	Karolinenfeld	12.07/ 47.86	468	41.9/3.9	FD	3/2008 – 3/2010	-
500	Erlbach	12.82/ 48.30	426	62.4/5.6	FD	5/2010 -	X
501	Harbach	12.61/ 48.42	467	32.8/9.6	FD	5/2010 -	X

campaigns have been conducted in 2008 and 2010, respectively [20], [33]. Focus of both campaigns was the Vils test site.

C. Continuous Soil Moisture Measurements

From the ten soil moisture measuring stations, an hourly data record of measured soil moisture exists starting in November 2007. Some of the stations were moved to different locations during their lifetime, some had to be removed for technical or logistical reasons. At all stations, soil moisture was measured in 5-cm depth with at least two probes installed horizontally. At most stations, additional probes are installed in different depths. Table I gives an overview of these stations including the surface sand and clay contents, the operation period and an indication whether the station is situated inside the Vils test site. The measurement devices used are IMKO Trime-ES time domain reflectometer (TDR) probes (theoretical accuracy $\pm 0.01 - \pm 0.03$ m^3 m^{-3} [46]) and Decagon ECHO-TE and EC-5 frequency domain (FD) probes (theoretical accuracy ± 0.03 m^3 m^{-3} [47], [48]). To monitor the quality of the stations, independent handheld soil moisture measurements were conducted regularly (typically every 2–4 weeks) starting in March 2008 at the stations with Delta-T Theta FD probes (theoretical accuracy ± 0.05 m^3 m^{-3} [49]) and gravimetric samples (theoretical accuracy ± 0.02 m^3 m^{-3} [50]). These handheld measurements were conducted in such a manner that 20 FD measurements were taken inside a circle with a diameter of 3 m around the station and three gravimetric samples taken within 1 m of the station. Station 125 is not used in this analysis as it is situated in a moor and not representative for a considerable area.

D. SMOS Validation Campaign Data Set

In spring and early summer 2010, the SMOS validation campaign took place in the UDC on eight days from 17 May

This article has been accepted for inclusion in a future issue of this journal. Content is final as presented, with the exception of pagination.

4   IEEE TRANSACTIONS ON GEOSCIENCE AND REMOTE SENSING

to 8 July 2010. On five of those days two L-band radiometers, EMIRAD (owned by the Technical University of Denmark) and HUT-2-D (owned by the Aalto University, Finland) and a thermal camera (supplied by the Max-Planck Institute for Meteorology, Hamburg), were flown on the Skyvan aircraft. Soil moisture, land use, and vegetation status were recorded by several ground teams on all eight days in five focus areas spread over the Vils test site. All focus areas were located around one or two of the soil moisture stations and had a size of about 3 km by 7 km. In each of the focus areas, soil moisture was measured on two grids with different resolution using Delta-T Theta FD probes. The coarser grid covered the whole focus area with 60 sampling points along transects, while the finer grid covered an area with a size of about 1 km^2 with 60–100 sampling points. The coarse-grid data will be used in the present study. At all sampling points, multiple soil moisture measurements were taken to decrease uncertainty resulting in more than 9000 samples in the course of the campaign.

The resolution of sampling points was chosen in such a way to best represent the different land cover classes while being coarse enough to allow an efficient sampling of a large area. In preparation of the SMOS validation campaign 2010, two extensive field campaigns were used to assess the soil moisture variability across different scales and the number of samples needed to be able to calculate the soil moisture mean of the focus areas in the Vils test site with an appropriate accuracy. [17] have developed an empirical model to study the number of samples necessary to measure the area-averaged soil moisture mean of a certain area to a certain degree of accuracy during field campaigns. They state that a number of 18 point samples is sufficient to measure the area-averaged soil moisture mean of an area of 800×800 m^2 and 30 samples for an area of 50×50 km^2 with an accuracy better than 0.03 m^3 m^{-3} with 95% confidence [17]. As this model was developed with data from the Central U.S., it may only be transferable to areas with similar climatic, topographic, and land surface features to the study area. Also, the empirical model may underestimate the amount of samples needed if some assumptions made may not hold [17]. Still, these numbers provide an indication about the order of magnitude of the amount of samples needed for a representative mean value of soil moisture.

Therefore, the means of measured soil moisture in the focus areas are considered representative for the sampled area. As the location of the focus areas has been chosen carefully in such a manner to best represent the heterogeneity of the Vils test site and the Vils test site is relatively homogeneous related to land cover, topography, soils, and climate, it is assumed that the soil moisture mean of all focus areas is representative for the Vils test site. Destructive biomass sampling was performed in selected areas. Due to the long duration of the campaign and different weather conditions, vegetation and soil moisture changed significantly in the course of the campaign. A more detailed overview of the airborne campaign is given in [20]. To study the conditions during the campaign in more depth, Figs. 3 and 4 show the temperature, precipitation, and soil moisture conditions during the campaign. An area of more than 192 km^2 was land cover mapped in the course of the campaign.
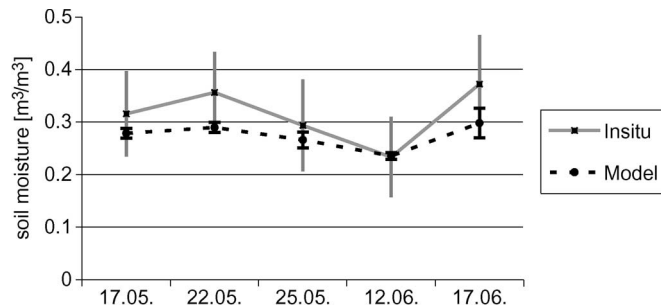

Fig. 3.   Large-scale comparison of measured and modeled soil moisture means for the Vils test site for the flight days during the SMOS validation campaign 2010.
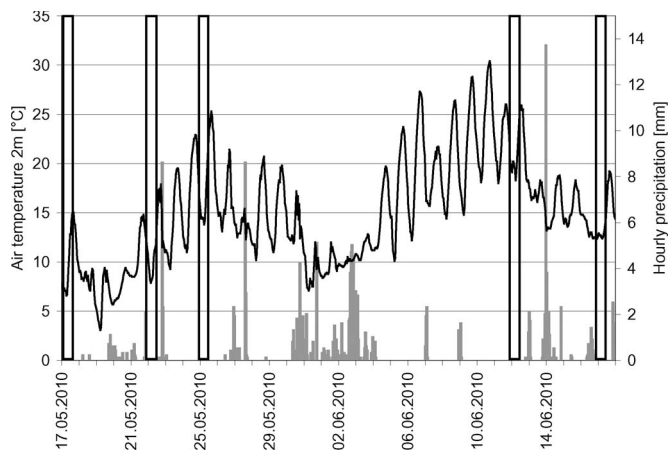

Fig. 4.   Hourly temperature (black line) and precipitation (grey bars) measured at the meteorological station Engersdorf (118) during the SMOS validation campaign 2010. Black bars indicate the flight days.

E. Airborne Data

The EMIRAD data are used in this study as reference for the validation of the radiative transfer modeling. The aircraft flight track with four flight lines inside the Vils test site is shown in Fig. 5 for one campaign day. A similar pattern was flown on all campaign days. EMIRAD is a fully polarimetric radiometer operating at L-band with an antenna system consisting of two Potter horns, one pointed nadir and the other one 40° aft. A detailed technical description of the instrument's characteristics is given in [51]. The EMIRAD footprint size is of the order of 2 km for the nadir antenna and about 4 km for the 40° looking antenna for an average flight altitude of 2 km above ground. Raw data were delivered as calibrated contemporaneous measurements in antenna geometry and were postprocessed before usage. This included temporal aggregation of the data, geocoding, and the geometric rotation from X/Y plane to H/V plane around the polarization rotation angle at boresight. During the geolocation, the 3-dB EMIRAD footprints were projected on the ground using a high-resolution digital elevation model and information on aircraft speed and orientation. In addition to that, RFI filtering was performed using RFI flags provided together with the data. The RFI flagging is being done with the kurtosis method, which is a widely used approach [51], [52]. As RFI cannot be removed completely using this flag, all data above a threshold of 300 K are discarded afterward. The RFI filtering is necessary as RFI is present in the EMIRAD
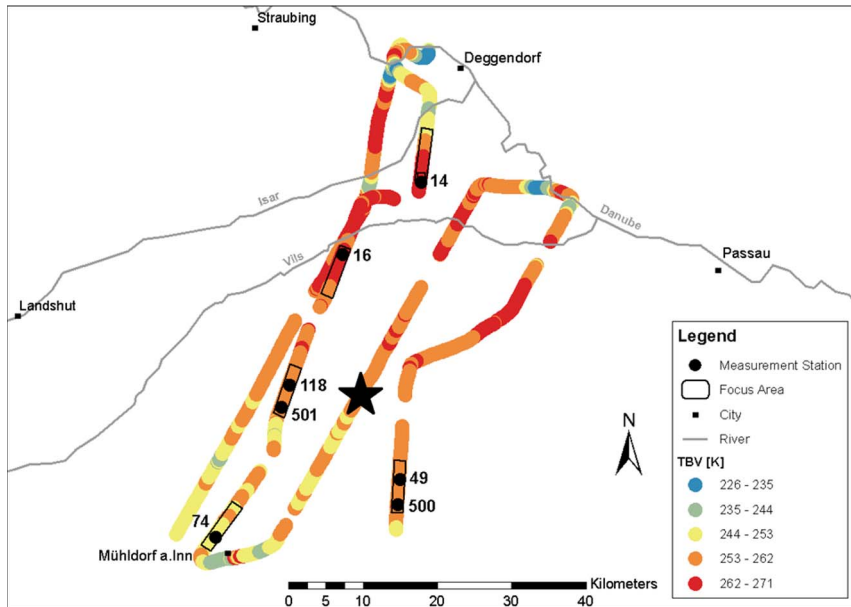
Fig. 5. Flight line with EMIRAD brightness temperature data (vertical polarization) for the SMOS validation campaign flights inside Vils test site on June 12, 2010. The Vils test site soil moisture stations are marked with black dots, the focus areas with black rectangles, the central ISEA grid point 2027099 with a star.

data measured in the UDC and makes part of the radiometer data unusable [51]. After processing, the data is available for the two incidence angles 0° and 40° for vertical and horizontal polarizations.

III. COUPLED LAND SURFACE AND RADIATIVE TRANSFER MODEL

For the present study, the land surface model PROMET (process-oriented multiscale evapotranspiration model) [44] was coupled with the microwave emission model L-MEB (L-band emission of the biosphere) [53] to be able to model the soil moisture and temperature fields as well as the resulting microwave emissions in the L-band for the entire UDC.

A. PROMET

The PROMET hydrologic land surface model is used to simulate fields of land surface states on a 1-km grid with hourly resolution in the UDC. It is spatially distributed and describes all relevant water and energy fluxes [38] related to the radiation balance, vegetation, soil, snow, and aerodynamic processes. The soil moisture dynamics are simulated with a modified version of the Richards equation for flow in unsaturated media [54]. The soil water retention model of [55] is used to relate soil suction head to soil moisture content. A detailed description of the model physics is given in [44]. The model is based on high-resolution spatial input data like soil and land cover maps and meteorological forcing data as input for the calculations. The meteorological station network providing the meteorological forcing is collocated with the *in situ* soil moisture network and consists of more than 130 stations. The land cover map has been derived from high-resolution satellite imagery and statistical information on community level.

The model has been validated in different test sites on different scales with good results [38], [39], [44], [56]. The soil water

model in particular has been validated in different test sites using *in situ* soil moisture measurements of soil moisture profiles and remote sensing observations with good results [43], [57]. Very good agreements between soil moisture profile measurements and simulations were found (RMSE $= 0.016$ m^3 m^{-3}) by [57]. Model simulations are available for the period from 1st November 2008 until the end of 2010. For these model runs, we renounced to specifically tune the soil information used by PROMET with soil parameterizations derived from field studies at the measurement sites and intentionally used standard soil maps, which are part of the Global Soil Data Base. This allows to generalize the results of the uncertainty analysis beyond the UDC.

B. L-MEB

The land surface microwave emission results from the continuous soil vegetation layer and is affected by soil temperature, soil moisture, and vegetation opacity.

A microwave emission model coupled to PROMET is used to simulate brightness temperatures for the whole UDC. The zero-order τ–ω radiative transfer model [58] is used for that purpose. In this paper, the model utilized is L-MEB, which is also a part of ESA's SMOS Level 2 soil moisture processor [53]. It is used to simulate high-resolution (1 km) microwave L-band brightness temperatures using, among others, the soil moisture fields, temperatures, and vegetation parameters simulated by PROMET. Wigneron *et al.* [53] give a comprehensive overview about that model; therefore, it is only introduced here briefly.

The effects of soil and vegetation on the brightness temperature with horizontal and vertical polarization $(P = h, v)$ are considered through [53], [59]

$$T_{BP} = T_a + \gamma_a \left[e_{GP} \cdot T_G \cdot \gamma_P + T_C (1 - \omega_P)(1 - \gamma_P) \right.$$
$$\left. + TC(1 - \omega_P)(1 - \gamma_P)(1 - e_{GP})\gamma_P \right] \quad (1)$$

This article has been accepted for inclusion in a future issue of this journal. Content is final as presented, with the exception of pagination.

6

IEEE TRANSACTIONS ON GEOSCIENCE AND REMOTE SENSING

TABLE II
THE MODEL PARAMETERS USED FOR L-MEB

	h	QR	NRh/ NRv	tth/ ttv	ωh/ωv	b'	b"
Bare soil	0.1	0	0/-1	1/1	0/0	0	0
Crops general	0.15	0	0/-1	1/1	0/0	0.05	0
Wheat	0.1	0	0/-1	1/8	0/0	0.035	0
Corn	0.6	0	0/-1	2/1	0.05/ 0.05	0.05	0
Grass	1.3- 1.13*SM	0	1/0	1/1	0/0.05	0.04	0.03
Coniferous	1.2	0	1.8/2	0.9/ 0.8	0.07/ 0.07	τNAD= 0.65	0.
Deciduous	1.	0	1/2	0.6/ 0.5	0.07/ 0.07	τNAD=1.	0

where $T_{\rm BP}$ is the brightness temperature [K]; $T_{\rm a}$ is the upwelling atmospheric emission [K]; $\omega_{\rm P}$ is the single scattering albedo of the canopy [−]; $\gamma_{\rm a}$ and $\gamma_{\rm P}$ are the transmissivity of the atmosphere and canopy, respectively, [−] and $T_{\rm G}$ and $T_{\rm C}$ are the temperature of the ground and the canopy [K] , respectively. $e_{\rm GP}$ is the emissivity of the soil surface [−].

The reflectivity $(1 - e_{\rm GP})$ of a rough soil is typically described as a function of the Fresnel reflectivities of a smooth surface, modified by a surface roughness component. The vegetation parameters are the vegetation single scattering albedo $\omega_{\rm P}$ and the vegetation transmissivity $\gamma_{\rm P}$. The latter is described as a function of the vegetation optical thickness τ at nadir and the observation angle (Beer's law). The atmospheric effects are being neglected in this study as no spaceborne brightness temperature data is being used.

The effective temperature of the ground, $T_{\rm G}$, is calculated after the approach of [53] from the soil surface temperature and the temperature of a deeper soil layer, both provided by PROMET. $T_{\rm C}$ is approximated with the temperature of the vegetation surface as modeled by PROMET. The vegetation optical depth is calculated using modeled leaf area index values with the approach of [53]. The optical depth of forests is fixed to a defined value. The roughness parameter h over grass is soil moisture dependent [60], [61]. Table II gives an overview about the vegetation-dependant model parameters used for L-MEB. They are in line with the parameters used for [53], [62], and [63] (J.-P- Wigneron, personal communication).

IV. MODEL VALIDATION AND UNCERTAINTY ASSESSMENT

A. Soil Moisture

1) Local Scale Soil Moisture: To verify the accuracy of the continuous soil moisture measurements from the stations, the 5-cm means of the continuous surface soil moisture measurements (TDR, FD) have been compared to the means of the handheld measured FD surface soil moisture that has been measured regularly at all stations. Fig. 6 shows that comparison. The station measurements seem to slightly overestimate the handheld measurements during very dry conditions. R^2 is 0.63, and the root mean squared error (RMSE) is 0.052 m^3 m^{-3}. There is no systematic bias but as indicated by the standard
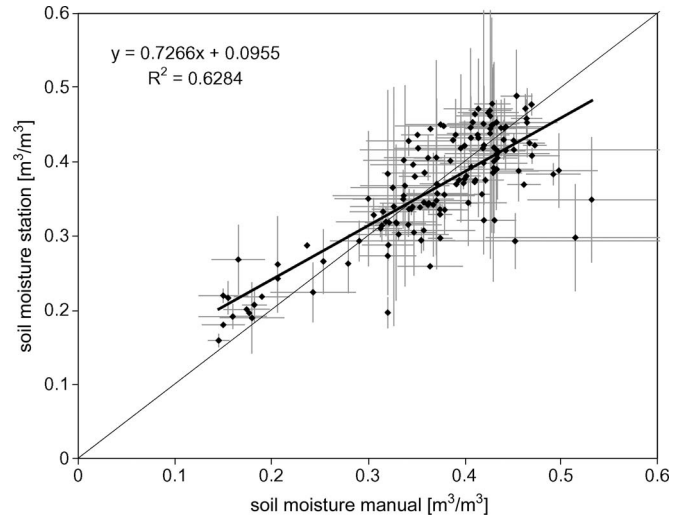
Fig. 6. Local comparison of continuously measured surface soil moisture at the stations with handheld and simultaneously measured surface soil moisture.
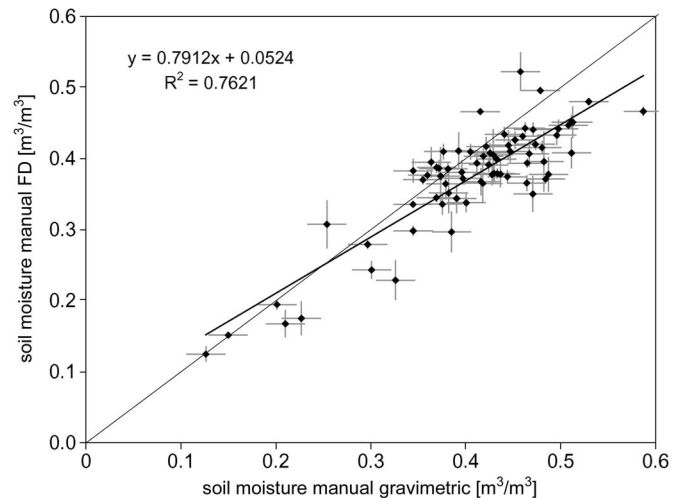

Fig. 7. Local comparison of manually measured surface soil moisture with handheld FD probes and gravimetric samples.

deviation bars and some outliers, the soil moisture variability within those measurements can be quite high even within a few meters around the station. The standard deviations of both data sets regularly exceed 0.10 m^3 m^{-3}.

To validate the handheld FD measurements, they were taken simultaneously with gravimetric samples. The comparison of the latter two data sets is shown in Fig. 7. The handheld FD measurements seem to slightly underestimate soil moisture under very wet conditions. R^2 is 0.76, and the RMSE is 0.053 m^3 m^{-3}. There does not seem to be a systematic bias.

To validate PROMET on the local scale and estimate the uncertainties related to the soil moisture modeling, PROMET has been used to model point-scale surface soil moisture at all stations which then was compared to the station measurements. The results of the comparison for the months April to October are summarized in Table III. The R^2 for five stations is above 0.6, the RMSE is below 0.05 m^3 m^{-3} for three stations and above 0.10 m^3 m^{-3} for five stations. The gains and offsets of the regression lines and the mean values of the data sets are also given in the table. It is obvious that a bias leads to

This article has been accepted for inclusion in a future issue of this journal. Content is final as presented, with the exception of pagination.

SCHLENZ *et al.*: UNCERTAINTY ASSESSMENT OF THE SMOS VALIDATION

7

TABLE III
STATISTICS OF THE COMPARISON BETWEEN MODELED AND MEASURED
SOIL MOISTURE AT THE MEASURING STATIONS

No.	Name	RMSE / RMSE of anomalies [$m^3\,m^{-3}$]	Gain / Offset	Mean PROMET [$m^3\,m^{-3}$]	Mean station [$m^3\,m^{-3}$]	R^2
14	Neusling	0.041 / 0.033	0.881 / 0.011	0.284	0.307	0.64
16	Steinbeissen	0.076 / 0.036	0.626 / 0.067	0.288	0.359	0.79
49	Frieding	0.111 / 0.056	0.365 / 0.142	0.277	0.374	0.55
74	Lochheim	0.153 / 0.067	0.299 / 0.113	0.220	0.357	0.45
80	Rothenfeld	0.039 / 0.035	0.553 / 0.100	0.245	0.260	0.77
115	Wettlkam	0.047 / 0.038	0.536 / 0.163	0.317	0.294	0.64
118	Engersdorf	0.111 / 0.043	0.474 / 0.095	0.275	0.376	0.66
500	Erlbach	0.119 / 0.060	0.289 / 0.176	0.278	0.393	0.27
501	Harbach	0.149 / 0.053	0.428 / 0.101	0.275	0.420	0.59
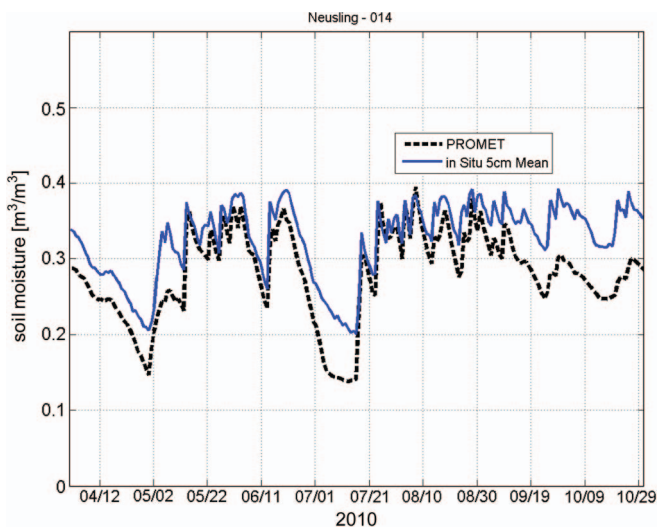
Fig. 8. Local comparison of measured and modeled 5-cm soil moisture for station Neusling for April to October 2010.

Fig. 9. Medium-scale comparison of area mean values of modeled and measured soil moisture in the five focus areas on the eight campaign dates of the SMOS validation campaign 2010.

high RMSE values at some stations. At the stations with high RMSE values, the deviation of the mean values of the two data sets compared are in the order of the RMSE value. The RMSE of anomalies is below 0.07 $m^3\,m^{-3}$ for all stations. PROMET tends to underestimate the soil moisture under wet conditions that occur mainly in spring and fall. This leads to an underestimation of the seasonal soil moisture dynamics by PROMET. The time series of the comparison with daily data for station 14 for the year 2010 is shown in Fig. 8.

2) Medium-Scale Soil Moisture: To see how well the model reproduces the medium-scale soil moisture dynamics, simulated soil moisture fields were compared with the distributed medium-scale measurements made during the 2010 field campaign. For that purpose, the mean value of all field measurements made on the coarse grid in one focus area was calculated for each campaign day and compared to the mean value of all model grid cells covering the same focus area.

The measurements used for this study are only the coarse-grid measurements to weight the whole focus area uniformly. Fig. 9 shows the comparison, each dot represents one focus area mean value which corresponds to about 300 independent soil moisture measurements. The model standard deviations are considerably smaller than the standard deviations of the measurements which are of the order of 0.07–0.08 $m^3\,m^{-3}$, on some days in some focus areas also exceed 0.1 $m^3\,m^{-3}$. The model tends to underestimate soil moisture under wet conditions which leads to an underestimation of soil moisture dynamics. The RMSE is 0.045 $m^3\,m^{-3}$ for that comparison and R^2 is 0.75. The RMSE of anomalies is 0.040 $m^3\,m^{-3}$.

3) Large-Scale Soil Moisture: To estimate how well the model is able to simulate soil moisture in extended areas on a SMOS-like scale, a comparison of measured and modeled mean soil moisture in the whole Vils test site was performed on basis of the ISEA grid. It is shown in Fig. 3. The mean values of the focus area means of measured soil moisture were compared to the mean values of simulated soil moisture for the central ISEA grid point in the Vils test site, ID 2027099. For this purpose, all model grid cells in the Vils test site were mapped to the ISEA grid with the nearest neighbor approach. For each day, all data mapped on a grid point were averaged. As the Vils test site is very homogeneous on that scale, it is assumed that the area mapped to one ISEA grid point is representative for a considerably larger area. For this analysis, only campaign days were used on which at least four out of the five focus areas had been sampled sufficiently. The days June 14 and July 8 had to be excluded because only one and three focus areas had been sampled, respectively, because of rain events starting in the course of the day. The RMSE of this analysis is 0.040 $m^3\,m^{-3}$, the RMSE of anomalies is 0.023 $m^3\,m^{-3}$.

B. Brightness Temperature

To assess the quality of the radiative transfer modeling with the coupled models PROMET and L-MEB, modeled brightness temperatures are compared to L-band radiometer

measurements. Apart from the point-like scale (e.g., with measurements from a ground-based radiometer), this can be done on a SMOS-like scale with airborne radiometer data. The latter approach is subject of this chapter. All 1-km brightness temperature data available from the coupled models and all airborne EMIRAD radiometer data were mapped to the same geometry based on SMOS's ISEA grid. This was done with the nearest neighbor approach for the five SMOS validation campaign days with airborne L-band radiometer measurements. During the mapping of EMIRAD footprints to the ISEA grid, the center coordinates of the EMIRAD footprints were used for the decision whether an EMIRAD footprint lied inside the area being mapped to an ISEA grid point. The central ISEA grid point in the Vils test site, ID 2027099, was used as comparison reference. For each day, all data mapped on that grid point were averaged. It is assumed that the results are valid for larger areas as the Vils test site is very homogeneous. This comparison includes some approximations. The defined look angles ($0°$, $40°$) of the radiometer are only valid in the center of the elliptical radiometer footprint. Near the edges of the footprint, the look angle deviates from the defined one. As the signal from the center has a larger influence on the overall measurement than the signal near the edges of the footprint due to the antenna diagram, the modeled brightness temperatures have only been produced for the center angle ($0°$, $40°$).

This comparison was performed for the $40°$ look angle brightness temperatures as well as the $0°$ look angle brightness temperature. Fig. 10 shows the result of that comparison for vertical and horizontal polarizations for $40°$ incidence angle; Fig. 11 shows the comparison for the $0°$ brightness temperature in vertical polarization. Horizontal polarization data are not shown here, as for an incidence angle of $0°$, both polarizations show essentially the same behavior. For $40°$ on three of the five campaign days, the simulated and observed brightness temperatures show a good agreement, while larger discrepancies are observed on days 22 May and 17 June, resulting in an RMSE of 16.52 K for H polarization and 13.14 K for V polarization. The model tends to simulate higher brightness temperatures than EMIRAD measurements, particularly for vertical polarization, and particularly for the two days mentioned above. For the vertical polarization in $0°$, the picture is very similar. The two days that show the largest deviation between model and measurement lead to an RMSE of 12.09 K (12.97 K for horizontal polarization). The reasons for these discrepancies will be discussed below. Fig. 4 shows that there are precipitation events between all five EMIRAD overflight days, even though one has to bear in mind that the data shown are only representative for one meteorological station that is close to the center of SMOS grid point 2027099. This emphasizes that both the environmental conditions and the brightness temperatures are very dynamic, and their variability is much larger than what can be seen in the measurements of the five campaign days. The surface temperature during the EMIRAD overflights varies between about 7 and 18 °C in the course of the campaign and the focus area means of soil moisture between 0.169 and 0.392 $m^3 \, m^{-3}$.

The vegetation conditions change significantly in the course of the campaign. The mean vegetation height of maize for
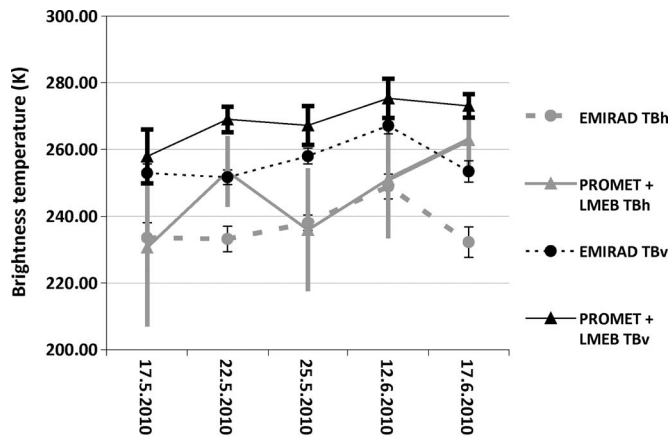

Fig. 10. Large-scale comparison of modeled and measured (EMIRAD) $40°$ brightness temperatures (V and H polarization) on the five flight days during the SMOS validation campaign 2010 based on the ISEA grid.

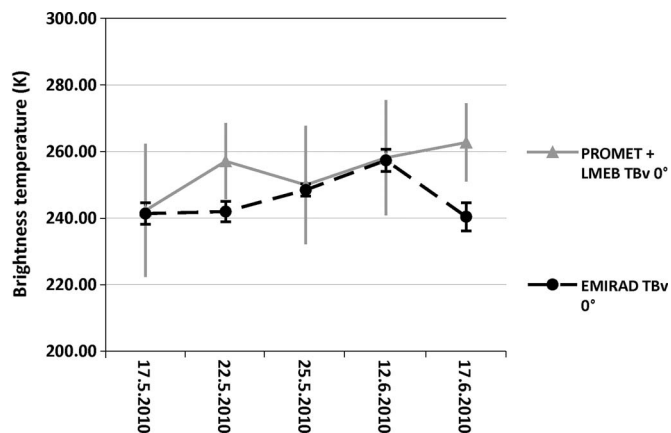Fig. 11. Large-scale comparison of modeled and measured (EMIRAD) NADIR ($0°$) brightness temperatures (V polarization) on the five flight days during the SMOS validation campaign 2010 based on the ISEA grid.

example varies between 7.2 and 44.5 cm, that of winter wheat between 40.2 and 79.5 cm. The measured vegetation heights during the campaign have been used to improve the vegetation parameterization in L-MEB.

V. DISCUSSION

A. Soil Moisture Measurements

Comparisons of different *in situ* data sets have been made to assess the accuracy of the data sets that will be used as reference data in the further analysis.

By looking at the comparisons shown above, one has to bear in mind several issues related to the different measurement techniques. Each technique has its own unique measurement principle and sampling volume resulting in different representations of the natural soil heterogeneities (e.g., soil type variations, air bubbles, stones, vegetation material, etc.) or soil moisture gradients in the soil profile in the measurements. Care has been taken to minimize those effects. The different measurements sample different soil volumes which results in the data sets compared being valid for slightly different soil layers. While the continuously measuring probes are installed horizontally

This article has been accepted for inclusion in a future issue of this journal. Content is final as presented, with the exception of pagination.

SCHLENZ *et al.*: UNCERTAINTY ASSESSMENT OF THE SMOS VALIDATION

9

in 5-cm depth and measure an integrated signal of a varying soil volume depending on soil moisture content, the vertical handheld FD measurements are valid for the upper 6 cm and the gravimetric samples are valid for the upper 4 cm of the soil. In addition, the measurements were not taken at exactly the same locations in order not to disturb the soil around the installed probes. Instead, the locations for the different measurements can be situated up to about 3 m apart from each other. As soil moisture variability can be quite high even on that scale, which is shown by the sometimes considerable standard deviations in Figs. 6 and 7, a sufficient amount of samples has been taken at all sampling days to minimize the effects of soil heterogeneity.

Considering all mentioned obstacles in determining representative soil moisture values for extended areas, the comparisons shown above seem to support the thesis that the soil moisture measured at the stations and with handheld FD probes shows the expected variability and is therefore reliable enough to be used in further analysis. However, the uncertainties of the measurements should be kept in mind when using them as reference data set.

B. Soil Moisture Modeling at the Local Scale

The local scale soil moisture comparison between model and measurements show that the model is able to capture the temporal and spatial dynamics of the soil moisture reasonably well, but at some stations has a considerable offset when it comes to absolute values, particularly under wet conditions, which reduces the dynamic range of the model. These offsets are due to discrepancies between the soil parameters derived from the large-scale soil maps used to parameterize PROMET and the individual soil properties at the specific location chosen for the soil moisture measurements. We decided to not tune the PROMET simulations to the soil properties of the specific measurement locations to determine the range of uncertainty that is introduced into the soil moisture simulations by the underlying soil map.

When looking at this, one has to keep in mind the uncertainties related to the soil moisture measurements. The standard deviation of the mean of the 5 cm *in situ* measurements indicate for example that different probes in the same depth sometimes have considerable deviations in their measurements. At station Frieding, for example, where the RMSE between model and measurement is relatively high, the mean standard deviation of the 5 cm means of the *in situ* measurements is 0.097 m^3 m^{-3} and regularly exceeds 0.1 m^3 m^{-3}, while in Neusling and Steinbeissen, where the RMSE is relatively low, the mean standard deviations of the measurements are below 0.01 m^3 m^{-3}. In Harbach and Lochheim, standard deviations exceed 0.05 m^3 m^{-3} regularly. In addition, Frieding is an example of a station, where the station *in situ* soil moisture is regularly higher than the soil moisture of the handheld FD measurements. This is particularly true during wet periods. As the FD measurements are validated with gravimetric samples, this is an indicator for less reliable measurements.

Stations Erlbach and Harbach are the only ones not situated next to a meteorological station. Even though they are less than 4 km away from the next meteorological station, it is obvious in the data that the meteorological forcing data used for modeling at those stations are inaccurate as some precipitation events that occurred at the meteorological station were not registered at the soil moisture stations. Therefore, the modeled soil moisture values at those stations are less reliable. On a larger scale, however, this should become insignificant.

C. Soil Moisture Modeling on the Medium Scale

The comparison of measured and modeled focus area means of soil moisture during SMOS validation campaign 2010 seems to perform better than the local scale soil moisture comparisons. They may be valid mainly for spring and summer, but they represent a considerable area of more than 100 km^2 of very heterogeneous land cover due to very small field sizes in the Vils test site. Both temporal and spatial variability of soil moisture are high during the campaign and are captured quite well.

The comparison of measured and modeled focus area means of soil moisture is affected considerably by the different scales of the two data sets. The high natural soil moisture variability of an area sized about 3 km $\times$ 7 km with heterogeneous land cover (e.g., forest, bare soil, wheat, grassland) leads to high standard deviations as seen in Fig. 9. The standard deviations of the modeled values are often smaller due to the model resolution of 1 km which leads to a strongly reduced variety of land covers and natural conditions appearing in a focus area. In fact, the land cover map used for the model could introduce substantial errors when differing substantially from the actual land cover in the field. A comparison of mapped land cover with the land cover map used for modeling shows that the shares of the three main agricultural land cover types, grassland, winter wheat, and maize, which cover more than 58% (model map: 61) of the Vils test site, are very similar in both maps: Winter wheat: 16% (14), grassland: 23% (28), maize: 19% (19). This means that the error due to the land cover map used in the model is expected to be small if the mean value of several pixels is considered. However, when looking at smaller areas with only a few pixels of model output, the statistical nature of the land cover distribution in the model can introduce considerable deviations. For this reason, mean values per focus area are used for the comparison rather than looking at *in situ* measurements located in a single PROMET pixel.

As mentioned earlier, deviations between modeled and measured soil moisture may always result from inaccurate forcing data. At this time of year, convective precipitation events are quite common in the area, and it is obvious in the data of measurement stations Harbach and Erlbach that some rain events that occurred in a focus area were missed by the meteorological stations delivering the forcing data as input for soil moisture modeling.

D. Soil Moisture Modelling on the Large Scale

As shown in Section IV, the large-scale comparison between measured and modeled soil moisture on basis of the ISEA grid for the Vils test site produces a smaller RMSE than that on the medium and local scale. This may be due to deviations between measurement and model resulting from small-scale

This article has been accepted for inclusion in a future issue of this journal. Content is final as presented, with the exception of pagination.

10   IEEE TRANSACTIONS ON GEOSCIENCE AND REMOTE SENSING

heterogeneity getting more and more insignificant when the scale increases. Measurement errors, land cover distribution, and small-scale precipitation events play a less significant role here. Of course, the sample size of six days is not very large, hampering a more detailed analysis, but for distributed measurements in an area as large as the Vils test site, it is hardly possible to get substantially larger data sets.

E. Brightness Temperature Modeling

Considering all the highly temporally and spatially variable parameters needed for the L-band emission modeling and the heterogeneity and small field size of the area, the results of the brightness temperature modeling look very promising.

The L-band emission of a surface depends mainly on surface temperature, surface soil moisture, vegetation properties, and soil properties like roughness. Therefore, the brightness temperature simulation is very sensitive to the soil moisture and temperature simulations that are used as input as well as the vegetation and soil properties used for the parameterization of the model. The overestimation of modeled brightness temperature can partly be explained by the underestimation of modeled soil moisture. It is obvious that on the two days, 22 May and 17 June, the deviation between both data sets is larger than on the other days. This is in line with the soil moisture estimate for those two days being less accurate than for the others when compared to soil moisture measurements in the field as can be seen in Fig. 3. The larger standard deviations of the model, when compared to the radiometer measurements, can be explained with the relatively large footprint of EMIRAD (approximately 4×4 km for $40°$ incidence angle), which leads to an integration over a variety of land cover types within every footprint. Therefore, the brightness temperature from one footprint to the next will not change considerably, leading to very small standard deviations when averaged. PROMET, on the other hand, models pure pixels containing only one land cover type per pixel (e.g., water, forest, bare soil, barren, grass) which have certain physical parameters related to them (e.g., surface temperature, soil moisture, vegetation parameters, roughness) leading to a high variability of brightness temperatures from one pixel to the next. As these pure pixels are then mapped and averaged on the ISEA grid, they produce the observed high standard deviations.

F. Implications for the SMOS Validation

1) Soil Moisture: For the SMOS validation, it will be important to know the dimension of the uncertainties related to the data sets used for validation. In the case of soil moisture, the uncertainties seem to reduce from local to medium to large scale. While having a mean RMSE value in the range of 0.09 m^3 m^{-3} for the soil moisture comparisons on the local scale and 0.045 m^3 m^{-3} on the medium scale, the RMSE value for the SMOS-like scale is in the order of 0.040 m^3 m^{-3}. The RMSE of anomalies on that scale is 0.023 m^3 m^{-3} which is better than the accuracy target of the SMOS soil moisture product, 0.04 m^3 m^{-3} random error [14], [15]. It is important to mention that all model runs, regardless of scale or area, have been performed with the same set of soil parameters to

make comparisons across scales and different areas possible. Therefore, these results are also transferable to other areas inside the UDC, even though the data sets used for the modeling (e.g., soil map, forcing data) may introduce different errors in different parts of the catchment. Due to the extensive data collected in the Vils test site and most of the comparisons being done here, the uncertainty analysis in this paper is most reliable in the Vils test site. Going from local to large scale, the time series of soil moisture measurements reduces to a few sampled days, while the spatial distribution of samples increases substantially. Therefore, the significance of the results on the large scale may be limited when it comes to long-term soil moisture dynamics, while the significance of the local scale results may be limited in terms of spatial distribution. As all results, regardless of scale and area used, point in the same direction, the results related to soil moisture uncertainty seem quite robust.

On the local scale, it is obvious that the RMSE values are not sufficient to describe model quality as simple offsets result in high RMSE values while the soil moisture dynamics may still be captured quite well by the model. Concerning SMOS validation, this means that in addition to comparing absolute values, it is necessary to also study how well specific soil moisture dynamics are captured. Considering soil moisture anomalies instead of using only absolute values might prove valuable for the SMOS validation [36].

Using a very similar data set of modeled soil moisture and station measurements for 2008 and 2009 in the Vils test site using the triple collocation method, [32] found that PROMET is commonly underestimating the soil moisture dynamical range at large scales (gain around 0.5). The correlation coefficients were of the order of 0.7 and the mean offsets about 0.09 m^{3}m^{-3}. Similar relationships between PROMET and measured soil moisture on different scales were found in this study (Fig. 9, Table I). Loew and Schlenz [32] concluded that the large-scale random error of PROMET soil moisture is better than 0.025 m^3 m^{-3}, which is in line with the findings of the current study.

2) Brightness Temperatures: The results of the brightness temperature simulations indicate that a validation of SMOS brightness temperature products is possible with an uncertainty in the range of 12–16 K RMSE for the period, area, and the incidence angles studied. As the data used in this study is only from five campaign days and the comparison was only performed on the large scale, the results are less robust than the soil moisture results. In addition, the model complexity of the coupled models makes it difficult to estimate wether the results in other areas or during other seasons would be similar. Still, considering the complexity of the approach, the results seem very promising. As the influence of soil moisture errors on the modeling seems to explain most of the observed deviations in brightness temperatures, the radiative transfer model does not seem to introduce large errors here.

VI. CONCLUSION

It was shown in this paper how soil moisture and L-band passive microwave emission can be modeled in different regions

of the UDC under varying soil and vegetation conditions with a coupled land surface and radiative transfer model.

Soil moisture modeling results have been compared to measurements on a local scale over three years and in the course of the SMOS validation campaign 2010 in an area about the size of a SMOS footprint with spatially distributed measurements. The soil moisture behavior has been captured with satisfying results in time as well as in space (R^2 mostly between 0.5–0.7). The absolute soil moisture deviations between model and measurement have a mean RMSE in the order of 0.09 m^3 m^{-3} for local measurements and 0.040 m^3 m^{-3} for large-scale values. The RMSE of anomalies is 0.023 m^3 m^{-3} on the large scale.

As the model tends to underestimate soil moisture under wet conditions, which leads to a reduced soil moisture dynamical range, a rescaling of land surface model soil moisture data might reduce the uncertainty of the SMOS validation.

The brightness temperature simulations have been compared with airborne radiometer measurements based on the SMOS ISEA grid for the Vils test site for five days of measurements under varying soil moisture and vegetation conditions. The overall performance is very promising (RMSE around 12–16 K). Uncertainties related to such a complex modeling approach and the measurements are manifold and have been discussed.

Approaches to improve brightness temperature modeling will have to take into account the possibility that the L-MEB parameters that have been used so far will have to be adapted to local conditions and new findings concerning brightness temperature modeling. The roughness parameter h for example plays an important role in L-band emission modeling [64]–[66] but has not been altered in the course of this study. To further improve the brightness temperature modeling, it would be possible to use the relationships found between modeled and measured soil moisture to rescale soil moisture before using it as input to the radiative transfer model.

The modeled soil moisture and brightness temperature maps in the UDC can be used for the validation of data products from SMOS and other remote sensing instruments. As the uncertainties assessed in this study lie well in the margin of uncertainty that SMOS has shown so far (e.g., dry bias of -0.11 to 0.3 m^3/m^3 when compared to *in situ* measurements and model simulations [36]) and all data sets described in the current paper point in the same direction, this study can provide a valuable contribution to SMOS validation activities.

REFERENCES

[1] P. A. Dirmeyer, "Using a global soil wetness data set to improve seasonal climate simulation," *J. Clim.*, vol. 13, no. 16, pp. 2900–2922, Aug. 2000.

[2] M. Jung, M. Reichstein, P. Ciais, S. I. Seneviratne, J. Sheffield, M. L. Goulden, G. Bonan, A. Cescatti, J. Chen, R. de Jeu, A. J. Dolman, W. Eugster, D. Gerten, D. Gianelle, N. Gobron, J. Heinke, J. Kimball, B. E. Law, L. Montagnani, Q. Mu, B. Mueller, K. Oleson, D. Papale, A. D. Richardson, O. Roupsard, S. Running, E. Tomelleri, N. Viovy, U. Weber, C. Williams, E. Wood, S. Zaehle, and K. Zhang, "Recent decline in the global land evapotranspiration trend due to limited moisture supply," *Nature*, vol. 467, no. 7318, pp. 951–954, Oct. 2010.

[3] A. Loew, T. Holmes, and R. de Jeu, "The European heat wave 2003: Early indicators from multisensoral microwave remote sensing?" *J. Geophys. Res.*, vol. 114, no. D5, p. D05 103, 2009.

[4] E. M. Fischer, S. I. Seneviratne, D. Lüthi, and C. Schär, "Contribution of land-atmosphere coupling to recent European summer heat waves," *Geophys. Res. Lett.*, vol. 34, no. 6, p. L06 707, 2007.

[5] E. M. Fischer, S. I. Seneviratne, P. L. Vidale, D. Lüthi, and C. Schär, "Soil moisture-atmosphere interactions during the 2003 European summer heat wave," *J. Clim.*, vol. 20, no. 20, pp. 5081–5099, Oct. 2007.

[6] S. I. Seneviratne, D. Luthi, M. Litschi, and C. Schar, "Land-atmosphere coupling and climate change in Europe," *Nature*, vol. 443, no. 7108, pp. 205–209, Sep. 2006.

[7] D. Entekhabi, G. R. Asrar, A. K. Betts, K. J. Beven, R. L. Bras, C. J. Duffy, T. Dunne, R. D. Koster, D. P. Lettenmaier, D. B. Mclaughlin, W. J. Shuttleworth, M. T. Van Genuchten, M.-Y. Wei, and E. F. Wood, "An agenda for land-surface hydrology research and a call for the second international hydrological decade," *Bull. Amer. Meteorol. Soc.*, vol. 80, no. 10, pp. 2043–2057, 1999.

[8] F. Aires, C. Prigent, and W. B. Rossow, "Sensitivity of satellite microwave and infrared observations to soil moisture at a global scale: 2. Global statistical relationships," *J. Geophys. Res.*, vol. 110, no. D11, p. D11 103, 2005.

[9] C. Prigent, F. Aires, W. B. Rossow, and A. Robock, "Sensitivity of satellite microwave and infrared observations to soil moisture at a global scale: Relationship of satellite observations to in situ soil moisture measurements," *J. Geophys. Res.*, vol. 110, no. D7, p. D07 110, 2005.

[10] J. P. Wigneron, J. C. Calvet, T. Pellarin, A. A. Van de Griend, M. Berger, and P. Ferrazzoli, "Retrieving near-surface soil moisture from microwave radiometric observations: Current status and future plans," *Remote Sens. Environ.*, vol. 85, no. 4, pp. 489–506, Jun. 2003.

[11] W. Wagner, V. Naeimi, K. Scipal, R. de Jeu, and J. Martínez-Fernández, "Soil moisture from operational meteorological satellites," *Hydrogeology J.*, vol. 15, no. 1, pp. 121–131, Feb. 2007.

[12] W. Wagner, G. Blöschl, P. Pampaloni, J.-C. Calvet, B. Bizzarri, J.-P. Wigneron, and Y. Kerr, "Operational readiness of microwave remote sensing of soil moisture for hydrologic applications," *Nordic Hydrol.*, vol. 38, no. 1, pp. 1–20, 2007.

[13] Y. H. Kerr, P. Waldteufel, J.-P. Wigneron, J.-M. Martinuzzi, J. Font, and M. Berger, "Soil moisture retrieval from space: The Soil Moisture and Ocean Salinity (SMOS) mission," *IEEE Trans. Geosci. Remote Sens.*, vol. 39, no. 8, pp. 1729–1735, Aug. 2001.

[14] Y. H. Kerr, P. Waldteufel, J. P. Wigneron, S. Delwart, F. Cabot, J. Boutin, M. J. Escorihuela, J. Font, N. Reul, C. Gruhier, S. E. Juglea, M. R. Drinkwater, A. Hahne, M. Martín-Neira, and S. Mecklenburg, "The SMOS mission: New tool for monitoring key elements of the global water cycle," *Proc. IEEE*, vol. 98, no. 5, pp. 666–687, May 2010.

[15] *Mission Objectives and Scientific Requirements of the Soil Moisture and Ocean Salinity (SMOS) Mission*, Eur. Space Agency (ESA), Noordwijk, The Netherlands, 2002.

[16] Z. Bartalis, W. Wagner, C. Anderson, H. Bonekamp, V. Naeimi, and S. Hasenauer, "Validation of coarse resolution microwave soil moisture products," in *Proc. IEEE IGARSS*, 2008, pp. II-173–II-176.

[17] J. S. Famiglietti, D. Ryu, A. A. Berg, M. Rodell, and T. J. Jackson, "Field observations of soil moisture variability across scales," *Water Resour. Res.*, vol. 44, no. 1, p. W01 423, 2008.

[18] S. Delwart, C. Bouzinac, P. Wursteisen, M. Berger, M. Drinkwater, M. Martin-Neira, and Y. H. Kerr, "SMOS validation and the COSMOS campaigns," *IEEE Trans. Geosci. Remote Sens.*, vol. 46, no. 3, pp. 695–704, Mar. 2008.

[19] S. Bircher, J. E. Balling, N. Skou, and Y. Kerr, "SMOS Validation by means of an airborne campaign in the Skjern River Catchment,

This article has been accepted for inclusion in a future issue of this journal. Content is final as presented, with the exception of pagination.

12   IEEE TRANSACTIONS ON GEOSCIENCE AND REMOTE SENSING

Western Denmark," *IEEE Trans. Geosci. Remote Sens.*, 2011, DOI: 10.1109/TGRS.2011.2170177, to be published.

[20] J. T. Dall'Amico, F. Schlenz, A. Loew, and W. Mauser, "Airborne campaigns in the upper Danube catchment in the context of the calibration and validation of SMOS," presented at the ESA Living Planet Symposium 2010, Bergen, Norway, submitted for publication.

[21] M. Zribi, M. Parde, J. Boutin, P. Fanise, D. Hauser, M. Dechambre, Y. Kerr, M. Leduc-Leballeur, G. Reverdin, N. Skou, S. Sobjaerg, C. Albergel, J. C. Calvet, J. P. Wigneron, E. Lopez-Baeza, A. Rius, and J. Tenerelli, "CAROLS: A new airborne L-band radiometer for ocean surface and land observations," *Sensors*, vol. 11, no. 1, pp. 719–742, 2011.

[22] R. Panciera, J. P. Walker, J. D. Kalma, E. J. Kim, J. M. Hacker, O. Merlin, M. Berger, and N. Skou, "The NAFE'05/CoSMOS data set: Toward SMOS soil moisture retrieval, downscaling, and assimilation," *IEEE Trans. Geosci. Remote Sens.*, vol. 46, no. 3, pp. 736–745, Mar. 2008.

[23] A. K. Sahoo, P. R. Houser, C. Ferguson, E. F. Wood, P. A. Dirmeyer, and M. Kafatos, "Evaluation of AMSR-E soil moisture results using the in-situ data over the Little River Experimental Watershed, Georgia," *Remote Sens. Environ.*, vol. 112, no. 6, pp. 3142–3152, Jun. 2008.

[24] K. Y. Vinnikov, A. Robock, N. A. Speranskaya, and C. A. Schlosser, "Scales of temporal and spatial variability of midlatitude soil moisture," *J. Geophys. Res.*, vol. 101, no. D3, pp. 7163–7174, 1996.

[25] M. H. Cosh, T. J. Jackson, R. Bindlish, and J. H. Prueger, "Watershed scale temporal and spatial stability of soil moisture and its role in validating satellite estimates," *Remote Sens. Environ.*, vol. 92, no. 4, pp. 427–435, Sep. 2004.

[26] M. H. Cosh, T. J. Jackson, P. Starks, and G. Heathman, "Temporal stability of surface soil moisture in the Little Washita River watershed and its applications in satellite soil moisture product validation," *J. Hydrol.*, vol. 323, no. 1–4, pp. 168–177, May 2006.

[27] W. T. Crow, D. Ryu, and J. S. Famiglietti, "Upscaling of field-scale soil moisture measurements using distributed land surface modeling," *Adv. Water Resour.*, vol. 28, no. 1, pp. 1–14, Jan. 2005.

[28] C. Rüdiger, J.-C. Calvet, C. Gruhier, T. R. H. Holmes, R. A. M. de Jeu, and W. Wagner, "An intercomparison of ERS-scat and AMSR-E soil moisture observations with model simulations over France," *J. Hydrometeor.*, vol. 10, no. 2, pp. 431–447, Apr. 2009.

[29] C. Albergel, J. C. Calvet, P. de Rosnay, G. Balsamo, W. Wagner, S. Hasenauer, V. Naeimi, E. Martin, E. Bazile, F. Bouyssel, and J. F. Mahfouf, "Cross-evaluation of modelled and remotely sensed surface soil moisture with in situ data in southwestern France," *Hydrol. Earth Syst. Sci.*, vol. 14, no. 11, pp. 2177–2191, 2010.

[30] S. Juglea, Y. Kerr, A. Mialon, J. P. Wigneron, E. Lopez-Baeza, A. Cano, A. Albitar, C. Millan-Scheiding, M. Carmen Antolin, and S. Delwart, "Modelling soil moisture at SMOS scale by use of a SVAT model over the Valencia Anchor Station," *Hydrol. Earth Syst. Sci.*, vol. 14, no. 5, pp. 831–846, 2010.

[31] D. G. Miralles, W. T. Crow, and M. H. Cosh, "Estimating spatial sampling errors in coarse-scale soil moisture estimates derived from point-scale observations," *J. Hydrometeor.*, vol. 11, no. 6, pp. 1423–1429, Dec. 2010.

[32] A. Loew and F. Schlenz, "A dynamic approach for evaluating coarse scale satellite soil moisture products," *Hydrol. Earth Syst. Sci.*, vol. 15, no. 1, pp. 75–90, 2011.

[33] J. T. Dall'Amico, F. Schlenz, A. Loew, and W. Mauser, "Smos soil moisture validation: Status at the Upper Danube cal/val site eight months after launch," in *Proc. IEEE IGARSS*, 2010, pp. 3801–3804.

[34] G. Strasser, K. Schneider, and W. Mauser, "The use of ERS SAR data derived soil moisture distributions for SVAT-model validation," in *Proc. IEEE IGARSS*, 1999, vol. 4, pp. 1921–1923.

[35] H. Bach and W. Mauser, "Methods and examples for remote sensing data assimilation in land surface process modeling," *IEEE Trans. Geosci. Remote Sens.*, vol. 41, no. 7, pp. 1629–1637, Jul. 2003.

[36] J. T. Dall'Amico, F. Schlenz, A. Loew, and W. Mauser, "First results of SMOS soil moisture validation in the Upper Danube Catchment," *IEEE Trans. Geosci. Remote Sens.*, 2011. DOI: 10.1109/TGRS.2011.2171496, to be published.

[37] F. Schlenz, T. Gebhardt, A. Loew, and W. Mauser, "L-band radiometer experiment in the SMOS test site Upper Danube," presented at the Earth Observation Water Cycle Conf., Rome, Italy, 2009.

[38] W. Mauser and S. Schädlich, "Modelling the spatial distribution of evapotranspiration on different scales using remote sensing data," *J. Hydrol.*, vol. 212/213, pp. 250–267, Dec. 1998.

[39] R. Ludwig and W. Mauser, "Modelling catchment hydrology within a GIS based SVAT-model framework," *Hydrol. Earth Syst. Sci.*, vol. 4, no. 2, pp. 239–249, 2000.

[40] H. Bach, M. Braun, G. Lampart, and W. Mauser, "Use of remote sensing for hydrological parameterisation of Alpine catchments," *Hydrol. Earth Syst. Sci.*, vol. 7, no. 6, pp. 862–876, 2003.

[41] R. Ludwig, W. Mauser, S. Niemeyer, A. Colgan, R. Stolz, H. Escher-Vetter, M. Kuhn, M. Reichstein, J. Tenhunen, A. Kraus, M. Ludwig, M. Barth, and R. Hennicker, "Web-based modelling of energy, water and matter fluxes to support decision making in mesoscale catchments—The integrative perspective of GLOWA-Danube," *Phys. Chem. Earth*, vol. 28, no. 14/15, pp. 621–634, 2003.

[42] M. Probeck, R. Ludwig, and W. Mauser, "Fusion of NOAA-AVHRR imagery and geographical information system techniques to derive subscale land cover information for the upper Danube watershed," *Hydrol. Process.*, vol. 19, no. 12, pp. 2407–2418, Aug. 2005.

[43] A. Loew, R. Ludwig, and W. Mauser, "Derivation of surface soil moisture from ENVISAT ASAR wide swath and image mode data in agricultural areas," *IEEE Trans. Geosci. Remote Sens.*, vol. 44, no. 4, pp. 889–899, Apr. 2006.

[44] W. Mauser and H. Bach, "PROMET—Large scale distributed hydrological modelling to study the impact of climate change on the water flows of mountain watersheds," *J. Hydrol.*, vol. 376, no. 3/4, pp. 362–377, Oct. 2009.

[45] A. Loew, "Impact of surface heterogeneity on surface soil moisture retrievals from passive microwave data at the regional scale: The Upper Danube case," *Remote Sens. Environ.*, vol. 112, no. 1, pp. 231–248, Jan. 2008.

[46] *TRIME-ES Manual*, IMKO Micromodultechnik GmbH, Ettlingen, Germany, 2001.

[47] *ECHO-TE/EC-TM—Water Content, EC and Temperature Sensors—Operator's Manual*, Decagon Devices, Inc., Pullman, WA, 2008.

[48] *EC-20, EC-10, EC-5 Soil Moisture Sensors—User's Manual*, Decagon Devices, Inc., Pullman, WA, 2009.

[49] *ThetaProbe Soil Moisture Sensor, Type ML2x, User Manual, ML2x-UM-1.21, UMS Version 2004*, Delta-T Devices Ltd., Cambridge, U.K., 2004.

[50] G. C. Topp and T. P. Ferre, "Measuring soil water content," in *Encyclopedia of Hydrological Sciences*, vol. 2, M. G. Anderson, Ed. Chichester, U.K.: Wiley, 2005, pp. 1077–1088.

[51] N. Skou, S. Misra, J. E. Balling, S. S. Kristensen, and S. S. Sobjaerg, "L-band RFI as experienced during airborne campaigns in preparation for SMOS," *IEEE Trans. Geosci. Remote Sens.*, vol. 48, no. 3, pp. 1398–1407, Mar. 2010.

[52] M. Parde, M. Zribi, P. Fanise, and M. Dechambre, "Analysis of RFI issue using the CAROLS L-band experiment," *IEEE Trans. Geosci. Remote Sens.*, vol. 49, no. 3, pp. 1063–1070, Mar. 2011.

[53] J. P. Wigneron, Y. Kerr, P. Waldteufel, K. Saleh, M. J. Escorihuela, P. Richaume, P. Ferrazzoli, P. de Rosnay, R. Gurney, J. C. Calvet, J. P. Grant, M. Guglielmetti, B. Hornbuckle, C. Mätzler, T. Pellarin, and M. Schwank, "L-band Microwave Emission of the Biosphere (L-MEB) model: Description and calibration against experimental data sets over crop fields," *Remote Sens. Environ.*, vol. 107, no. 4, pp. 639–655, Apr. 2007.

[54] J. Philip, "The theory of infiltration: 1. The infiltration equation and its solution," *Soil Sci.*, vol. 83, pp. 345–357, 1957.

[55] R. Brooks and A. Corey, "Hydraulic properties of porous media," Colorado State Univ., Fort Collins, CO, Tech. Rep., Hydrology paper 3, 1964.

[56] U. Strasser and W. Mauser, "Modelling the spatial and temporal variations of the water balance for the Weser catchment 1965–1994," *J. Hydrol.*, vol. 254, no. 1–4, pp. 199–214, Dec. 2001.

[57] V. R. N. Pauwels, W. Timmermans, and A. Loew, "Comparison of the estimated water and energy budgets of a large winter wheat field during AgriSAR 2006 by multiple sensors and models," *J. Hydrol.*, vol. 349, no. 3/4, pp. 425–440, Feb. 2008.

[58] C. Mätzler, *Thermal Microwave Radiation. Applications for Remote Sensing*. London, U.K.: Inst. Eng. Technol., 2006.

[59] I. H. Woodhouse, *Introduction to Microwave Remote Sensing*. London, U.K.: Taylor & Francis, 2006.

[60] R. Panciera, J. P. Walker, J. D. Kalma, E. J. Kim, K. Saleh, and J.-P. Wigneron, "Evaluation of the SMOS L-MEB passive microwave soil moisture retrieval algorithm," *Remote Sens. Environ.*, vol. 113, no. 2, pp. 435–444, Feb. 2009.

[61] K. Saleh, Y. H. Kerr, P. Richaume, M. J. Escorihuela, R. Panciera, S. Delwart, G. Boulet, P. Maisongrande, J. P. Walker, P. Wursteisen, and J. P. Wigneron, "Soil moisture retrievals at L-band using a two-step inversion approach (COSMOS/NAFE'05 Experiment)," *Remote Sens. Environ.*, vol. 113, no. 6, pp. 1304–1312, Jun. 2009.

[62] K. Saleh, J. P. Wigneron, P. Waldteufel, P. de Rosnay, M. Schwank, J. C. Calvet, and Y. H. Kerr, "Estimates of surface soil moisture under

grass covers using L-band radiometry," *Remote Sens. Environ.*, vol. 109, no. 1, pp. 42–53, Jul. 2007.

[63] J. P. Grant, J. P. Wigneron, A. A. Van de Griend, A. Kruszewski, S. S. Søbjærg, and N. Skou, "A field experiment on microwave forest radiometry: L-band signal behaviour for varying conditions of surface wetness," *Remote Sens. Environ.*, vol. 109, no. 1, pp. 10–19, Jul. 2007.

[64] F. Schlenz, A. Loew, J. T. Dall'Amico, and W. Mauser, "SMOS rehearsal campaign 2008: Data analysis and soil moisture retrieval at the Upper Danube test site," presented at the Earth Observation Water Cycle Conf., Rome, Italy, 2009.

[65] J. P. Wigneron, A. Chanzy, Y. H. Kerr, H. Lawrence, J. Shi, M. J. Escorihuela, V. Mironov, A. Mialon, F. Demontoux, P. de Rosnay, and K. Saleh-Contell, "Evaluating an improved parameterization of the soil emission in L-MEB," *IEEE Trans. Geosci. Remote Sens.*, vol. 49, no. 4, pp. 1177–1189, Apr. 2011.

[66] R. Panciera, J. P. Walker, and O. Merlin, "Improved understanding of soil surface roughness parameterization for L-band passive microwave soil moisture retrieval," *IEEE Geosci. Remote Sens. Lett.*, vol. 6, no. 4, pp. 625–629, Oct. 2009.

Florian Schlenz (M'08) was born in Forchheim, Germany, 1980. He received the Diplom degree in physical geography with remote sensing and computer science from the University of Munich, Munich, Germany, in 2007.

He has been with the Department of Geography, University of Munich, since 2007, and works as a researcher on the project SMOSHYD (Integrative analysis of SMOS soil moisture data) which aims at the calibration and validation of SMOS data in the Upper Danube Catchment as well as at the study of scaling issues. His research interests include hydrological and radiative transfer modeling as well as airborne and satellite-based remote sensing of soil moisture, including the analysis of field data and passive microwave radiometer data.

Mr. Schlenz is a member of the European Geosciences Union.

Johanna T. dall'Amico received the B.Sc. degree in mathematics from the University of Reading, Reading, U.K., in 2007 and the Diplom degree in geography with remote sensing and mathematics from the University of Munich, Munich, Germany, in 2008. She is currently working toward the Ph.D. degree at the Department of Geography, University of Munich. In 2005, she was a visiting student at the Natural Environment Research Council Environmental Systems Science Centre in Reading, U.K., working on remote sensing applications for fluvial flood mapping and modeling.

Since 2007, she has been with the University of Munich, working on the project SMOSHYD (Integrative analysis of SMOS soil moisture data) which aims at the calibration and validation of SMOS data in the Upper Danube Catchment as well as at the study of scaling issues. Therefore, her current research interests include airborne and satellite remote sensing of soil moisture and its spatial variability, including the analysis of ground data as well as ancillary remote sensing data.

Alexander Loew (M'04) received the M.S. and the Ph.D. degrees in geography from University of Munich (LMU), Munich, Germany in 2001 and 2004, respectively.

From 2001 to 2008, he was a PostDoc with the LMU, working on the retrieval of bio- and geophysical parameters from microwave remote sensing data. In 2007, he was a Visiting Scientist with the NASA Goddard Space Flight Center, Greenbelt, MD. In 2009, he joined the Max Planck Institute for Meteorology, Hamburg, Germany. Currently, he is leading a research group on Terrestrial Global Remote Sensing, focusing on global-scale remote sensing for climate studies. His research interests include the quantitative retrieval of geophysical parameters from remote sensing data, the development of image processing algorithms, coupling of land surface process models with microwave scattering and emission models, and the development of land surface process models and data assimilation techniques. He is an editor for *Hydrology and Earth System Science* and acts as a Reviewer for several national and international journals.

Wolfram Mauser (M'92) was born in Innsbruck, Austria, in 1955. He received the M.S. degrees in experimental physics and geography/hydrology and the Ph.D. degree in hydrology from the University of Freiburg, Freiburg, Germany, in 1979, 1981, and 1984, respectively.

In 1981, he worked with the University of Maryland, College Park and the Goddard Space Flight Center, Greenbelt, MD, in the field of remote sensing and hydrology. From 1984 to 1991, he was an Assistant Professor with the Department of Hydrology, Institute for Physical Geography, University of Freiburg. In 1991, he was appointed Full Professor for geography and geographical remote sensing, Department of Geography, University of Munich, Germany. From 2003 to 2009, he was Chairman of the German National Committee for Global Change Research. He has been working in the field of remote sensing and hydrology within the major European research programs. He was appointed Principal Investigator (PI) by the European Space Agency (ESA) for its ERS-1, ERS-2, and ENVISAT program and is PI for the Shuttle Radar Topography Mission and Soil Moisture and Ocean Salinity mission. He was member of ESA's Mission Advisory Group of the Earth Explorer Surface Processes and Ecosystem Changes Through Response Analysis Mission. He took part in the MAC-Europe, E-MAC, and DAISEX-campaign. His special research interest is the development and validation of spatially distributed land surface processes models and image processing algorithms as well as model assimilation procedures for microwave and hyperspectral optical data.

Publication 2

Schlenz, F., Fallmann, J., Marzahn, P., Loew, A., and Mauser, W.: Characterization of Rape Field Microwave Emission and Implications to Surface Soil Moisture Retrievals, Remote Sensing, 4, 247-270, 2012. (published online: http://www.mdpi.com/2072-4292/4/1/247/)

Article

Characterization of Rape Field Microwave Emission and Implications to Surface Soil Moisture Retrievals

Florian Schlenz [1,*]**, Joachim Fallmann** [2]**, Philip Marzahn** [1]**, Alexander Loew** [3] **and Wolfram Mauser** [1]

[1] Department of Geography, University of Munich, Luisenstr. 37, D-80333 Munich, Germany;
     E-Mails: p.marzahn@iggf.geo.uni-muenchen.de (P.M.); w.mauser@lmu.de (W.M.)

[2] Institute of Meteorology and Climate Research, Karlsruhe Institute of Technology,
     D-82467 Garmisch-Partenkirchen, Germany; E-Mail: joachim.fallmann@kit.edu

[3] Max-Planck-Institute for Meteorology, KlimaCampus, D-20146 Hamburg, Germany;
     E-Mail: alexander.loew@zmaw.de

* Author to whom correspondence should be addressed; Tel.: +49-89-2180-6695;
     Fax: +49-89-2180-6675; E-Mail: f.schlenz@iggf.geo.uni-muenchen.de.

Abstract: In the course of Soil Moisture and Ocean Salinity (SMOS) mission calibration and validation activities, a ground based L-band radiometer ELBARA II was situated at the test site Puch in Southern Germany in the Upper Danube Catchment. The experiment is described and the different data sets acquired are presented. The L-band microwave emission of the biosphere (L-MEB) model that is also used in the SMOS L2 soil moisture algorithm is used to simulate the microwave emission of a winter oilseed rape field in Puch that was also observed by the radiometer. As there is a lack of a rape parameterization for L-MEB the SMOS default parameters for crops are used in a first step which does not lead to satisfying modeling results. Therefore, a new parameterization for L-MEB is developed that allows us to model the microwave emission of a winter oilseed rape field at the test site with better results. The soil moisture retrieval performance of the new parameterization is assessed in different retrieval configurations and the results are discussed. To allow satisfying results, the periods before and after winter have to be modeled with different parameter sets as the vegetation behavior is very different during these two development stages. With the new parameterization it is possible to retrieve soil moisture from multiangular brightness temperature data with a root mean squared error around

0.045–0.051 m³/m³ in a two parameter retrieval with soil moisture and roughness parameter H_r as free parameters.

Keywords: passive microwave remote sensing; radiometry; L-band; soil moisture; roughness; Soil Moisture and Ocean Salinity (SMOS); L-MEB

1. Introduction

Controlling the energy- and mass exchanges between the Earth's surface and the atmosphere, the water content of the upper soil layer plays an important role within the global, regional and local water cycle and thus, the global climate system. Evaporation rates, surface runoff, infiltration as well as plant growth and photosynthetic activity are controlled by the water content of the soil [1,2]. Observations of soil moisture serve as input for numerical weather and climate prediction models and are needed for hydrologic modeling, flood and drought monitoring and other water and energy cycle applications [2,3].

Several remote sensing techniques have been tested for measuring variations of soil moisture on different scales [4–7]. Amongst these, passive microwave systems have proven to be very promising as this technique benefits from being almost independent from solar radiation and weather conditions. Microwave emissions show a direct relationship to soil moisture through the soil's dielectric constant and have a sensitivity to land surface roughness and vegetation cover [8].

At L-Band (21 cm, 1.4 GHz), soil moisture in the first centimeters of the soil has a significant impact on the emitted brightness temperature T_B (about 2 K per 0.01 [m³/m³] over bare soil [2]). The SMOS (Soil Moisture and Ocean Salinity) mission (launched in 2009) was designed to measure soil moisture and ocean salinity from space with a repetition rate of 1–3 days and a spatial resolution of 35–50 km with the unique MIRAS (microwave imaging radiometer with aperture synthesis) 2D interferometric L-band radiometer (1.4 GHz) [2]. Through the exceptional measurement technique it is possible to separate vegetation- and soil moisture dynamics through multiangular (0° to 55°) brightness temperature measurements [2].

To investigate passive microwave remote sensing of soil moisture under different canopy types, a variety of campaigns with ground- or aircraft-based L-Band radiometers were carried out in the past [9]. These experiments are being used to develop, improve and calibrate radiative transfer modeling which is essential for soil moisture retrieval from passive microwave data. In preparation for the SMOS mission, several dedicated ground radiometer experiments were conducted. Examples for these experiments are the long term radiometer field experiment SMOSREX [10] that is carried out over bare and vegetated soil near Toulouse in South France with the (LEWIS) L-Band radiometer and the Bray 2004 experiment in the Les Landes forest near Bordeaux [11]. Further Schwank *et al.* performed a L-Band radiometer experiment at the test site Eschikon near Zurich, Switzerland for clover grass in 2007 [12] as well as in 2004 over a freezing soil [13] which was successfully used for the parameterization and assimilation into a hydrological model [14,15]. Wigneron *et al.* [9] gives an overview about the L-Band radiometer experiments that have been used for the development of the radiative transfer model used in the SMOS L2 soil moisture processor. A new generation of L-Band

radiometers are the ELBARA II radiometers (ETH L-Band Radiometer 2nd generation) that are used throughout Europe for dedicated studies in the SMOS context [16]. Examples are the experiments in Valencia, Spain [17], Sodankyla, Finland [18], Grenoble, France and Puch near Munich, Germany [19].

It is the scope of this paper to describe the experiment carried out in Puch in Southern Germany as well as describe the microwave emission of winter oilseed rape as measured in Puch and establish a parameterization that allows modeling the brightness temperature with the radiative transfer model L-MEB that is also used in the SMOS L2 soil moisture processor. The soil moisture retrieval capabilities of L-MEB over winter oilseed rape are assessed.

Although many microwave emission experiments with different vegetation types have taken place in the past, there is no study to the author's knowledge about winter oilseed rape, consequently no parameters are known for representing it in L-MEB. In Germany, rape was one of the three most important crops grown in 2010. With around 155,000 ha, rape plays an important role within the renewable energy sector because it serves as basis for alternative energy- and industrial-production [20]. Therefore it should be of interest how that crop behaves in radiative transfer modeling.

In Section 2, the field experiment is described according to geographical location of the test site and data sets being used in the present study. The following Section 3 elaborates on the model L-MEB and how it is being used. Section 4 presents the results of the microwave emission modeling and the soil moisture retrieval capabilities of the model for the land use winter oilseed rape. A discussion of the results as well as a conclusion is added to complete the paper.

2. Field Experiment

2.1. Test Site

In the course of SMOS cal/val activities, one of the passive microwave radiometers ELBARA II was installed on a well instrumented experimental farm of the Bavarian State Research Center for Agriculture (LfL) in Puch, about 30 km west of Munich in Southern Germany in the center of the SMOS test site Upper Danube [19,21,22] (Figure 1). The intention of the experiment was to measure brightness temperatures (TB) constantly over two vegetative surfaces: grassland and farmland, which was in this case cultivated with winter oilseed rape. Extensive ancillary environmental data have been collected in addition to constant measuring stations.

The location of the radiometer has the geographical coordinates 11.2136°E and 48.1845°N and it is 556 m a.s.l. [19]. It is situated in the temperate latitudes of Central Europe within the region of the northern Alpine foreland. The climate can be described as temperate humid with a maximum of precipitation during summer [23]. The soil type was classified as sandy loam with a sand content of 22% and a clay content of 6% and a bulk soil density of 1.2 g/cm³. The radiometer test site is surrounded by a flat agricultural area. At the border of two fields of different land use (grassland and farmland), the passive microwave radiometer ELBARA II had been installed on a scaffolding of 4 m in such a way that it was possible to rotate the radiometer in order to measure over two types of land use. Due to technical restraints the viewing angles over the two fields could only be varied between 50° and 70°. Schwank *et al.* [16] give a detailed overview of the technical details of the radiometer. In the surroundings of the radiometer, ground measurements (vegetation height, leaf area index (LAI),

phenology, vegetation water content (VWC), soil roughness, soil moisture, snow parameters) were conducted on a regular basis and continuous hourly measurement stations of soil moisture and soil temperature were set up. Data of the meteorological station of the Bavarian State Research Center for Agriculture next to the radiometer were used for completing the data set.

Figure 1. The Upper Danube catchment in Europe; the radiometer test site is marked with a circle.
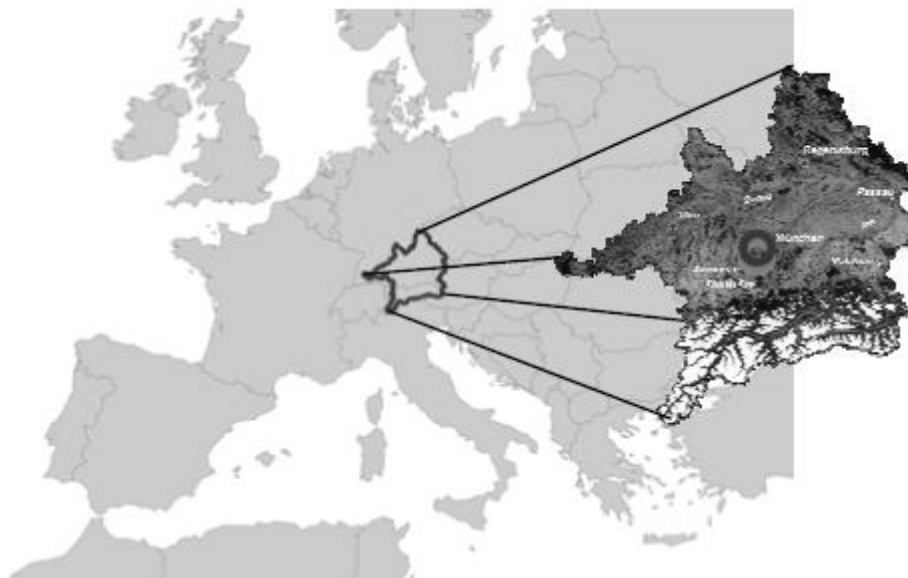
Figure 2 shows the radiometer ELBARA II with angle of aperture α and incidence angle θ and the location of ground truth measurements.

Figure 2. Radiometer ELBARA II with angle of aperture α, incidence angle θ and the two halfaxes a and b of the elliptical footprint on the left; location of ground measurements (LAI and handheld soil moisture (FDR) inside the field of view (FOV), vegetation water content (VWC) outside the FOV; soil moisture and soil temperature stations for both fields are located to the right of the radiometer, the meteorological station to the left of the radiometer.
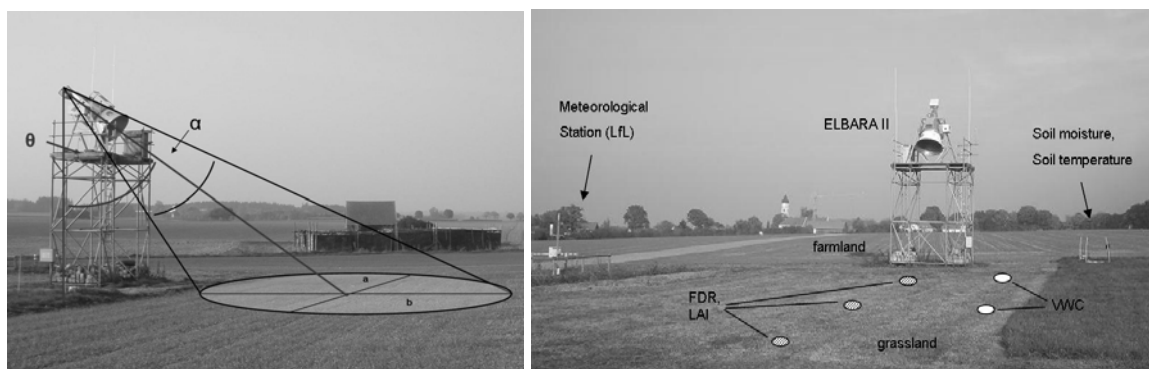
2.2. Measurements

All ground measurements were collected from 1 October 2009 until 14 July 2010. The period of 287 days is approximately the duration of the vegetation period of winter oilseed rape at the location

Puch. Days with snow cover or frozen ground were removed from the data sets for the current analysis. In addition to these gaps some technical problems resulted in data loss which extended the data gaps in winter. All measurements related to soil moisture and vegetation characteristics were carried out on a weekly basis if the weather conditions permitted it.

2.2.1. Meteorological and Soil Moisture Measurements

From the start of the experiment in October 2009 to July 2010 the mean temperature measured 2 m above the soil surface was 9.3 °C. The total precipitation during the campaign was 599.5 mm, with a maximum daily rain event on 2 June 2010 of 28.8 mm·d^{-1}.

Soil moisture and soil temperature stations at two locations (farmland and grassland) next to the radiometer tower were installed at the beginning of the campaign to record the development of soil moisture and soil temperature profiles. Soil water content and temperatures were measured hourly with horizontally installed IMKO Trime-TDR (time domain reflectometry) probes in several depths (5, 10, 20 and 40 cm for soil moisture and 2, 5 and 50 cm for soil temperature). For quality control of the station measurements, handheld measurements of soil water content were conducted on a weekly basis at the stations and inside the field of view (FOV) of the radiometer at three sampling points. As the station measurements seem very reliable they are considered representative for the radiometer FOV. Figure 3 shows the development of the measured surface soil moisture and the precipitation throughout the study period.

Figure 3. Daily soil moisture measured at a depth of 5 cm and precipitation as daily sum for the whole campaign period; the data gaps are due to technical problems during winter-time.
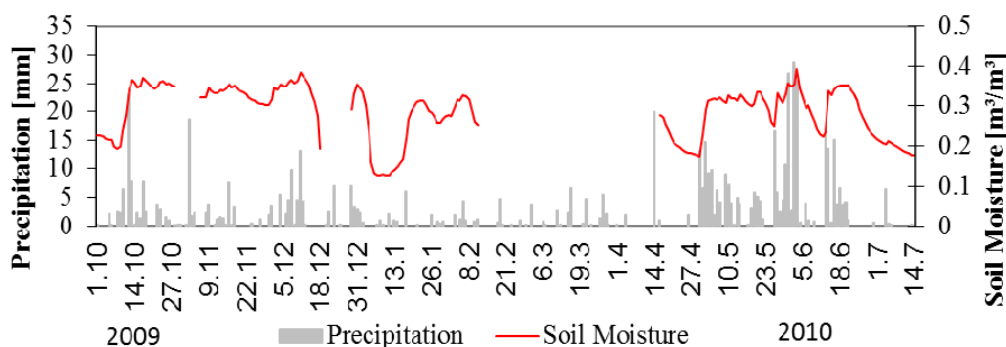
2.2.2. Vegetation Measurements

The vegetation on the farmland area that is subject of this study was winter oilseed rape (brassica napus), sowing is dated to 21 August 2009. About 30 days after seeding, the first sprouts became visible. During presence of vegetation, the LAI was measured using a LAICOR LAI-2000 [24], the vegetation water content [kg·m^{-2}] was measured through destructive measurements. The LAI and vegetation height were measured at the sampling points inside and outside the FOV while the vegetation water content was only measured outside the FOV in order to not disturb the radiometer measurements (Figure 3). The development of the LAI as well as the VWC is shown in Figure 4.

Figure 4. Development of vegetation water content and leaf area index for the duration of the experiment.
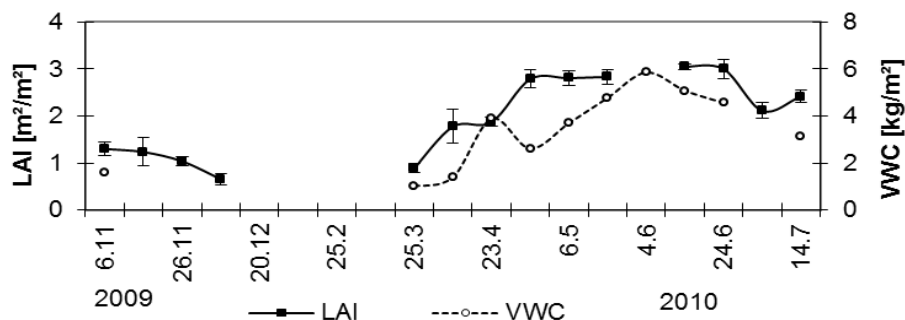
The vegetation height ranged from 15 cm in the beginning of November 2009 to 135 cm at the end of the growing period mid of July 2010. The LAI increased from 1.5 to 3 m^2/m^2 and the water content from 0.5 to approx. 6 kg/m^2. The correlation of LAI and VWC gives an R^2 of 0.77 and a regression function of $VWC = 1.571 \times LAI - 0.320$.

The typical vegetation development of winter rape as described in [25] was confirmed by the measurements of vegetation height, LAI, VWC and observations of phenology. After emergence of the first plants in autumn, the three parameters: height, LAI and VWC increased until the daily mean temperature fell below a value of 5 °C. With this temperature the first plants start to degenerate, until the beginning of winter period, with nearly no 'vital vegetation' left (see Figure 5). This effect also shows in rape leaves turning brown during winter. The snow layer during winter protected the plants from frost. During snow cover the maximum snow height reached 17cm at the beginning of February.

Figure 5. Photographs of the winter rape canopy demonstrating stages of phenology at the beginning of October (top left), middle of November(top centre) and middle of December (top right) as well as May (bottom left) and July (bottom right).

With the end of winter, the former horizontally oriented leaves then turned to vertical growth with the formation of branches until the canopy reached its maximum height. With the end of the growing period, the plants lost most of their leaves, only the pods remained. The winter break naturally divides the vegetation growth into two periods with very different appearance of the plants.

The vegetation grew with a rate of about 0.87 cm day^{-1} from 40 to 140 cm, during the main growing period of 92 days from 25 March until 24 June 2010. The density of dry-matter increased with

approximately 44 g·m^{-2}·d^{-1} during the same time.

2.2.3. Surface Roughness Measurements

A photogrammetric approach was chosen for roughness measurements at the test site due to its 3 dimensional output and highly accurate estimates [26]. For sampling soil surface roughness, a rectangular scaffold with the dimensions of 1 × 2.5 m^2 was laid onto the ground and used as a reference frame for the orientation of the image block. As the sample plots were entirely covered by vegetation during the test period, all the plants in the sampling area were cut off and removed without disturbing the soil surface. Highly precise ground control points (GCP) attached to the scaffold made it possible, to generate a digital elevation model (DEM) out of overlapping photos shot from around 2.5 m height by using image matching techniques. More detailed information of the measurement technique is given in [27]. Figure 6 shows an example of one DEM with heights in cm and relative to the lower edge of the scaffold containing a tractor track (this one was not used in the current study as it is not representative for the radiometer FOV). From the DEM it was possible to calculate the RMS-Height s (standard deviation of height) [cm] for the entire area, which gives a direct information on the (vertical) roughness condition [28,29].

As [30] was able to establish a clear relationship between s and H$_r$ but obtained no improvement in the parameterization of H$_r$ by using additional information like the autocorrelation length, s is the only parameter considered in this study.

Figure 6. Digital elevation model of a roughness measurement performed in October 2009, clearly visible is the tractor track on the right. The heights are relative to the lower edge of the scaffold.

2.0
Height [cm]
-10.5
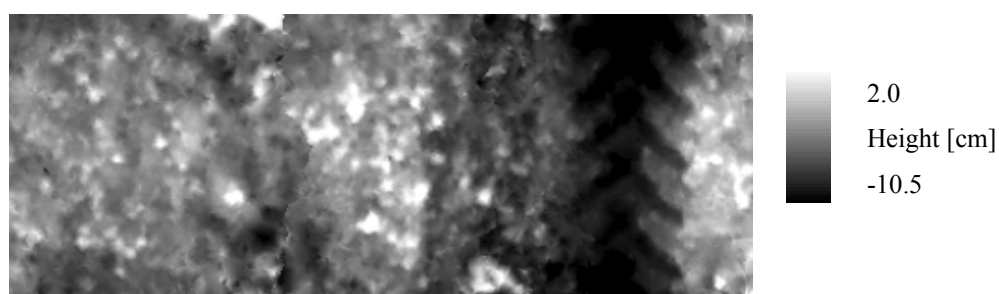
Roughness measurements were conducted in September 2009, March and September 2010. The results from the roughness measurements are listed in Table 1. The value s describes the standard deviation of surface heights related to the lower edge of the scaffold in cm. At three locations within the field roughness measurements were taken near the radiometer FOV and then averaged.

Table 1. Results from the roughness measurements.

Time	s [cm]
September 2009	1.161
March 2010	1.005
September 2010	1.312

s varies from 1.0 to 1.3 cm in the course of the measurement period which is not considered a

significant change in roughness. As expected the roughness decreased slightly during winter (from September to March).

2.2.4. Ground Based Radiometer

The microwave radiometer ELBARA II operating at 1.4 GHz was designed for remote sensing at the field scale to detect emissivities of different surface types and conditions in a passive manner. ELBARA is a DICKE-radiometer, equipped with a dual-polarized conical horn antenna with −3 dB full beam width of 12° and symmetrical and identical beams with small side lobes [12]. By applying this technology it is possible to determine the horizontal and vertical polarization component of the upwelling electromagnetic radiation. Internal hot and cold loads stabilized at 338 and 278 K attend every measurement for calibration. To detect man-made EM noise, the radiometer works simultaneously at two overlapping channels, one between 1,400 and 1,418 MHz and the other between 1,409 and 1,427 MHz [12]. The footprint dimension (Table 2) varies with incidence angle θ, which reaches from 50° to 70° with an increment of 5° and sky measurements at 140° (for calibration). The angle of the aperture is α = 6.5°. The width and length of the elliptic footprint were calculated based on the −3 dB beamwidth, the installation height and the incidence angle [12].

Table 2. Footprint dimensions of the elliptic 3 dB footprint at incidence angle θ.

Incidence Angle [°]	FOV Length [m]	FOV Width [m]	FOV Area [m²]
50	10.41	4.78	38.92
55	12.04	5.2	49.19
60	13.82	6.82	74.06
65	21.51	7.46	125.74
70	41.91	10.32	340.41

For the analysis of the radiometer data only the angles 50–65° were used, because of the increasing fraction of sky radiance detected at angles above 65° [12]. Systematic errors were corrected by referring all the temperatures to the measured zenith temperatures T^p_{zenith} (p = h,v) [12]. For each incidence angle 2 measurements per hour were performed. Figure 7 shows the evolution of brightness temperatures over the experiment period for two angles and both horizontal and vertical polarizations.

Figure 7. Measured ELBARA brightness temperatures (TB) for angle 50° (left) and 65° (right) for both vertical and horizontal polarization.
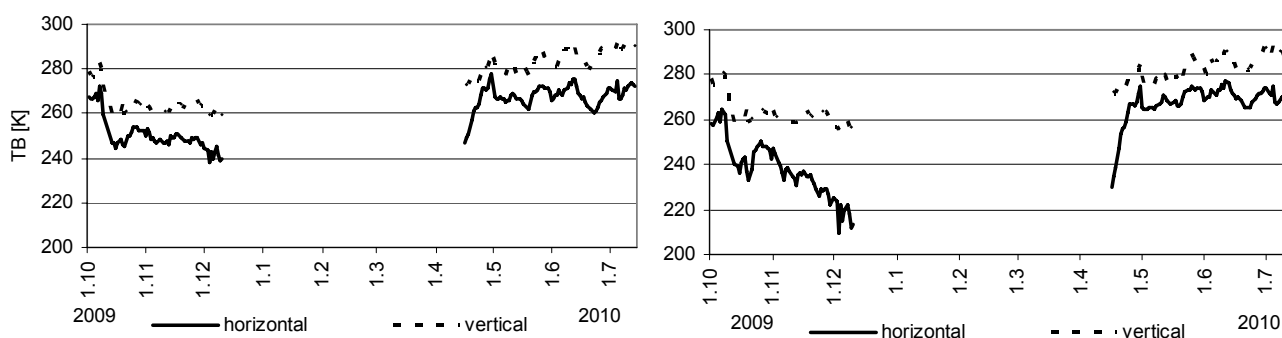
The data gap is due to technical problems during the freezing period. Because of the direct relationship between emission of radiation and water content of the soil, strongly connected to the dielectric properties, the radiometer signal reacts inversely to the development of soil moisture [31] as can be seen in Figure 8.

Figure 8. Development of TB and soil moisture in 5 cm depth – 50°, horizontal polarisation.
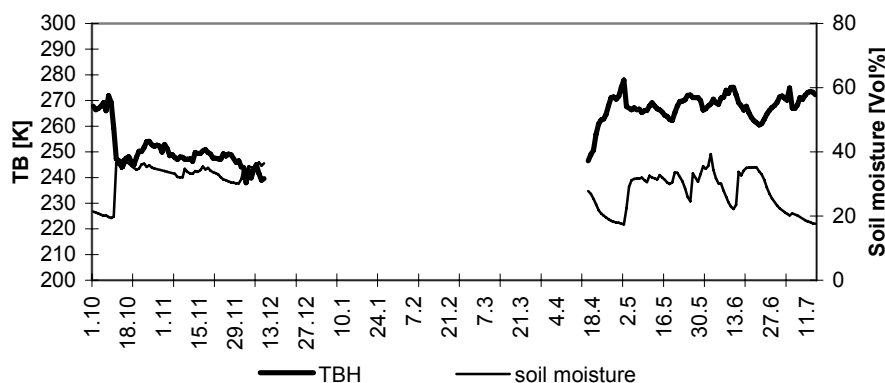
Next to the radiometer horn, thermal infrared measurements were performed with the IR radiometer Everest Interscience 4,000.4 ZH. This device is sensitive in the spectral range from 8 to 15 μm, the temperature range is 243–1,033 K and the accuracy is ±1% of reading [12]. These measurements were used for constantly detecting the physical temperature of the soil surface the radiometer is pointed at.

3. Model and Methods

3.1. Microwave Radiative Transfer Model

The microwave radiative transfer model L-MEB (**L-Band M**icrowave **E**mission of the **B**iosphere) is used in this study to simulate the microwave emission of a vegetated surface at L-Band. A detailed description of the model physics is provided by [9], therefore only a brief overview is given here.

The basis of L-MEB is the Tau (τ)-Omega (ω) model [9], which simulates the overall brightness temperature TB of a natural surface. This simple radiative transfer model uses two parameters to characterize the land surface: the vegetation optical depth τ and the single scattering albedo ω. They are used to parameterize vegetation attenuation and scattering effects. In several studies, the τ-ω-model has usually been found to be an accurate approach to model the L-Band emission from a vegetation canopy [9].

Using that model, the overall emission from a two layer medium (soil and vegetation) is for each polarization (horizontal and vertical) the sum of the three terms soil emission attenuated (scattered and absorbed) by the vegetation layer, direct vegetation emission and vegetation emission reflected by the soil and attenuated again by the vegetation. It results in a polarized (p = h,v) brightness temperature (TB_P):

$$TB_P = (1 - \omega_p)\,(1 - \gamma_p)\,(1 + \gamma_p\,r_{Gp})\,T_C + (1 - r_{Gp})\,\gamma_p\,T_G \tag{1}$$

where T_C and T_G are the vegetation and the effective soil temperatures, r_{Gp} is the soil reflectivity, γ_p the vegetation attenuation factor, expressed by the vegetation optical depth and ω_p the vegetation single scattering albedo [9].

The effective temperature of the soil is composed of a contribution of signals from different soil layers in different depths. According to the sensing depth variation with soil moisture content, the soil moisture is also taken into account here [32]. Thus in L-MEB the following equation is used to parameterize T_G:

$$T_G = T_{Deep} + C_t (T_{Surf} - T_{Deep}) \tag{2}$$

T_{Deep} here refers to the temperature at 50 cm and T_{Surf} to the temperature at 2 cm depth. Note, that Equation (2) neglects multiple scattering effects within the soil layer [9]. The higher the soil moisture is, the smaller is the depth, the radiation signal originates from [12]. Accounting for this effect, Wigneron *et al.* [9] changed Equation (2), parameterizing the factor C as function of soil moisture as follows:

$$C_t = (SM/w_0)^{bw0} \tag{3}$$

where SM is the soil moisture in a depth of 5cm, which has a strong influence on emission characteristics of a surface. W_0 and bw_0 are semi-empirical parameters according to textural properties. Wigneron *et al.* [9] use the values $w_0 = 0.3$ m³/m³ and $bw_0 = 0.3$ as default values in L-MEB.

The reflectivity r_{Gp} at the soil/atmosphere interface is dependent upon the dielectric properties of the soil, originating from the dielectric roughness that depends on soil moisture, temperature, salinity, texture and geometrical roughness [16]. Referring to [33], the dielectric roughness is a function of the dielectric permittivity ε_S and of surface roughness effects. For the lower frequency range (1–20 GHz), several models have been developed to relate ε_S to soil parameters such as moisture, bulk density or proportion of sand and clay. In L-MEB the model of DOBSON [34] or MIRONOV [35] is used to calculate ε_S. Freezing also affects ε_S seriously, but is not accounted for within this study [33].

In L-MEB the geometrical roughness is expressed through the parameters H_r (mean roughness), $N_{H,V}$ (polarization dependent roughness), and Q_R (frequency dependent roughness). The latter has no influence in the region of 1.4 GHz and thus is set to zero in L-MEB [30]. According to [30], there is an exponential relation between the standard deviation of heights of the soil surface s and H_r. According to that functional relation, for the case of the Puch experiment, the measured s in the field would correspond to a roughness parameter H_r of approximately 0.5.

In the L-Band the scattering effects, represented by the single scattering albedo ω_p (where the subscript P stands for polarization) are generally found in the literature to be low. For most low vegetation types, ω_p is below 0.05 [9]. The vegetation attenuation factor γ_p is mainly expressed by the vegetation optical depth τ_p through the equation

$$\gamma_p = \exp(-\tau_p/\cos\theta) \tag{4}$$

with τ_p as vegetation optical depth and θ as incidence angle. As presented in the following, τ_p is expressed as a function of the overall vegetation optical depth at nadir ($\theta = 0°$).

τ_p is generally found to be linearly related to the total vegetation water content VWC [kg/m²], using the b-parameter. For calculation of the vegetation optical depth through $\tau = b \times VWC$, a value of $b = 0.12 \pm 0.03$ was found to be representative for most agricultural crops.

Some results of previous studies showed a strong relationship between vegetation optical depth and LAI. Through this, and because of the relationship between LAI and VWC ($R^2 = 0.95$ for fallow at SMOSREX [10]), it is possible to calculate the vegetation optical depth from LAI through the linear equation:

$$\tau = b_1 \times \text{LAI} + b_2 \tag{5}$$

Although the calculation of the vegetation optical depth with the water content is assumed to be more stable, in this study we decided to retrieve τ from the LAI because the LAI can be derived on the global scale from satellite data which is important for the global application of SMOS.

3.2. Methods

Due to the lack of L-MEB parameterizations for rape in a first step the brightness temperature modeling ability of L-MEB over winter oilseed rape was tested by using the SMOS default parameters for Central European crops to parameterize L-MEB and compare the simulated with measured brightness temperatures. After that it was tried to develop a better L-MEB parameterization for the land use winter oilseed rape. In order to do that, a sensitivity study was conducted to find the parameters with the most pronounced effect on the modeling. Next, different parameter retrievals are performed to estimate the L-MEB parameters needed for a proper modeling. In the end, the soil moisture retrieval capabilities of the new parameterization are assessed.

To test the suitability of the SMOS default parameters for Central European crops that are also used in the SMOS L2 soil moisture retrieval algorithm (Table 3) [36] for the radiative transfer modeling over winter oilseed rape, L-MEB was used with the default parameters to model the brightness temperatures in a simple forward modeling approach. The results are compared with the measured brightness temperatures from the radiometer ELBARA II. To enable a comparison with other retrievals carried out later, L-MEB is also used to assess the soil moisture retrieval performance of the default parameters in a one parameter retrieval. The parameters in Table 3 correspond to the default values as described in [36] that are in accordance with the operational version of the SMOS L2 soil moisture processor. As the H_r value is implemented as a piecewise function of soil moisture in the SMOS L2 soil moisture processor, the H_r value in Table 3 corresponds to the maximum value of H_r that is being used in the processor.

Table 3. The different parameterizations used for L-band microwave emission of the biosphere (L-MEB) in this study. The first one corresponds to the Soil Moisture and Ocean Salinity (SMOS)   default parameterization for Central European Crops, the other two have been developed within this study for the period before (early period) and after winter (late period).

Parameter	w0/bw0	tth/ttv	ωh/ωv	H_r	N_H	Nv	Q_r	b_1	b_2	b
SMOS default	0.3/0.3	1/1	0/0	0.1	2	0	0	0.06	0	-
Early period	0.3/0.3	1/1	0.07/0	0.71	0	−1	0	0.12	0.08	-
Late period	0.3/0.3	1/1	0/0	0.93	0	−1	0	0.09	0.08	0.07

The above mentioned continuous soil moisture measurements in 5 cm depth and the soil temperature measurements in 2 cm and 50 cm depth were used as input for the model together with the LAI measurements that were interpolated. The soil parameters and the air temperature that are needed for the modeling were also taken from the measurements described above.

To analyze which parameters affected the modeling result the most for our experiment, a sensitivity study was performed. Within this study, all the parameters mentioned above, were tested for their

sensitivity to the modeling results in the forward modeling approach described above. As a result, the b-parameters controlling the vegetation optical depth τ, H_r characterizing the surface roughness and the single scattering albedo ω (only valid for the first period of the experiment) had a considerable impact on the modeling result. All the other parameters remained 'default' for the entire experiment.

Because of the afore mentioned structural difference of winter rape in early and late growing period which leads to a very different vegetation behavior at L-Band, the study handles the part before and after winter break separately. Due to data gaps in the radiometer data the winter break extends into April. The first period in 2009 is 71 days long and contains 39 vegetation days (mean-temperature >5 °C) while the second period in 2010 is 90 days long and contains 90 vegetation days.

The procedure for finding the best possible L-MEB parameterization for winter oilseed rape at the specific test site Puch was basically the same for both periods, with different results in each case. An iterative inversion approach was used to retrieve different combinations of L-MEB parameters from the multiangular ELBARA II measurements using different ground data sets as input. The procedure is outlined in the following:

At first a three parameter (3P)-retrieval is conducted with soil moisture, vegetation optical depth and roughness as free parameters while measured soil temperatures are used as input to L-MEB. The result is analysed and the retrieved parameters are compared to the ground measurements. Especially the relationship between measured LAI and VWC and retrieved vegetation optical depth as well as the relationship between retrieved roughness and measured roughness are investigated.

To establish a relationship between the retrieved vegetation optical depth and the measured LAI and VWC the b-parameters for this relationship were estimated by establishing a linear regression between measured LAI and VWC and the retrieved vegetation optical depth (see Equation (5)).

It is assumed that the new b-parameters and the mean value of the retrieved roughness parameter H_r can be treated as a possible new parameterization for L-MEB over winter oilseed rape in Puch. In the following steps this new parameterization is assessed.

The retrieved vegetation optical depth is compared to a calculated vegetation optical depth using the new b-parameters and interpolated values of measured LAI and VWC to see how well the new b-parameters are able to reproduce the retrieved vegetation optical depth.

The soil moisture retrieval capabilities of this parameterization is tested by comparing the retrieved soil moisture from a one parameter (1P)-retrieval (only soil moisture as free parameter; roughness fixed at the above mentioned mean value of retrieved roughness from the 3P-retrieval; vegetation optical depth calculated from the interpolated LAI measurements with the new b-parameters) to measured soil moisture.

As the roughness does not seem to be constant it is analyzed if there is a relationship between soil moisture and roughness by calculating a linear regression between measured soil moisture and retrieved roughness. This has been reported by different authors for grass [37,38].

To assess the influence of roughness on the soil moisture retrieval result two additional retrievals are carried out:

A 1P-soil moisture retrieval where H_r is not constant but a function of measured soil moisture
A two parameter (2P)-retrieval with soil moisture and roughness as free parameters

The performance of the different dielectric models of DOBSON and MIRONOV in the 3P-retrieval

are compared as well as other authors found that the MIRONOV model is better under certain conditions than the DOBSON model which is currently the default model in the SMOS processor [30].

In the end the soil moisture retrieval capabilities of the new parameterization are summarized and the influence of the different parameters assessed.

4. Results and Discussion

4.1. SMOS Default Parameterization and Sensitivity Study

A comparison of the time series of measured and forward modeled brightness temperatures using the default parameters for crops shows that there is a considerable deviation between both data sets. Figure 9 shows the comparison for an incidence angle of 50°.

Figure 9. Comparison between simulated and measured TB on the basis of using the standard parameters according to literature—horizontal polarization.
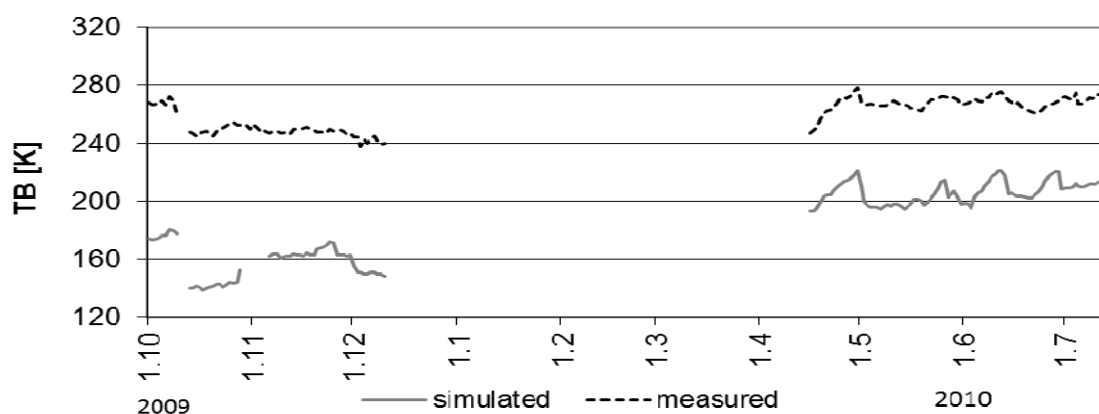
With root mean squared errors of 75.7 K for horizontal and 29.6 K for vertical polarization, there are considerable deviations between both time series. L-MEB severely underestimates the measurement when parameterized with the 'SMOS default parameters'. When used for a 1-P soil moisture retrieval these parameters lead to RMSE values of 0.354 m^3/m^3 and 0.283 m^3/m^3 soil moisture for the first and second period respectively under the current conditions which is not satisfying.

The sensitivity study conducted to find the parameters that need to be changed revealed that vegetation and roughness parameterization have to be adapted to the specific features of winter oilseed rape at the location Puch. According to [9] the vegetation optical depth Tau is positively correlated to the brightness temperature, in the way, that an increasing Tau leads to an increase of the TB. To minimize the deviation between the measured and the retrieved TB, a new set of b-parameters had to be found for the land use winter oilseed rape. Another aspect which leads to an increase of the modeled value is an increase of the roughness condition, here in form of the parameter H_r [9]. For this reason, the vegetation optical depth (mainly the b-parameters) as well as the roughness conditions in form of the parameter H_r had to be adapted to the specific conditions of the test site.

A roughness parameter of $H_r = 0.8$ was found to produce good results. Another result of the sensitivity study was that the forward modeling approach delivers the best results for the early growing period when a single scattering albedo of 0.07 is used. As this value is also reported in literature

for different crops [39] it was decided to use it throughout this study for the early growing period. The b-parameters that were found to produce best results lie in the order of $b_1 = 0.135 − 0.14$ and $b_2 = 0.08 − 0.1$.

With the above described insights it is possible to find parameterizations for L-MEB that enable forward modeling of the 50° brightness temperatures with an RMSE between 1.5 K and 7.1 K for both periods and both polarizations. If higher incidence angles are used (e.g., 70°) the RMSE increases to 24 K, as L-MEB is known to work less efficiently at high incidence angles. Therefore it is expected that the usage of several angles in a soil moisture retrieval from measured brightness temperatures will be able to produce reasonable results even if they will not be as good as the forward modeling results for 50°. It was not possible to model the periods before and after winter break with one set of parameters satisfyingly because of the afore mentioned difference in vegetation behavior at L-Band due to the structural difference of winter rape in both periods. Therefore the two periods are treated separately.

The sensitivity study was also used to find initial values and uncertainties for the parameters that produce best retrieval results. They are listed in Table 4.

Table 4. The initial values (and standard deviations) that are used for all the retrievals within this study for the retrieved parameters soil moisture, roughness parameter H_R and vegetation optical depth.

	Soil moisture [m³/m³]	H_R [-]	Vegetation optical depth [-]
Early period	0.3 (0.1)	0.8 (0.1)	0.2 (1.0)
Late period	0.35 (0.1)	0.8 (0.1)	0.3 (1.0)

4.2. Retrieval Results for Early Growing Period

The roughness and vegetation optical depth that were retrieved using the 3P-retrieval for the early growing period are shown in Figure 10.

Figure 10. Development of vegetation optical depth at NADIR (tau_3P) and roughness parameter H_r (H_r _3P) as a result of a 3P-retrieval. Also shown is the calculated Tau (tau_calc).
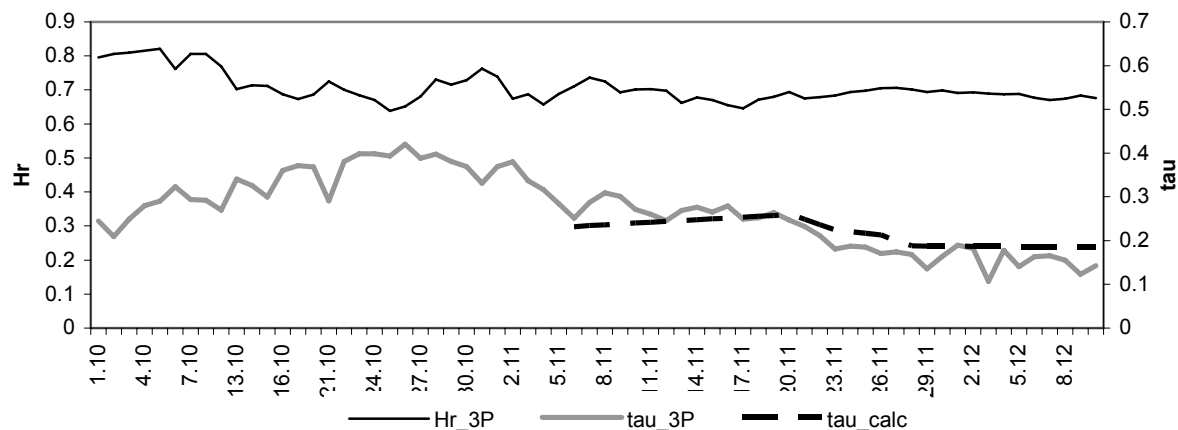
A rise of the vegetation optical depth is visible for the first part of the period. A decrease in physical temperature leads to a decrease of plant vitality and thus to a decrease of vegetation optical depth in the second half. With the loss of plant vitality and VWC, the retrieved roughness seems to become smoother. The mean vegetation optical depth in this period is 0.27, the mean H_r is 0.71 which is of the same order as the value of 0.8 that was found in the sensitivity study but is considerably higher than the value around 0.5 that was estimated from the roughness measurements. The roughness seems to decrease slightly in the course of this period.

Referring to [9] there is a linear relationship between measured leaf area index (LAI) and vegetation optical depth. Equation 5 is used to calculate the two b-parameters from the linear regression between measured LAI and retrieved vegetation optical depth. The R² for this relationship is 0.6, the regression equation was $\tau = 0.12 \times LAI + 0.08$. Referring to Equation (5) that means: $b_1 = 0.12$ and $b_2 = 0.08$. It is important to mention that this regression is based on only four LAI measurements and therefore may not be very reliable. Nevertheless, these two b-parameters together with the mean retrieved H_r parameter are considered a possible extension to the L-MEB parameterization for winter oilseed rape in such an early growing stage and are evaluated in the following. The new parameterization is summarized in Table 3. Because of the lack of data, a relationship between VWC and vegetation optical depth could not be established.

A comparison between the retrieved vegetation optical depth and a calculated one using the measured LAI values together with the new b-parameters in Equation (5) is shown by Figure 10.

Both lines follow a similar trend even though the calculated Tau shows less variability, which is as expected due to the small amount of LAI measurements that have been interpolated for this comparison. The RMSE is 0.03. Calculated Tau values are only available after November 6 as this was the start of the LAI measurements.

A comparison between the retrieved and measured soil moisture is shown in Figure 11. The retrieved soil moisture follows the overall evolution of the measured soil moisture except on the first days of the experiment, but the variability is considerably higher in the retrieved soil moisture. This may be an indication that the radiometer "sees" a different, more dynamic, soil layer (e.g., 0–2 cm) than what is being measured by the TDR probes (5 cm horizontally). R^2 for this comparison is 0.76 and the root mean squared error 0.057 m^3/m^3.

The soil moisture retrieval capabilities of the new parameterization are tested by retrieving soil moisture in a 1P-retrieval from the ELBARA measurements. Roughness is parameterized with a constant H_r value of 0.71 and the vegetation optical depth is calculated with the new b-parameters from interpolated LAI measurements. The resulting soil moisture can be seen in Figure 11 together with measured soil moisture and the retrieved soil moisture from the 3P-retrieval. R^2 decreases to 0.33 and the RMSE increases to 0.086 m^3/m^3 for the comparison with the measured soil moisture. Obviously, the 1P-retrieval works considerably less well than the 3P-retrieval for soil moisture. One has to bear in mind that the retrievals that use a calculated Tau can only be performed for the time after 6 November as no LAI measurements are available before that. Therefore these comparisons are not as reliable as the period analyzed is relatively short. The retrieved soil moisture shows more variability than the measured one. All in all the measured soil moisture shows a very low dynamic after the first days of this period.

Figure 11. Comparison between the soil moisture of the 3P-retrieval (sm_3P), the 1P-retrieval (sm_1P(H_r = 0.71)) with a constant value of H_r = 0.71 and the measured soil moisture at the location Puch.
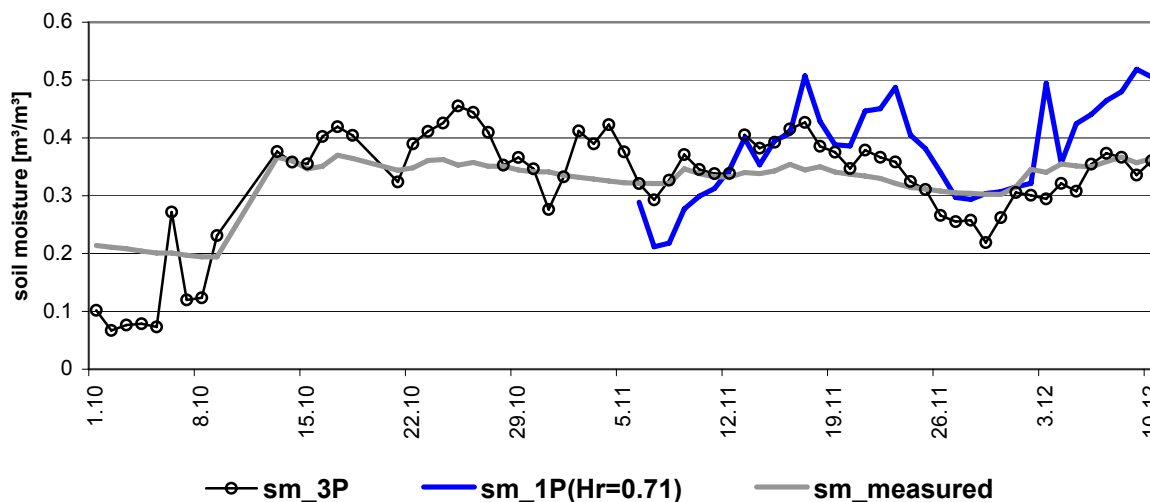
To study whether the changing roughness from the 3P-retrieval is dependent on soil moisture which has been reported earlier [37,38,40] and is also accounted for in the SMOS algorithm, the correlation between both datasets is calculated, the result is shown in Figure 12. With increasing soil moisture, H_r is decreasing.

Figure 12. Correlation between measured soil moisture and retrieved roughness parameter H_r for early (left) and late (right) growing period.
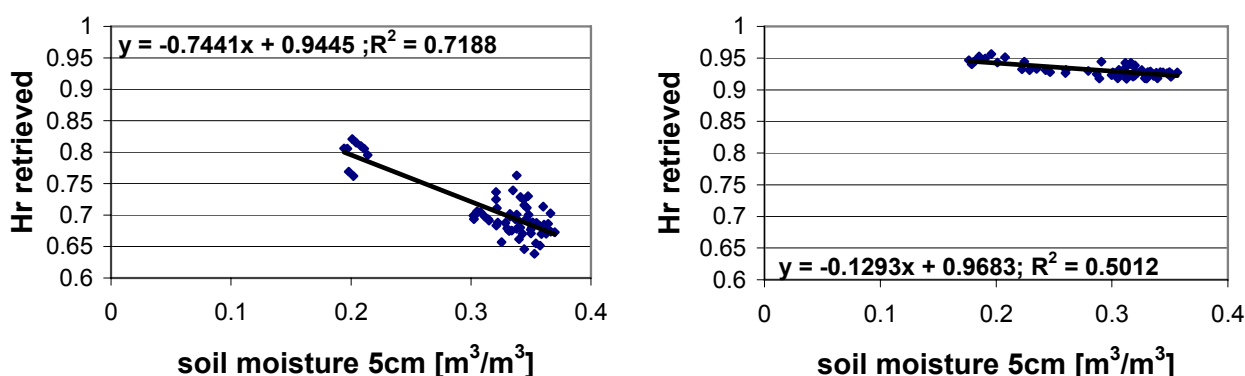
If this linear regression is used to parameterize H_r as a function of soil moisture during a 1P-soil moisture retrieval, the result is very similar to the 1P-retrieval with constant H_r (see Table 5). The two H_r values have nearly the same evolution over time (not shown). If H_r is left free in a 2P-retrieval where soil moisture and H_r are retrieved the retrieved soil moisture follows very closely the evolution of the 3P-retrieved soil moisture (not shown) after November 6. Before that date no 2-P retrieval is possible due to a lack of LAI measurements. The RMSE is even lower than in the 3-P-retrieval but R² is considerably lower for the 2-P-retrieval which is probably due to the low soil moisture dynamic after November 6 (Table 5).

Table 5 summarizes the soil moisture retrieval results for the different retrievals carried out.

Table 5. Results from different soil moisture retrievals for the early and late growing period. During the 3P-retrieval soil moisture, tau and H_r are free parameters. Soil moisture and H_r are free in both 2P-retrievals while for one tau is calculated from LAI (2P(sm; H_r)_lai) and for the other tau is calculated from VWC (2P(sm; H_r)_vwc). Two different 1P-retrievals with soil moisture as free parameter have been carried out. One with a constant H_r value (1P(H_r = 0.xx)) and one with H_r parameterized as a function of soil moisture (1P(H_r = f(sm))).

Period	Retrieval	R^2	RMSE [m^3/m^3]	Gain	Offset
Early	3P(sm;tau; H_r)	0.76	0.057	1.7	0.21
	2P(sm; H_r))_lai	0.33	0.045	1.61	−0.21
	1P(H_r =0.71)	0.33	0.086	2.57	−0.48
	1P(H_r =f(sm))	0.22	0.078	1.88	−0.22
Late	3P(sm;tau;H_r)	0.70	0.049	0.80	0.02
	2P(sm; H_r))_lai	0.40	0.051	0.60	0.12
	2P(sm; H_r)_vwc	0.35	0.076	0.84	0
	1P (H_r =0.93)	0.16	0.108	0.69	0.14
	1P(H_r =f(sm))	0.14	0.097	0.59	0.15

To test the influence of the dielectric model used in L-MEB the 3P-retrieval is also done with the MIRONOV dielectric model and compared to the above mentioned results produced with the DOBSON model. The effect is very small. The RMSE between modeled and simulated soil moisture is 0.004 m^3/m^3 higher (0.061 m^3/m^3) by using MIRONOV than that one by using DOBSON.

4.3. Retrieval Results for Late Growing Period

The late growing period is treated analogue to the early period. The difference is that the soil moisture is being retrieved from a surface, densely covered with winter oilseed rape plants. Plants with horizontally oriented, small leaves and low plant column density, are now turning to plants with vertical stems, leaves, flowers and later pods.

Figure 13 shows roughness and vegetation optical depth as retrieved during the 3P-retrieval together with soil moisture.

Figure 13. Development of retrieved vegetation optical depth (tau_3P) and roughness parameter H_r (hr_3P).
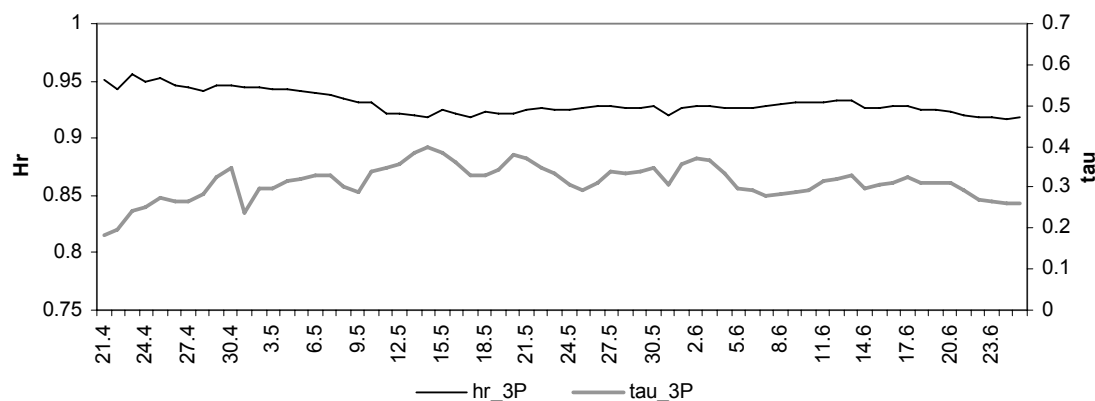
Vegetation optical depth shows an increase at the beginning which can be connected to vertical plant growth. The vegetation height increased from about 70 cm mid of April to 130 cm mid of May. Since that point of time no further vertical growth was detected. The soil roughness remains at a more or less constant level but tends to decrease slightly in the beginning. It is considerably higher than during the first period. The mean value of H_r is 0.93 and the vegetation optical depth totaled at a mean of 0.29.

Using Equation (5) the b-parameters for the second period were also estimated by using a linear regression between LAI and retrieved vegetation optical depth. The relationship shows an R^2 of 0.6 and the equation of the linear regression line reads as follows: $\tau = 0.09 \times LAI + 0.08$. Consequently $b_1 = 0.09$ and $b_2 = 0.08$. Because of having several VWC measurements in this period, it was also possible to establish a relationship between VWC and the retrieved vegetation optical depth, which provides a b-parameter of $b = 0.07$. Summarizing these results we get a possible L-MEB parameterization for the late growing period (Table 3).

Figure 14 compares the retrieved vegetation optical depth to that one calculated with the LAI and the water content of the plants (VWC) using the new b-parameters.

Figure 14. Comparison between calculated vegetation optical depth on the basis of water content (tau_calc_vwc) or LAI (tau_calc_lai) and tau retrieved (tau_3P).
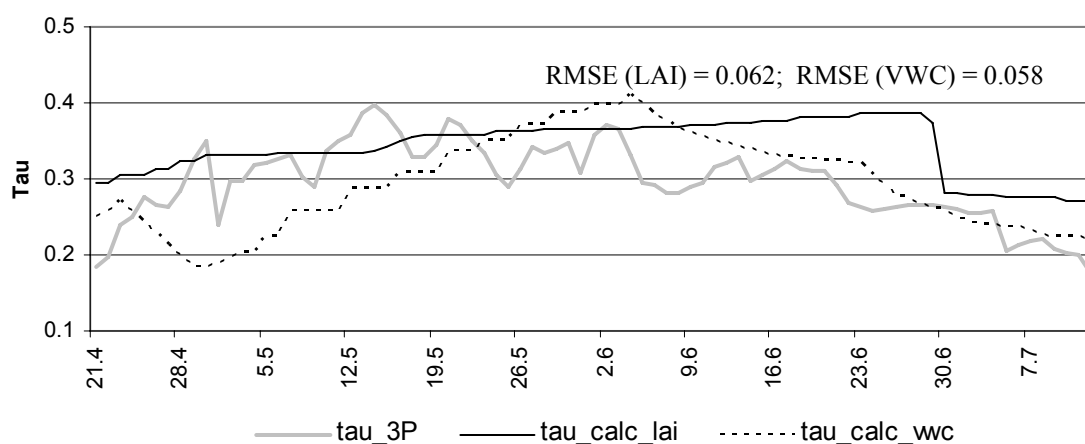
Throughout the whole period, the calculated vegetation optical depths generally follow the trend of the retrieved value. Here again the retrieved values show a higher variability. The deviation between the two calculated and the retrieved vegetation optical depth is similar but evolves differently over time. Both calculated Taus have their maximum at different points in time. The one calculated from VWC develops more smoothly.

The soil moisture retrieval capabilities of the new parameterization for the late growing period are also tested by retrieving soil moisture in a 1P-retrieval from the ELBARA measurements. Roughness is parameterized with a constant H_r value of 0.93 (compare Figure 13) and the vegetation optical depth is calculated with the new b-parameters from interpolated LAI measurements. The resulting soil moisture can be seen in Figure 15 together with measured soil moisture and the retrieved soil moisture from the 3P-retrieval.

Figure 15. Comparison between the soil moisture of the 3P-retrieval (sm_3P), the 1P-retrieval (sm_1P(H$_r$ =0.93)) with a constant value of H$_r$ = 0.93, the 2P-retrieval with tau calculated from LAI measurements(sm_2P_lai) and the measured soil moisture at the location Puch.
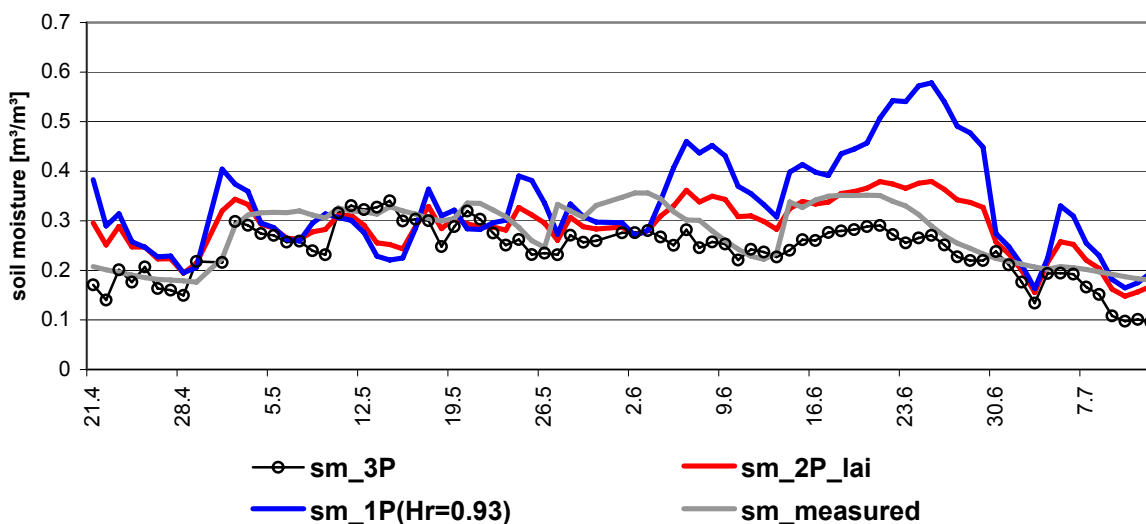
The picture is similar to the early growing period. The general trend of the soil moisture could be reproduced with the retrieved soil moisture but there are also considerable deviations. The 1P-retrieval results in a considerably higher RMSE and lower R² (see Table 5) than the 3P-retrieval. Especially in June the retrieved soil moisture from the 1-P retrieval is considerably higher than the measured one.

To investigate if the roughness is dependant on soil moisture Figure 12 compares retrieved roughness to measured soil moisture. There is a weak relationship between both variables. With increasing soil moisture, roughness decreases, but only marginally from around 0.95 to around 0.92.

If the established linear regression is used to express the roughness as a function of soil moisture during a 1P-soil moisture retrieval no considerable improvement can be observed. While the RMSE decreases by 0.011 [m³/m³] the R² decreases as well (Table 5). The evolution over time is very similar (not shown).

As a 2P-retrieval with soil moisture and roughness as free parameters leads to clearly improved results, it is probable that the roughness value leads to large errors if not left free (see Table 5 and Figure 15). Using VWC instead of LAI for the calculation of the vegetation optical depth does not lead to an improvement (Table 5). Especially in June, where the deviation between measured soil moisture and retrieved soil moisture from the 1P-retrieval is very high, the 2P-retrieval leads to considerable improvements. As the LAI reaches its maximum values at this time it is probable that vegetation effects lead to the high deviations between measured and retrieved soil moisture. As Tau is parameterized in the same way in both retrievals it is assumed that the parameter H$_r$ incorporates some vegetation effects.

As in the early growing period the DOBSON dielectric model leads to better results than the MIRONOV model in the 3-P retrieval. The soil moisture RMSE increases by 0.020 m³/m³ to 0.069 m³/m³ when using MIRONOV instead of DOBSON.

4.4. Discussion of the Chosen Approach

One has to bear in mind that the dataset used for this study has two main drawbacks. Firstly the ELBARA data used was measured at angles between 50 and 65° which is only a rather small angle window at high angles. L-MEB is known to be less efficient at high incidence angles. For that reason angles above 55° are filtered out in the SMOS soil moisture retrieval [36]. Secondly the soil moisture was measured in a depth of 5cm which may be lower than the sensing depth of the ELBARA as reported by [41]. Therefore the observed deviation between measured and retrieved soil moisture may include an error that is being made when one assumes that the ELBARA is sensing the soil moisture measured in 5cm depth. The rather high incidence angles at the edge of the region where soil moisture retrievals can still deliver satisfying results complicate things further.

In addition to that only a small number of LAI measurements during the early growing period makes it necessary to keep the uncertainties in mind that originate from this.

During the second period the vegetation optical depth is very high during the main growing season which decreases the soil moisture sensitivity of the ELBARA data. The VWC has values around 6 kg/m² at this time.

When the results from the L-MEB modeling with the SMOS default parameters are discussed it has to be kept in mind that those parameters were only used as a starting point for the modeling due to the lack of a rape parameterization for L-MEB. If the conclusions drawn here are to be considered in the context of a satellite application several factors have to be considered that differ from point scale to satellite scale, e.g., the scale of the instrument footprint or the footprint heterogeneity.

5. Conclusions

A new parameterization for the radiative modeling of L-Band microwave emission from a rape field was developed. Significant differences were found between early and late rape development stages that led to the development of two different parameterizations for the two development stages.

It was especially important to adapt the roughness parameter H_r and the b-parameters to local conditions. In case of the early growing period the single scattering albedo has also been adapted. All other parameters have been taken from literature and correspond to the parameters used for the SMOS L2 processor.

Using the SMOS default parameterization in L-MEB for forward modeling of the microwave emission led to a clear offset in the order of 30 K−75 K for vertical and horizontal polarization respectively. This corresponds to a soil moisture retrieval RMSE above 0.28 m³/m³ in a 1-P retrieval.

It was not possible to find one parameterization that allowed satisfying microwave emission modeling results for the periods before and after winter for winter oilseed rape. Remarkable is the considerably increased roughness parameter H_r after winter as it would be expected that the soil becomes smoother in winter. This may be connected to the different development stages of the rape plants during the two periods. Apparently the roughness parameter H_r includes a vegetation dependant component. It was interesting to see that the retrieved values for the roughness parameter H_r lied consistently over the expected range that was found in studies over different crops and was estimated from measurements [9,30]. A value of 0.7–0.9 is considered a very rough soil by these studies, which

was not observed in Puch. Other studies however found similar values of H_r [42] and also conclude that a constant value of H_r or a simple linear regression with soil moisture could lead to significant retrieval errors due to a dynamic roughness parameter. Panciera *et al*. [42] also concludes that a dielectric component in the microwave roughness which is related to soil moisture microscale heterogeneity might be responsible for this effect.

It does not seem to be possible to establish a parameterization for L-MEB that allows a satisfying 1P-soil moisture retrieval from the ELBARA data described above under the apparent conditions in Puch. As a 2P-retrieval with soil moisture and roughness as free parameters leads to clearly improved results the roughness parameterization seems to be responsible for a considerable part of the encountered problems. The uncertainties in the vegetation optical depth modeling, that are clearly existent seem to have a smaller impact on the soil moisture retrieval. Another aspect that can explain the retrieval quality is the fact that no angles below 50° were available which is not ideal as L-MEB is known to be less efficient at high incidence angles. The observed relationship between soil moisture and H_r does not help to improve soil moisture retrievals considerably.

Still, the 3P-retrievals show that it is possible to retrieve soil moisture with an RMSE in the order of 0.049–0.057 m³/m³ and a R^2 of 0.70–0.76 with multiangular ELBARA II data above 50° if the roughness and vegetation optical depth are left free, which is promising. When doing a 2P retrieval (soil moisture and roughness free) with the usage of the newly found b-parameters to calculate vegetation optical depth from LAI the retrieved soil moisture shows RMSE values of around 0.045–0.051 m³/m³ with R^2 values of 0.33 and 0.40 for early and late growing period respectively.

Under the reported conditions the DOBSON dielectric model performs better than the MIRONOV model.

As this study is the first to the authors' knowledge that has studied the passive microwave emission from rape fields, the gained insights into the radiative transfer modeling over rape fields can surely add to the existing knowledge in the field of passive microwave remote sensing over different crops.

Acknowledgments

References

1. Jung, M.; Reichstein, M.; Ciais, P.; Seneviratne, S.I.; Sheffield, J.; Goulden, M.L.; Bonan, G.; Cescatti, A.; Chen, J.; de Jeu, R.; *et al.* Recent decline in the global land evapotranspiration trend due to limited moisture supply. *Nature* **2010**, *467*, 951-954.

2. Kerr, Y.H.; Waldteufel, P.; Wigneron, J.-P.; Martinuzzi, J.-M.; Font, J.; Berger, M. Soil moisture retrieval from space: The Soil Moisture and Ocean Salinity (SMOS) mission. *IEEE Trans. Geosci. Remote Sens.* **2001**, *39*, 1729-1735.

3. Entekhabi, D.; Asrar, G.R.; Betts, A.K.; Beven, K.J.; Bras, R.L.; Duffy, C.J.; Dunne, T.; Koster, R.D.; Lettenmaier, D.P.; Mclaughlin, D.B.; *et al.* An agenda for land-surface hydrology research and a call for the second international hydrological decade. *Bull. Am. Meteorol. Soc.* **1999**, *80*, 2043-2057.

4. Wagner, W.; Naeimi, V.; Scipal, K.; de Jeu, R.; Martínez-Fernández, J. Soil moisture from operational meteorological satellites. *Hydrogeol. J.* **2007**, *15*, 121-131.

5. Aires, F.; Prigent, C.; Rossow, W.B. Sensitivity of satellite microwave and infrared observations to soil moisture at a global scale: 2. Global statistical relationships. *J. Geophys. Res.* **2005**, *110*, D11103.

6. Loew, A.; Ludwig, R.; Mauser, W. Derivation of surface soil moisture from ENVISAT ASAR wide swath and image mode data in agricultural areas. *IEEE Trans. Geosci. Remote Sens.* **2006**, *44*, 889-899.

7. Mauser, W.; Rombach, M.; Bach, H.; Demircan, A.; Kellndorfer, J. Determination of spatial and temporal soil-moisture development using multitemporal ERS-1 data. *Proc. SPIE* **1995**, *2314*, 502-515.

8. Wagner, W.; Blöschl, G.; Pampaloni, P.; Calvet, J.-C.; Bizzarri, B.; Wigneron, J.-P.; Kerr, Y. Operational readiness of microwave remote sensing of soil moisture for hydrologic applications. *Nord. Hydrol.* **2007**, *38*, 1-20.

9. Wigneron, J.P.; Kerr, Y.; Waldteufel, P.; Saleh, K.; Escorihuela, M.J.; Richaume, P.; Ferrazzoli, P.; de Rosnay, P.; Gurney, R.; Calvet, J.C.; *et al.* L-band Microwave Emission of the Biosphere (L-MEB) Model: Description and calibration against experimental data sets over crop fields. *Remote Sens. Environ.* **2007**, *107*, 639-655.

10. de Rosnay, P.; Calvet, J.-C.; Kerr, Y.; Wigneron, J.-P.; Lemaître, F.; Escorihuela, M.J.; Sabater, J.M.; Saleh, K.; Barrié, J.; Bouhours, G.; *et al.* SMOSREX: A long term field campaign experiment for soil moisture and land surface processes remote sensing. *Remote Sens. Environ.* **2006**, *102*, 377-389.

11. Grant, J.P.; Wigneron, J.P.; Van de Griend, A.A.; Kruszewski, A.; Søbjærg, S.S.; Skou, N. A field experiment on microwave forest radiometry: L-band signal behaviour for varying conditions of surface wetness. *Remote Sens. Environ.* **2007**, *109*, 10-19.

12. Schwank, M.; Matzler, C.; Guglielmetti, M.; Fluhler, H. L-band radiometer measurements of soil water under growing clover grass. *IEEE Trans. Geosci. Remote Sens.* **2005**, *43*, 2225-2237.

13. Schwank, M.; Stahli, M.; Wydler, H.; Leuenberger, J.; Matzler, C.; Fluhler, H. Microwave L-band emission of freezing soil. *IEEE Trans. Geosci. Remote Sens.* **2004**, *42*, 1252-1261.

14. Loew, A.; Schwank, M.; Schlenz, F. Assimilation of an L-band microwave soil moisture proxy to compensate for uncertainties in precipitation data. *IEEE Trans. Geosci. Remote Sens.* **2009**, *47*, 2606-2616.

15. Loew, A.; Schwank, M. Calibration of a soil moisture model over grassland using L-band microwave radiometry. *Int. J. Remote Sens.* **2010**, *31*, 5163-5177.

16. Schwank, M.; Wiesmann, A.; Werner, C.; Mätzler, C.; Weber, D.; Murk, A.; Völksch, I.; Wegmüller, U. ELBARA II, An L-band radiometer system for soil moisture research. *Sensors* **2009**, *10*, 584-612.

17. Cano, A.; Saleh, K.; Wigneron, J.-P.; Antolín, C.; Balling, J.; Kerr, Y.; Kruszewski, A.; Millán-Scheiding, C.; Søbjærg, S.; Skou, N. The SMOS Mediterranean Ecosystem L-Band characterisation EXperiment (MELBEX-I) over natural shrubs. *Remote Sens. Environ.* **2010**, *114*, 844-853.

18. Rautiainen, K.; Lemmetyinen, J.; Pulliainen, J.; Vehviläinen, J.; Drusch, M.; Kontu, A.; Kainulainen, J.; Seppänen, J. L-Band radiometer observations of soil processes in boreal and sub-arctic environments. *IEEE Trans. Geosci. Remote Sens.* **2011**, in press.

19. Schlenz, F.; Gebhardt, T.; Loew, A.; Marzahn, P.; Mauser, W. L-Band Radiometer Experiment in the SMOS Test Site Upper Danube. In *Proceedings of EGU General Assembly 2010*, Vienna, Austria, 2–7 May 2010; p. 9677.

20. FNR e.V. *Jahresbericht 2009/2010*; Fachagentur Nachwachsende Rohstoffe e.V. (FNR): Gülzow-Prüzen, Germany, 2010.

21. Dall'Amico, J.T.; Schlenz, F.; Loew, A.; Mauser, W.; Kainulainen, J.; Balling, J.; Bouzinac, C. Airborne and ground campaigns in the Upper Danube Catchment: Data sets for calibration, validation and downscaling of SMOS data. *IEEE Trans. Geosci. Remote Sens.* **2011**, submitted.

22. Delwart, S.; Bouzinac, C.; Wursteisen, P.; Berger, M.; Drinkwater, M.; Martin-Neira, M.; Kerr, Y.H. SMOS Validation and the COSMOS Campaigns. *IEEE Trans. Geosci. Remote Sens.* **2008**, *46*, 695-704.

23. Teuling, A.J.; Hupet, F.; Uijlenhoet, R.; Troch, P.A. Climate variability effects on spatial soil moisture dynamics. *Geophys. Res. Lett.* **2007**, *34*, L06406.

24. LI-COR, Inc. *LAI-2000 Plant Canopy Analyzer: Instruction Manual*; LI-COR, Inc.: Lincoln, NL, USA, 2003.

25. Behrens, T.; Diepenbrock, W. Using digital image analysis to describe canopies of winter oilseed rape (*Brassica napus L.*) during vegetative developmental stages. *J. Agron. Crop Sci.* **2006**, *192*, 295-302.

26. Rieke-Zapp, D.H.; Rosenbauer, R.; Schlunegger, F. A photogrammetric surveying method for field applications. *Photogramm. Rec.* **2009**, *24*, 5-22.

27. Marzahn, P.; Rieke-Zapp, D.; Ludwig, R. Assessment of soil surface roughness statistics for microwave remote sensing applications using a simple photogrammetric acquisition system. *ISPRS* **2011**, submitted.

28. Taconet, O.; Ciarletti, V. Estimating soil roughness indices on a ridge-and-furrow surface using stereo photogrammetry. *Soil Till. Res.* **2007**, *93*, 64-76.

29. Marzahn, P.; Ludwig, R. On the derivation of soil surface roughness from multi parametric PolSAR data and its potential for hydrological modeling. *Hydrol. Earth Syst. Sci.* **2009**, *13*, 381-394.

30. Wigneron, J.P.; Chanzy, A.; Kerr, Y.H.; Lawrence, H.; Shi, J.; Escorihuela, M.J.; Mironov, V.; Mialon, A.; Demontoux, F.; de Rosnay, P.; Saleh-Contell, K. Evaluating an improved parameterization of the soil emission in L-MEB. *IEEE Trans. Geosci. Remote Sens.* **2011**, *49*, 1177-1189.

31. Woodhouse, I.H. *Introduction to Microwave Remote Sensing*; Taylor and Francis: London, UK, 2006.

32. Holmes, T.R.H.; de Rosnay, P.; de Jeu, R.; Wigneron, R.J.P.; Kerr, Y.; Calvet, J.C.; Escorihuela, M.J.; Saleh, K.; Lemaître, F. A new parameterization of the effective temperature for L-band radiometry. *Geophys. Res. Lett.* **2006**, *33*, L07405.

33. Mätzler, C. *Thermal Microwave Radiation. Applications for Remote Sensing*; Institution of Engineering and Technology: London, UK, 2006.

34. Dobson, M.C.; Ulaby, F.T.; Hallikainen, M.T.; El-Rayes, M.A. Microwave dielectric behavior of wet soil-Part II: Dielectric mixing models. *IEEE Trans. Geosci. Remote Sens.* **1985**, *GE-23*, 35-46.

35. Mironov, V.; Bobrov, P. Spectroscopic microwave dielectric model of moist soils. In *Advances in Geoscience and Remote Sensing*; Jedlovec, G., Ed.; InTech: Vukovar, Croatia, 2009; pp. 279-302.

36. Kerr, Y.; Waldteufel, P.; Richaume, P.; Davenport, P.; Ferrazzoli, P.; Wigneron, J.-P. *SMOS Level 2 Processor Soil Moisture Algorithm Theoretical Basis Document (ATBD) V 3.5*; CBSA, UoR, TV and INRA: Toulouse, France, 2011.

37. Saleh, K.; Kerr, Y.H.; Richaume, P.; Escorihuela, M.J.; Panciera, R.; Delwart, S.; Boulet, G.; Maisongrande, P.; Walker, J.P.; Wursteisen, P.; Wigneron, J.P. Soil moisture retrievals at L-band using a two-step inversion approach (COSMOS/NAFE'05 Experiment). *Remote Sens. Environ.* **2009**, *113*, 1304-1312.

38. Panciera, R.; Walker, J.P.; Kalma, J.D.; Kim, E.J.; Saleh, K.; Wigneron, J.-P. Evaluation of the SMOS L-MEB passive microwave soil moisture retrieval algorithm. *Remote Sens. Environ.* **2009**, *113*, 435-444.

39. Van de Griend, A.A.; Wigneron, J.P. On the measurement of microwave vegetation properties: Some guidelines for a protocol. *IEEE Trans. Geosci. Remote Sens.* **2004**, *42*, 2277-2289.

40. Escorihuela, M.J.; Kerr, Y.H.; de Rosnay, P.; Wigneron, J.P.; Calvet, J.C.; Lemaitre, F. A simple model of the bare soil microwave emission at L-band. *IEEE Trans. Geosci. Remote Sens.* **2007**, *45*, 1978-1987.

41. Escorihuela, M.J.; Chanzy, A.; Wigneron, J.P.; Kerr, Y.H. Effective soil moisture sampling depth of L-band radiometry: A case study. *Remote Sens. Environ.* **2010**, *114*, 995-1001.

42. Panciera, R.; Walker, J.P.; Merlin, O. Improved understanding of soil surface roughness parameterization for L-band passive microwave soil moisture retrieval. *IEEE Geosci. Remote Sens. Lett.* **2009**, *6*, 625-629.

Publication 3

Schlenz, F., dall'Amico, J. T., Mauser, W., and Loew, A.: Analysis of SMOS brightness temperature and vegetation optical depth data with coupled land surface and radiative transfer models in Southern Germany, Hydrol. Earth Syst. Sci. Discuss., 9, 1-48, 2012. (accepted; doi: 10.5194/hessd-9-1-2012)

Hydrology and Earth System Sciences Discussions

Analysis of SMOS brightness temperature and vegetation optical depth data with coupled land surface and radiative transfer models in Southern Germany

F. Schlenz[1], J. T. dall'Amico[1], W. Mauser[1], and A. Loew[2]

[1]Department of Geography, University of Munich, Munich, Germany
[2]Max-Planck-Institute for Meteorology, KlimaCampus, Hamburg, Germany

Title Page

Abstract	Introduction
Conclusions	References
Tables	Figures

|◄ | ►|
◄ | ►

| Back | Close |

Full Screen / Esc

Printer-friendly Version

Interactive Discussion

Abstract

Soil Moisture and Ocean Salinity (SMOS) L1c brightness temperature and L2 optical depth data are analysed with a coupled land surface (PROMET) and radiative transfer model (L-MEB) that are used as tool for the analysis and validation of passive
5 microwave satellite observations. The coupled models are validated with ground and airborne measurements under contrasting soil moisture, vegetation and temperature conditions during the SMOS Validation Campaign in May and June 2010 in the SMOS test site Upper Danube Catchment in Southern Germany with good results. The brightness temperature root-mean-squared errors are between 6 K and 9 K and can partly
10 be attributed to a known bias in the airborne L-band measurements. The L-MEB parameterization is considered appropriate under local conditions even though it might possibly further be optimised. SMOS L1c brightness temperature data are processed and analysed in the Upper Danube Catchment using the coupled models in 2011 and during the SMOS Validation Campaign 2010 together with airborne L-band brightness
15 temperature data. Only low to fair correlations are found for this comparison ($R < 0.5$). SMOS L1c brightness temperature data do not show the expected seasonal behaviour and are positively biased. It is concluded that RFI is responsible for most of the observed problems in the SMOS data products in the Upper Danube Catchment. This is consistent with the observed dry bias in the SMOS L2 soil moisture products which
20 can also be related to RFI. It is confirmed that the brightness temperature data from the lower SMOS look angles are less reliable. This information could be used to improve the brightness temperature data filtering before the soil moisture retrieval. SMOS L2 optical depth values have been compared to modelled data and are not considered a reliable source of information about vegetation due to missing seasonal behaviour
25 and a very high mean value. A fairly strong correlation between SMOS L2 soil moisture and optical depth was found ($R = 0.65$) even though the two variables are considered independent in the study area. The value of coupled models as a tool for the analysis

Title Page

Abstract	Introduction
Conclusions	References
Tables	Figures

|◄ | ►|
◄ | ►

| Back | Close |

Full Screen / Esc

Printer-friendly Version

Interactive Discussion

Please note the remarks at the end of the manuscript.

of passive microwave remote sensing data is demonstrated by extending this SMOS data analysis from a few days during a field campaign to a long term comparison.

1 Introduction

The European Space Agency's (ESA) Soil Moisture and Ocean Salinity (SMOS) mission was launched in November 2009 to monitor surface soil moisture and ocean salinity globally with a temporal resolution of 2–3 days and a spatial resolution in the order of 43 km (Kerr et al., 2010). Soil moisture is derived from multiangular interferometric passive microwave L-band brightness temperature measurements at 1.4 GHz and delivered on an ISEA (icosahedral Snyder equal area projection) grid with a mean distance between grid points of 12.5 km (Kerr et al., 2010). Potential applications of spaceborne soil moisture products are numerical weather forecasting, land surface hydrology, agricultural applications and climate research (Dirmeyer, 2000; Entekhabi et al., 1999; Bolten et al., 2010). An accuracy target of $0.04\,\mathrm{m^3\,m^{-3}}$ soil moisture random error is set for the SMOS L2 soil moisture measurements (Kerr et al., 2010; ESA, 2002). A central question for the validation of SMOS is whether and under which conditions this level of accuracy can be reached. This paper aims at contributing to answer this question.

It is important to validate remotely sensed soil moisture products properly in order to ensure good product quality that is a prerequisite for the application of the data. This is especially important as SMOS follows a novel technological concept. Validation of passive microwave soil moisture products is challenging due to the mismatch in scale between satellite products and point scale in situ measurements that are typically used for validation of remote sensing based soil moisture products (Bartalis et al., 2008; Prigent et al., 2005). In situ measurements for satellite validation are usually collected in field campaigns over extended areas and during short periods of time or over longer time spans at few selected measuring locations. In addition to other remote sensing data sets, the outputs of spatially distributed environmental process models

can make a valuable contribution to the validation of remotely sensed soil moisture products (Crow et al., 2005; Albergel et al., 2010; Juglea et al., 2010; dall'Amico et al., 2011a). These data sets can help to extend long-term validation activities to larger areas.

Some studies have thoroughly evaluated the SMOS L2 products so far. The performance of the products behaves differently from region to region and changes with time (dall'Amico et al., 2011a; Albergel et al., 2012; Jackson et al., 2011; Gruhier et al., 2010; Parrens et al., 2012). Generally the SMOS performance in Central Europe seems to be degraded compared to other regions of the world. For the Upper Danube Catchment in Southern Germany, that is also the area of interest in this study, Albergel et al. (2012), dall'Amico et al. (2011a) and dall'Amico (2012) have compared SMOS L2 soil moisture products to in situ and modelled reference data. They find mean correlation coefficients of 0.25–0.3 and a dry bias in the order of $0.23\,\mathrm{m^3\,m^{-3}}$–$0.267\,\mathrm{m^3\,m^{-3}}$ for the comparison of SMOS data with in situ data in 2010. For 2011 these figures improve considerably with a correlation coefficient of 0.52 and a dry bias of $0.15\,\mathrm{m^3\,m^{-3}}$ for the same comparisons (dall'Amico, 2012). In Europe the performance of the SMOS L2 soil moisture product was considerably affected by radio frequency interference (RFI) since the launch of SMOS (Albergel et al., 2012; Balling et al., 2011), but the amount of contaminated data has exhibited a decrease due to RFI mitigation efforts and switching off of RFI sources (Oliva et al., 2012). In 2010, several RFI sources were obvious in SMOS L1c data in Germany that have disappeared in 2011. Probably the improvement in SMOS performance in Southern Germany can at least partly be attributed to an improvement in the RFI situation.

Despite these improvements, the validation studies so far show that more work is still necessary to further improve the quality of the SMOS L2 soil moisture products in order to meet the mission target. Therefore it should be studied where the problems in the SMOS L2 soil moisture product originate from and how improvements could be achieved. Especially the pronounced dry bias in Germany and other regions needs further investigation. It needs to be clarified whether it is RFI-induced or has to do

with radiative transfer modelling uncertainties or other retrieval problems. Therefore it is essential to validate and study the radiative transfer modelling in the L-band of the microwave domain on the SMOS scale as SMOS soil moisture products are inverted through an iterative inversion method from L-band passive microwave observations (Kerr et al., 2010). The radiative transfer model used in the SMOS L2 soil moisture processor is the L-band Microwave Emission of the Biosphere (L-MEB) model (Wigneron et al., 2007) that serves as a forward model in the soil moisture inversion. Uncertainties in the parameterization of the radiative transfer model can result in errors in the retrieved variables (in most retrievals soil moisture and optical depth). As the L-MEB parameterizations used for the SMOS soil moisture retrieval have mostly been derived from studies with ground or airborne L-band radiometer measurements on the local scale it is possible that scaling issues introduce additional uncertainties. The vegetation optical depth, that is simultaneously retrieved with soil moisture and delivered in the SMOS L2 product, could be a valuable source of information about vegetation characteristics. However, Jackson et al. (2011) concludes that it does not contain reliable information in the US. This could point towards retrieval problems and should also be investigated in other parts of the world.

Few studies have validated and analysed the SMOS L1c products over vegetated surfaces which is important if the radiative transfer modelling abilities in the SMOS processing are to be studied. Examples are Albergel et al. (2011), Bircher et al. (2011), Montzka et al. (2011), Parrens et al. (2012). Albergel et al. (2011) and Parrens et al. (2012) have shown that there is still potential to improve soil moisture retrievals from SMOS brightness temperatures in Southern France. They used calibrated statistical relationships based on reference soil moisture values and additional information like leaf area index (LAI) simulated by a land surface model to produce better soil moisture estimates. Bircher et al. (2011) have compared SMOS L1c and airborne brightness temperatures with modelled brightness temperatures using in situ data as input on different spatial scales on one day in Denmark. They developed an improved L-MEB parameterisation for local conditions. Other studies rely either on ground based

or airborne radiometer data as reference with the drawbacks of the mismatch in scale between radiometer and SMOS footprint. Also, airborne campaigns typically yield relatively small datasets of only a few days. With the help of coupled land surface and radiative transfer models these datasets can be extended beyond the typical scale and duration of field campaigns and thereby can serve as a valuable extension for SMOS validation and data analysis activities.

This study aims at assessing how coupled land surface and radiative transfer models can contribute to the validation and analysis of passive microwave remote sensing data. Possible explanations for the apparent problems in the SMOS L2 soil moisture data in Southern Germany are assessed. For this reason, SMOS L1c brightness temperature and L2 vegetation optical depth data are analysed with modelled and airborne data. If RFI would be responsible for most of the L2 problems this should be visible in the SMOS L1c brightness temperatures as well. And if SMOS L1c brightness temperatures would perform better than L2 data, this would point towards a problem in the soil moisture retrieval. Retrieved SMOS L2 optical depth values are analysed as they play an important role in the soil moisture retrieval and could be a valuable source of information about vegetation characteristics. Another important aspect is the parameterization of the radiative transfer model used for the soil moisture retrieval. It has been reported e.g. by Bircher et al. (2011) and Panciera et al. (2009) that it might be necessary to optimize the parameterization under local conditions to obtain best results. To study this, the radiative transfer modelling is analysed with airborne data as reference under local conditions. It has been reported that brightness temperatures at certain angles may be more reliable than at others (Bircher et al., 2011; Hornbuckle et al., 2011). Such a finding could also be exploited to improve the soil moisture retrieval by using only certain angular ranges. It is not the intention of this paper to study SMOS L2 soil moisture data as this has thoroughly been done already by dall'Amico et al. (2011a) and dall'Amico (2012).

The study is conducted in the highly instrumented Vils test site in the Upper Danube Catchment in Southern Germany that has been used as a major SMOS cal/val test site

since 2007 (Delwart et al., 2008). Different extensive field campaigns have taken place here that produced time series of soil moisture station measurements. They are publicly available over the International Soil Moisture Network (ISMN) (Dorigo et al., 2011) http://www.ipf.tuwien.ac.at/insitu/. In addition to that ground based L-band radiometer measurements and spatially distributed data sets of soil moisture, vegetation and airborne L-band radiometer measurements are available (Schlenz et al., 2011; dall'Amico et al., 2011b; Schlenz et al., 2012). The land surface model PROMET (Mauser and Bach, 2009) has been coupled to the radiative transfer model L-MEB to model land surface states in the Upper Danube Catchment on a 1 km grid as well as the resulting microwave emissions in the L-band. The coupled model is used as a tool for the analysis of the SMOS passive microwave satellite observations. As the SMOS data perform considerably better in 2011 than in 2010 the study concentrates on 2011 data. In addition to 2011 data, data from the SMOS Validation campaign 2010 are used for model validation and a brief SMOS data analysis as this is the only period with extensive ground and airborne data available.

In Sect. 2 the study area and data sets as well as the models involved in this study are described. This is followed by the description of the methodology. Section 3 details and discusses the results of the model validation, followed by an analysis of the radiative transfer model parameterization under local conditions on the SMOS scale with airborne brightness temperatures from the SMOS Validation campaign 2010. Next, SMOS L1c brightness temperature data are analysed and compared with the airborne brightness temperatures from the SMOS Validation Campaign 2010 in this period. Afterwards a long term comparison with modelled brightness temperatures from April to October 2011 is performed. SMOS L2 optical depth is compared against model results and the SMOS L2 soil moisture product before the main findings are summarized in the Conclusions.

---

2 Material and methods

The flowchart in Fig. 1 illustrates the context of the different data sets and comparisons in this paper. The coupled models PROMET and L-MEB produce data sets (black) of soil moisture (SM), vegetation optical depth (Tau), and brightness temperatures (BT) that are compared to SMOS data (red). In situ soil moisture (green) and airborne brightness temperatures (blue) are used for model validation. Additional comparisons of airborne brightness temperatures with SMOS L1c brightness temperatures and SMOS L2 soil moisture and optical depth values are also carried out.

2.1 Study area and in situ data

The study area is the Vils test site in the SMOS test site Upper Danube Catchment in Southern Germany. This region has been the subject of a wide range of hydrological, remote sensing and global change studies, e.g. Mauser and Schädlich (1998), Ludwig and Mauser (2000), Bach et al. (2003), Ludwig et al. (2003), Probeck et al. (2005), Loew et al. (2006), Mauser and Bach (2009). The Vils test site has roughly the size of a SMOS footprint and is situated in the northeast of the Upper Danube Catchment in an undulating terrain that is used agriculturally. It has a temperate humid climate and is considered homogenous with respect to terrain and land cover. It does not contain large water bodies or cities. The three most important agricultural land cover types are winter wheat, maize and grass that cover more than 60 % of the area. Based on previous studies (Strasser et al., 1999; Bach and Mauser, 2003; Loew, 2008), this test site has carefully been chosen and used for SMOS calibration and validation (cal/val) studies since 2007 (Delwart et al., 2008). The test site has been instrumented with seven soil moisture profile stations that have been measuring between 2007 and 2011 and has been subject of extensive field campaigns, the most comprehensive one being the SMOS Validation Campaign from 17 May to 8 July 2010. Details of this campaign are given in dall'Amico et al. (2011b). During this field campaign airborne L-band radiometer measurements were performed together with more than 9000 soil moisture

and comprehensive vegetation parameter measurements that were collected in five selected focus areas sized roughly 3 by 7 km and distributed throughout the test site. The analysis in this study concentrates on the ISEA grid point 2027099 that is located in the centre of the Vils test site and the furthest away from any open water bodies. Two neighbouring grid points in the Vils test site have the IDs 2026586 and 2026587. Due to the homogeneity of the Vils test site the in situ and airborne measurements from the field campaigns are considered to be representative for the whole Vils test site. From the soil moisture stations the hourly 5 cm measurements from all available probes have been averaged per station and are being used as reference in this study. Figure 2 gives an overview of the Vils test site.

2.2 Airborne data

During the SMOS Validation Campaign the airborne L-band radiometer EMIRAD 2 (owned by the technical University of Denmark, Skou et al., 2010) was flown on five days onboard the Skyvan aircraft over the Vils test site to measure brightness temperatures emitted by the land surface over a representative portion of a SMOS footprint around SMOS morning overpass time. EMIRAD is a thoroughly validated radiometer that has been used in a variety of studies and is therefore used as reference in this study. EMIRAD has an antenna system consisting of two Potter horns, one pointed nadir and one 40° aft and has a footprint size of about 1.5 km for the nadir antenna and 2 km for the 40° looking antenna for an average flight altitude of 2 km above ground. The data processing is described in (Schlenz et al., 2011) and involved RFI filtering with RFI flags that were provided with the data and a threshold filtering. After processing the data were available for the two look angles 0° and 40° for vertical and horizontal polarization. A detailed description of the airborne campaign data set is given by (dall'Amico et al., 2011b). Contrasting soil moisture, temperature and vegetation conditions were observed in the course of the campaign (focus area mean values of soil moisture varied between 0.169 $m^3 m^{-3}$ and 0.392 $m^3 m^{-3}$, air temperatures during overflight were between 7 °C and 18 °C, vegetation heights ranged between 7 cm and 79 cm). For fur-

---

ther comparisons the EMIRAD data were mapped onto the ISEA grid with the nearest neighbour method.

2.3 SMOS data

SMOS L1c and L2 data are delivered on the ISEA grid with a mean distance between grid points of about 12.5 km, although the data have a mean resolution in the order of 43 km (Kerr et al., 2010). SMOS L1c brightness temperatures are valid for the whole SMOS footprint, which actual size is dependent on the incidence angle and therefore changes from one observation to the other. The SMOS L2 soil moisture and optical depth products are only valid for the nominal land cover class (low vegetation) within the footprint for which the soil moisture retrieval is carried out. Details about the geometry and other properties of the data products can be found in the Algorithm Theoretical Basis Document (ATBD) of the SMOS L2 Soil Moisture Processor (Kerr et al., 2011). Only SMOS data from morning orbits (around 06:00 a.m. local time) are used to avoid uncertainties related to differences between morning and evening overpasses that have been found by (Rowlandson et al., 2012).

In order to make the SMOS L1c data usable a comprehensive data processing chain has been developed and set up that helps to reduce the noise in the data and makes it easier to interpret. The processing consists of filtering, geometric and Faraday rotation and an incidence angle based analysis. The processing has been adapted from the official SMOS L2 soil moisture processing described in Kerr et al. (2011). In a first step observations that are RFI flagged or do not fulfil the spatial resolution requirements because the footprint is too large or elongated are filtered out by applying:

$$\frac{\text{axis1}}{\text{axis2}} > 1.5 \tag{1}$$

and

$$\sqrt{4 \cdot \text{axis1} \cdot \text{axis2}} > 3025 \tag{2}$$

where axis1 and axis2 are the half lengths of the major and minor axis of the 3 dB contour of the near elliptical SMOS footprint. Afterwards, several RFI filtering techniques are performed to detect strong RFI. These include a threshold filtering deleting all brightness temperatures above 300 K and below 200 K as only land surfaces are considered, the upper and lower thresholds for the imaginary part of full polarized brightness temperatures are −50 K and 50 K, respectively. Another test compares the amplitudes of the brightness temperatures to its expected range with:

$$50 < \sqrt{TB_X^2 + TB_Y^2} < 500 \qquad (3)$$

and filters out data exceeding these thresholds. Additional techniques are applied to filter for soft RFI. These are based on the fourth Stokes parameter ST4 that is required to be below the threshold of 50 K and the mean value of the halved first Stokes parameter of all observations for one pixel $\langle TBS1 \rangle = 0.5 * (TB_X + TB_Y)$. Following condition needs to be fulfilled to pass the test for brightness temperature observations:

$$\left(TBS1 - \langle TBS1 \rangle \right) > 5.0 + 4.0 \cdot DTB_X \qquad (4)$$

where DTB_X is the radiometric uncertainty related to TB_X. This test is only reasonable in homogenous areas where brightness temperature variations within one pixel do not arise from a large surface heterogeneity (e.g. coastlines). Most of these threshold have been taken from Kerr et al. (2011) while some are more strict than the values used in the SMOS L2 processing. They have been tested with airborne and SMOS brightness temperatures and proven to be valuable under local conditions.

L1c data are delivered as top of atmosphere (TOA) brightness temperatures in antenna geometry that need to be rotated to enable a comparison with brightness temperatures on the Earth's surface which is performed in the next step. The necessary rotations comprise a geometric rotation to correct for the transformation from antenna to Earth surface reference frame and the Faraday rotation to correct for the influence of the atmosphere on the brightness temperatures. The rotations are detailed in Kerr

---

et al. (2011). After the rotations, the vertical and horizontal polarized brightness temperatures are averaged into 10° bins that are centred around the designated angle to enable an incidence angle based analysis. A similar approach was chosen by Parrens et al. (2012).

This processing reduces the noise in the data considerably but outliers that are probably related to RFI are still present in the data.

The SMOS L2 optical depth data have been processed analogue to the SMOS L2 soil moisture processing as described in dall'Amico et al. (2011a). It involves a filtering using the DQX value and the flags FL_NO_PROD, FL_RFI_Prone_H, FL_RFI_Prone_V and FL_RAIN (Kerr et al., 2011). This processing reduces noise in the data by deleting some outliers with suspicious data but there are still outliers left in the data that are probably connected to RFI that is not detected by the methods and flags used.

dall'Amico (2012) have thoroughly analysed the SMOS L2 soil moisture data for April to October 2011 in the Vils test site with in situ data and PROMET simulations. They find correlation coefficients for the comparison between SMOS and in situ soil moisture in the Vils test site of around 0.52 and a dry bias of around 0.15 $m^3 m^{-3}$. For comparisons between modelled soil moisture and SMOS soil moisture the mean correlation coefficient in the Vils test site for 2011 is 0.54, the mean bias 0.13 $m^3 m^{-3}$.

2.4 Coupled land surface and radiative transfer modelling

The hydrological land surface model PROMET (PROcesses of Mass and Energy Transfer, Mauser and Bach, 2009) and the microwave emission model L-MEB (L-band emission of the biosphere, Wigneron et al., 2007) have been coupled to model land surface states (e.g. soil moisture, temperatures, vegetation parameters) and the resulting microwave emission to validate and analyse SMOS L1c brightness temperatures as well as SMOS L2 optical depth data. Two publications have already validated the models and discussed the uncertainties related to this modelling approach thoroughly. While Schlenz et al. (2011) have focussed on the validation and uncertainties related to the land surface modelling from point to SMOS-like scale in the Upper Danube Catchment

and brightness temperature modelling on the SMOS-like scale in the Vils test site, Schlenz et al. (2012) have analysed the radiative transfer modelling on the point scale in a test site roughly 100 km southwest of the Vils test site. Therefore it is referred to these publications for a more thorough discussion of the related uncertainties.

2.4.1 Land surface model PROMET

In the present study the hydrological land surface model PROMET is used to simulate fields of land surface states with an hourly resolution on a 1 km grid in the Upper Danube Catchment. A detailed description of the model physics is given by Mauser and Bach (2009) and Mauser and Schädlich (1998). The model describes all relevant water and energy fluxes related to the radiation balance, vegetation, soil, snow, and land-surface-atmosphere exchange processes. It is spatially distributed and based on high resolution spatial input data like land cover and soil maps and meteorological forcing data from station networks or regional climate models as input. In our case the meteorological station network delivering the meteorological forcing consists of more than 130 stations operated by the Bavarian State Research Center for Agriculture. The land cover map has been derived from high resolution satellite imagery and statistical information on community level, the soil map is taken from a combination of the European and German soil map and regional soil information supplied by the (BÜK, 1997). The soil moisture dynamics modelling is done in PROMET with a 4-layer soil model based on an explicit solution of the Richards equation for flow in unsaturated media (Philip, 1957) while the soil water retention model of (Brooks and Corey, 1964) is used to relate soil suction head to soil moisture content. The 4 soil compartments were selected to be situated at 0–2, 2–15, 15–50 and 50–150 cm depth for this study. For all comparisons between modelled and measured soil moisture the second soil layer is used, as its depth corresponds to the depth where most soil moisture measurements were performed. The average of the first two layers is used for brightness temperature modelling and SMOS comparisons as the penetration depth of microwaves in the L-band is typically 5 cm (Kerr et al., 2010). The model has been validated in different

test sites on different scales with good results by Mauser and Schädlich (1998), Ludwig and Mauser (2000), Mauser and Bach (2009), Loew et al. (2006), Strasser and Mauser (2001), Pauwels et al. (2008). Muerth (2008) evaluated the soil temperature modelling abilities of PROMET in the Upper Danube Catchment with measurements and remote sensing data with good results.

For the analysis of the 2011 data set the dynamic vegetation model within PROMET was used. It models the vegetation development dynamically depending on the soil and weather characteristics for all individual pixels. Plant development is simulated with a 2 layer canopy model, which iteratively closes the energy balance for the sub canopy soil surface and each layer of the canopy and thereby produces a canopy radiation temperature. Details are given in Hank (2008). The modelled vegetation parameters phenology, vegetation height, vegetation biomass and leaf area index (LAI) of this model, which evolve dynamically accoding to the course of the weather, have been compared to ground measurements with very good results by Hank (2008) in the centre of the Upper Danube Catchment for several test sites on wheat, oat, maize and grassland during several years. (Hank, 2008) assessed e.g. the modelled LAI with a mean R^2 of 0.925 (0.92) and a mean Nash-Sutcliffe coefficient of 0.83 (0.87) for wheat (maize).

Schlenz et al. (2011) have compared modelled soil moisture from PROMET with soil moisture measurements on different scales. The measurements were conducted on the local scale at nine soil moisture measuring stations in and around the Vils test site that have been measuring between November 2007 and November 2010 and on the regional scale with handheld probes during the SMOS Validation Campaign 2010 on 8 days between May and July 2010 in an area considered representative for the central SMOS grid point in the Vils test site (Schlenz et al., 2011). They concluded that the uncertainties of the soil moisture modelling decrease from local to regional scale with a mean root-mean-squared error (RMSE) of 0.094 m^3 m^{-3} on the local scale and 0.040 m^3 m^{-3} on the regional scale. The mean R^2 on the local scale is 0.60. A bias leads to high RMSE values especially in wet conditions which leads to an underestimation in the reproduction of the seasonal soil moisture dynamics through PROMET.

A detailed analysis of the soil moisture modelling uncertainties described by Schlenz et al. (2011) showed that four of the five stations with the highest RMSE values are located on the same soil type. As the laboratory soil texture analysis from soil samples taken at these stations differed substantially from the soil texture used in the model parameterization, that is derived from the Global Soil Data Base the soil parameterization was improved for this soil type based on the laboratory results of a soil texture analysis. This new parameterization in addition to other model improvements led to a clear reduction of the soil moisture modelling uncertainties. The mean RMSE of those four stations decreased from $0.122\,\mathrm{m^3\,m^{-3}}$ to $0.057\,\mathrm{m^3\,m^{-3}}$ while the mean R^2 increased from 0.52 to 0.70. Overall this new parameterization leads to a mean RMSE over all stations of $0.065\,\mathrm{m^3\,m^{-3}}$ and a mean R^2 of 0.71. Applied to the whole test site this new parameterization leads to a slightly improved RMSE of $0.039\,\mathrm{m^3\,m^{-3}}$ on the regional scale. Figure 3 shows the comparison of the modelled and measured 5 cm soil moisture mean of the five soil moisture stations that are within a 20 km radius around SMOS ID 2027099 for 2011. The deviations between both data sets are small.

Loew and Schlenz (2011) have used an extended version of the triple collocation method (Miralles et al., 2010) to assess relative soil moisture errors of PROMET, the in situ measurements from the stations in the UDC and coarse scale satellite soil moisture products. They conclude that the soil moisture random error of PROMET is better than $0.025\,\mathrm{m^3\,m^{-3}}$ on the SMOS scale which is consistent with similar findings of Schlenz et al. (2011).

2.4.2 Radiative transfer model L-MEB

The microwave emission model L-MEB, which is also part of ESA's SMOS Level 2 soil moisture processor, is used to simulate L-band brightness temperatures from the continuous soil vegetation layer in the Upper Danube Catchment on a 1 km resolution. A comprehensive description of the model is given by Wigneron et al. (2007). This zero-order Tau (τ)–Omega (ω) radiative transfer model uses PROMET soil moisture, soil surface temperature and LAI fields as input for the modelling. The polarized

---

($p = h, v$) brightness temperature TB_P [K] is calculated through a sum of the three terms soil emission attenuated (scattered and absorbed) by the vegetation, direct vegetation emission and vegetation emission reflected by the soil and attenuated by the vegetation again:

$$\mathrm{TB}_P = (1 - \omega_p)(1 - \gamma_p)(1 + \gamma_p r_{\mathrm{Gp}})T_C + (1 - r_{\mathrm{Gp}})\gamma_p T_G \tag{5}$$

where γ_p is the vegetation attenuation factor [–] and ω_p is the vegetation single scattering albedo [–]; T_G and T_C are the effective temperature of the ground and the canopy [K], respectively. r_{GP} is the reflectivity of the rough soil [–] which is typically described as a function of the Fresnel reflectivities of a smooth surface, modified by a surface component. The vegetation attenuation factor γ_p is described as a function of the vegetation optical depth τ at nadir and the observation angle. The effective temperature of the ground, T_G, is calculated from the surface and deep (50 cm) soil temperatures by the approach of Wigneron et al. (2007) and T_C is approximated by PROMET's air temperature. The vegetation optical depth is calculated using LAI values from PROMET with the approach of Wigneron et al. (2007). The optical depth of forests is fixed to a defined value. The roughness parameter H_R over grass is soil moisture dependent (Saleh et al., 2009).

The land cover specific L-MEB parameters used for the modelling are summarized in Table 1, they are in line with the parameters used by Wigneron et al. (2007); Saleh et al. (2007); Grant et al. (2007) and have been taken from a compilation of parameterisations of L-MEB based on experimental studies (J.-P. Wigneron, personal communication, 2012) that forms the basis of the SMOS L2 processor parameterisation. These parameters agree mostly with the default parameters that are being used in the operational version of the SMOS L2 processor for Central European Crops (Kerr et al., 2011). The rape parameterisation developed by Schlenz et al. (2012) has been added.

As different authors have reported that it might be necessary to parameterize L-MEB locally to obtain optimal results (Panciera et al., 2009; Bircher et al., 2011), the radiative transfer modelling abilities of the coupled models PROMET and L-MEB have been

validated on the local scale by Schlenz et al. (2012) near Munich over a rape field and on the SMOS scale by Schlenz et al. (2011) in the Vils test site. To test the suitability of the L-MEB parameters under local conditions (Schlenz et al., 2011) have compared modelled brightness temperatures to airborne measurements of brightness temperatures from the airborne L-band radiometer EMIRAD (Skou et al., 2010) on basis of the SMOS ISEA grid for the look angles 0° and 40° for five days during the SMOS Validation Campaign 2010. They concluded that the model performs very well on three of the campaign days while on two days there are deviations between model results and measurements. RMSE values for this comparison at the central ISEA ID in the Vils test site (2027099) are 16.52 K and 13.14 K for horizontal and vertical polarization of the 40° look angle and 12.97 K and 12.09 K for horizontal and vertical polarization of the 0° look angle, respectively. Through the usage of the improved land surface model now using a dynamic vegetation model these error values have decreased substantially to 8.39 K and 8.98 K for horizontal and vertical polarization of the 40° look angle and 6.80 K and 6.45 K for the horizontal and vertical polarization of the 0° look angle, respectively. As EMIRAD is a reliable radiometer that has been thoroughly calibrated and used in a variety of studies it is used as reference here. These comparisons are thoroughly discussed in Sect. 3.1.

Schlenz et al. (2012) have developed a new L-MEB parameterization for winter rape and tested the suitability of it for soil moisture retrievals from ground based multiangular L-band brightness temperature data of a ELBARA II radiometer (Schwank et al., 2009) situated in Puch near Munich in the Upper Danube Catchment. They also analysed the sensitivity of L-MEB to different parameterisations under local conditions. They conclude that the soil moisture retrieval with L-MEB works satisfyingly over rape and that the optical depth parameterisation and the roughness parameterisation are crucial for the radiative transfer modelling. These results are consistent with a variety of studies that stress the importance of correct optical depth and roughness parameterization for radiative transfer modelling, e.g. Bircher et al. (2011), Panciera et al. (2009).

For further comparisons the modelled brightness temperature data were mapped onto the ISEA grid with the nearest neighbour method.

2.5 SMOS L1c data analysis

After the performance of the L-MEB parameterization under local conditions has been analysed with a comparison between modelled and airborne brightness temperatures these airborne brightness temperatures are also compared to SMOS L1c data during the SMOS Validation Campaign 2010. Afterwards SMOS L1c data are compared to modelled brightness temperatures for a range of look angles for the year 2011.

2.5.1 Comparison with airborne brightness temperatures during the SMOS Validation Campaign 2010

During the SMOS Validation Campaign 2010 airborne brightness temperatures are available for the Vils test site from the EMIRAD radiometer for five days on which SMOS morning overpasses have taken place. Unfortunately only on two of those days SMOS L1c data with sufficient quality are available, and only on 17 June a value for the 0° look angle is available. Those data sets of EMIRAD and SMOS measurements are compared for the five campaign days at the central ISEA grid point in the Vils test site for the two EMIRAD look angles 0° and 40°. As Bircher et al. (2011) found out that neither using the EMIRAD antenna pattern nor the SMOS antenna pattern for weighting the brightness temperatures for a similar comparison between SMOS L1c, EMIRAD and modelled brightness temperatures improved the results over applying simple means, the same simplification was applied here. The results are presented in Sect. 3.2.1.

2.5.2 Comparison with modelled brightness temperatures in 2011

To enable a longterm analysis of SMOS L1c brightness temperatures under varying soil moisture and vegetation conditions, they are compared to modelled brightness
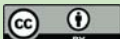
temperatures in 2011 from April to October on the basis of the ISEA grid to which the model data have been mapped with the nearest neighbour approach. For the ISEA grid points in the Vils test site these comparisons are performed for the angles 10°, 20°, 30°, 40° and 50° for both polarizations. They are presented and discussed in Sect. 3.2.2.

2.6 SMOS optical depth analysis

To study whether the optical depth values in the SMOS L2 soil moisture product that are obtained during the soil moisture retrieval contain valuable information, they are compared to modelled values of optical depth using vegetation parameters from the dynamic vegetation model PROMET for 2011. The modelled values are mapped to the ISEA grid using the nearest neighbour method and the time series for every ISEA grid point is compared to SMOS optical depth values. To test whether there is a relation between retrieved SMOS L2 soil moisture and optical depth the correlation for both data sets for 2011 is calculated. The results for the ISEA IDs in the Vils test site are presented and discussed in Sect. 3.3.

3 Results and discussion

3.1 Model validation and L-MEB parameterization under local conditions

In Sect. 2.4.1 it is reported that the land surface model PROMET and specifically the soil moisture submodel has been validated extensively in different studies and works well in the Upper Danube Catchment and especially the Vils test site. A RMSE of $0.039\,\mathrm{m^3\,m^{-3}}$ on the regional scale has been reported.

The radiative transfer modelling abilities under local conditions of the coupled models PROMET and L-MEB have been summarized in Sect. 2.4.2. To illustrate these results, Fig. 4 compares modelled brightness temperatures in the Vils test site on five days during the SMOS Validation Campaign 2010 with measurements from the airborne L-

band radiometer EMIRAD for the 40° look angle. The error bars indicate the standard deviations from the averaging.

The vertically polarized brightness temperature shows a relatively constant offset in the order of 5–10 K while the horizontally polarized brightness temperature does not. This can partly be explained with a systematic bias of $\sim 3.5\,\mathrm{K}$ that was observed for the EMIRAD 40° horizontal channel throughout the SMOS Validation Campaign 2010 as reported in Bircher et al. (2011). Since this only explains parts of the observed bias, other factors could also play a role here but due to the uncertainties related with the EMIRAD bias this issue is not further investigated. Possibly the L-MEB parameterisation could further be optimized. No systematic bias is observed for the 0° look angle (not shown), the RMSE is largely determined by deviations on the last day.

It is considered promising that on four of the five days the model works reliably despite contrasting soil moisture, temperature and vegetation conditions. This leads us to the overall conclusion that the coupled models work reliably and the parameterisations chosen for L-MEB are appropriate under the local conditions. Especially the roughness and vegetation optical depth parameterisation seem to be appropriate as the model performance does not change significantly during the first four days even though vegetation grows strongly during this time. For example, the mean vegetation height of all wheat fields in the focus areas increases from 40.2 cm to 77.9 cm during those four flight days. Growing vegetation increases the importance of correct vegetation parameterisation through an increase in vegetation optical depth. An incorrect soil roughness parameterisation would lead to a clear offset between model output and measurements in all angles and polarizations, especially at the beginning.

On the last day there is a considerable deviation between measurements and model output, that is also apparent for the 0° look angle (not shown). While the measured brightness temperatures decrease by about 15 K, the modelled vertically polarized brightness temperature decreases by only about 4 K and the horizontally polarized brightness temperature increases by about 5 K. It is not possible to give a simple explanation for this deviation between model output and measurements. Modelled soil

moisture and temperatures do not show any abnormality (soil moisture deviations between model and field measurement for the whole Vils test site are below $0.03\,m^3\,m^{-3}$ as for most of the other days, too). When compared to the earlier days the vegetation growth is considerably smaller between the last two days, all of the three most important plants wheat, maize and grass grow less than 8 cm on average in this time frame. A feature that is different on the last day in comparison to all other days is that the upper soil layer is very wet and that standing water is present in the area due to considerable precipitation events shortly before the EMIRAD overflight. This may be part of an explanation for the distinct behaviour of the brightness temperatures on this day. It is known that high soil moisture gradients in the upper soil layer, standing water and interception after precipitation events can lead to problems in the radiative transfer modelling which has also been reported by (Jackson et al., 2011; Rowlandson et al., 2012). Therefore the observed deviation does not necessarily point toward a parameterisation problem but should be further investigated. Overall the L-MEB parameterisation works very well under contrasting conditions and is considered appropriate under local conditions so that no further investigations on the parameterisation are performed. Yet, it is possible that the parameterisations could further be optimised under local conditions.

3.2 Analysis of SMOS L1c data

3.2.1 Comparison with airborne brightness temperatures during the SMOS Validation Campaign 2010

Figure 4 compares EMIRAD, SMOS and modelled brightness temperatures for the central ISEA grid point in the Vils test site for EMIRAD's 40° look angle at around 06:00 a.m. local time which corresponds to the SMOS morning overpass time. All 40° SMOS observations are larger than their EMIRAD counterpart while the 0° observation is lower. The RMSEs are 17.02 K and 28.05 K for the horizontal and vertical polarization of the 40° angle, respectively. For the 0° angle (not shown here) the RMSEs are 11.12 K and 11.55 K for the horizontal and vertical polarization, respectively. SMOS data show

the expected behaviour with vertically polarized brightness temperatures being higher than the horizontally polarized ones for 40° and both being essentially the same for 0°. But a RMSE between 11.12 K and 28.05 K can be considered a substantial deviation that may be attributed at least partly to RFI problems. Due to the small sample size this comparison is not considered reliable enough to draw further conclusions. Of course this comparison involves some approximations related to the different geometries of the two data sets. The SMOS L1c data are valid for a larger area than what is being mapped to each ISEA grid point in a nearest neighbour mapping approach. Hence the SMOS L1c data are valid for a larger area than the EMIRAD data. But as the Vils test site is very homogenous concerning soil, land cover, climate and topography it is assumed that this difference of geometries plays a very small role. In addition to that the centre of the SMOS footprint contributes more to the SMOS brightness temperature value than the edges due to the antenna pattern. This is being confirmed by the low variation of EMIRAD brightness temperatures of the neighbouring ISEA grid points. If a mean value of the three Vils ISEA grid points 2027099, 2026586 and 2026587 is calculated the deviation of this value from the 2027099 value never reaches 2 K. The homogeneity of the area is also the reason for the assumption that the EMIRAD data are representative for the whole area even though the EMIRAD flight lines do not cover the whole area. The flight pattern was planned carefully in order to best represent the variability present in the Vils test site.

3.2.2 Comparison with modelled brightness temperatures for the year 2011

To study SMOS L1c brightness temperatures in different seasons a long term comparison of SMOS L1c brightness temperature with modelled brightness temperatures has been performed for the central ISEA grid point for April to October 2011. The statistics for the analysis of modelled with SMOS L1c brightness temperatures are summarized in Table 2 for the look angles 10°, 20°, 30°, 40° and 50°.

It is apparent that the correlations between both data sets are only low to fair ($R < 0.45$) with RMSE values around 11–22 K. For horizontal polarization correlations

get better with increasing look angle, except for the 10° angle. The vertical polarization behaves similarly. These correlations are generally lower than the correlations between PROMET and SMOS L2 soil moisture which is 0.57 for the ID 2027099 in 2011 (dall'Amico, 2012). Concerning regressions and RMSE values the vertically polarized brightness temperatures perform better than the horizontally polarized ones. The bias for the horizontal polarization increases with increasing look angles. The regressions for the vertical polarization improve with increasing angles. Following radiative transfer theory, the horizontally polarized brightness temperatures are expected to decrease with increasing look angle, while the vertically polarized ones are expected to be generally higher and increase with increasing look angles. The expected behaviour is only observable for the vertically polarized observations.

In general the horizontally polarized brightness temperatures seem less reliable than the vertically polarized ones and the lower look angles perform inferior to the higher angles. One has to keep in mind that the significance of the results for the angles below 30° is lower due to the smaller sample size. The lower performance of SMOS data for the lower look angles is consistent with findings of Bircher et al. (2011) and may be related to the SMOS interferometric imaging technique.

As the correlations between SMOS L1c and modelled brightness temperatures are inferior to the correlations between SMOS L2 and modelled soil moisture, the problems in the SMOS L2 soil moisture product are considered to originate not primarily from a retrieval problem. A pure retrieval problem would mainly be visible in the L2 data, but not in L1c data, if the radiative transfer modelling works reliably. As it was shown in Sect. 3.1 that the radiative transfer modelling works reliably under most conditions in the study area, this points towards an RFI issue because it affects both L1c and L2 data. The mean positive bias in the SMOS brightness temperatures (compare Table 2) adds to this argumentation. Oliva et al. (2012) state that RFI can produce higher SMOS brightness temperatures which would lead to a dry bias in the soil moisture retrievals. The mean positive bias in the SMOS brightness temperatures can partly explain the observed dry bias in the SMOS L2 soil moisture products, that were found

---

by dall'Amico (2012). A more pronounced overestimation of brightness temperatures would be necessary to explain it entirely. However, as the SMOS L1c data processing described in Sect. 2.3 uses stricter filtering techniques than the official SMOS processor, it is possible that the bias is decreased due to a more efficient filtering of RFI.

Figures 5–8 show both time series for the 20° and 40° look angles for both polarizations from April to October 2011 and Fig. 9 shows the scatter plots for the same comparisons. The error bars in Figs. 5–8 represent the standard deviation of the spatial (PROMET) and angular (SMOS) averaging of the data. The PROMET standard deviations are relatively large due to the high spatial resolution of PROMET which leads to very different land cover classes being averaged (e.g. bare soil and forest). The behaviour of the additional look angles, that were modelled, is analogue to the 20° and 40° comparisons (not shown). Due to orbit geometry there are less SMOS observations available for 20° than for 40°. For the angles 10° to 30° in the horizontal polarization the SMOS brightness temperatures are considerably lower than the modelled ones for the summer months between end of May and end of August. For the other months it is the other way round for all angles. For the angles 40° and 50° both data sets have comparable mean values for the summer months. For vertical polarization the behaviour is similar. PROMET standard deviations are smaller in the summer months from around mid of June until mid of August because the optical depth variations are smaller during this time as most crops have relatively high LAI values (compare Fig. 10). In August winter wheat is being harvested leaving bare soil fields while maize shows very high LAI values, therefore the standard deviation increases substantially. If the other two ISEA IDs in the Vils test site 2026586 and 2026587 are considered the big picture for the brightness temperature comparison is very similar but the performance concerning correlation, RMSE and regression tends to be lower (not shown), which is analogue to SMOS L2 soil moisture data performance.

The seasonal behaviour of SMOS is not as expected. The expected increase of brightness temperatures in summer is not at all visible due to a sharp drop in brightness temperatures at the beginning of June. This seasonal behaviour is not observable in

the model data that serve as input for L-MEB. Soil moisture modelling for example seems to work equally well before and after the drop (Fig. 3). The drop in brightness temperatures coincides roughly with the end of the pronounced drying period in April and May, but obviously the model data does not react as extreme to the increase in soil moisture as the SMOS data. Obviously there is either a pronounced problem with the brightness temperature data that may be linked to RFI or an unresolved radiative transfer problem. As it has been shown in Sect. 3.1 that the radiative transfer modelling works reliably, it is concluded that these problems are also related to RFI.

Of course this comparison involves the same approximations that are mentioned in the previous section that are related to the different geometries of the data sets compared. But due to the already demonstrated homogeneity of the Vils test site this is not expected to have a substantial impact.

For the interpretation of these results it is important to keep the uncertainties in mind that are related to the modelling approach. In Sect. 2.4.1 it is shown that the uncertainties of the land surface model have been assessed thoroughly and are considered to be small. Soil moisture, temperature and vegetation modelling work reliably. The radiative transfer modelling uncertainties are assessed in Sect. 2.4.2 in May and June 2010 in the study area. Under contrasting soil moisture, vegetation and temperature conditions it works reliably in most instances with brightness temperature RMSE values between 6 K and 9 K. Parts of these deviations can be explained with a known offset in the reference radiometer. The comparisons in this section show considerably larger deviations during the same time of year. As both results were obtained under similar conditions in the same area, the radiative transfer modelling uncertainties are considered to play a minor role here.

3.3 Analysis of SMOS optical depth Tau

As the vegetation optical depth plays an important role in the SMOS soil moisture retrieval and could prove to be a valuable source of information about vegetation characteristics, it has been analysed for the year 2011. Figure 10 shows the time series of the

---

comparison between modelled and SMOS L2 optical depth for low vegetation for April to October 2011 at the central ISEA ID in the Vils test site. Error bars indicate the DQX value for SMOS and the standard deviation of the averaging for PROMET. Analogue to the brightness temperatures, the PROMET standard deviations are relatively high due to the high spatial resolution of PROMET. The correlation coefficient for this comparison is 0.33 and the bias (SMOS-PROMET) 0.18. The comparison looks similar when the two additional ISEA IDs in the Vils test site are considered. SMOS values are generally too high although the correlation coefficients differ for the IDs (correlation coefficient: -0.27 and 0.03 for ID 2026587 and 2026586, respectively; bias: 0.10 and 0.13 for ID 2026587 and 2026586, respectively) (not shown). The seasonal behaviour is different from ID to ID, while some peaks are constant in time. The seasonal pattern of vegetation optical depth for a temperate region with a high percentage of crops consists of an increase from spring until summer during the crop growth phase and a decrease in fall during ripening and harvesting. This is not clearly apparent in the SMOS data. The increase in April and May seems to be captured as well as a decrease in October but the variability of SMOS optical depth appears very high with several peaks throughout the year compared to typical vegetation phenology. The mean value of 0.40 is relatively high when compared to model simulations and typical values found in literature that range between maximum values of 0.3 and 0.4 for low vegetation (Wigneron et al., 2007; Saleh et al., 2007). A visual comparison to MODIS NDVI data from (ORNL-DAAC, 2012) did not deliver any similarity with SMOS optical depth either. It does not seem to have a physical meaning which was also found by (Jackson et al., 2011) in the US. The high variability, the unclear seasonal pattern and the high values of optical depth could indicate that SMOS optical depth also depends on other parameters than vegetation. Possibly RFI in the brightness temperatures or parameters in the radiative transfer modelling that are compensated by Tau could play a role here.

To test whether there is a relationship between SMOS retrieved soil moisture and optical depth, both data sets were compared. Although a visual comparison of the time series does not allow any conclusions, the scatter plot (Fig. 11) shows a clear

relationship with a correlation coefficient of 0.65, which is similar for the other Vils IDs. This is the largest correlation coefficient determined in the whole study and per se surprising as soil moisture and optical depth are considered independent variables in our area. This clearly indicates a retrieval problem. Modelled soil moisture and optical depth show no significant correlation ($R = 0.053$) for the same comparison.

4   Conclusion and outlook

The land surface model PROMET and the radiative transfer model L-MEB have been coupled and used as a tool for the analysis of SMOS passive microwave satellite observations. The coupled models have been shown to work well in determining the L-band microwave emission under varying soil moisture, vegetation and temperature conditions during the SMOS Validation Campaign 2010. Their output has been compared to ground data and airborne L-band brightness temperature measurements. A considerable part of the observed brightness temperature RMSE, which is around 6 K–9 K, is attributed to a known bias in the airborne L-band measurements. Therefore the L-MEB parameterizations used in this study are considered reliable enough to be used for SMOS validation activities. However, a further optimisation under local conditions may still be possible. A known uncertainty factor that should further be investigated is the brightness temperature behaviour shortly after precipitation events.

SMOS L1c brightness temperature data have been compared to airborne brightness temperatures on two days during the SMOS Validation Campaign 2010 from which no reliable conclusions can be drawn due to the small data set.

Next, an extensive comparison of SMOS L1c with modelled brightness temperatures from April to October 2011 was performed in the Vils test site. SMOS L1c brightness temperatures do not show the expected seasonal behaviour and are positively biased. SMOS L1c data do not perform better than L2 soil moisture data in the Vils test site, which could have pointed towards a pure retrieval problem. It is concluded that RFI is responsible for most of the observed problems in the SMOS L2 soil moisture product.

This is consistent with the observed dry bias in the SMOS L2 soil moisture products which can be related to RFI as stated by (Oliva et al., 2012). It is confirmed that the brightness temperature data from the lower SMOS look angles are less reliable which has also been reported by (Bircher et al., 2011). This information could be used to improve the brightness temperature data filtering before the SMOS soil moisture retrieval.

SMOS L2 optical depth values have been compared to modelled data using vegetation parameters from the dynamic vegetation model in PROMET. SMOS optical depth does not seem to be a reliable source of information about vegetation characteristics due to missing seasonal behaviour and very high values. This could originate from RFI or soil moisture retrieval problems. Indeed a strong correlation between SMOS L2 soil moisture and optical depth was found that was not expected ($R = 0.65$). This points clearly towards retrieval problems and should be further investigated.

As it has been shown that the radiative transfer modelling abilities of the coupled models are reliable in most instances under local conditions when compared to airborne data, it seems probable that RFI is responsible for most of the observed problems in the SMOS data. Therefore RFI mitigation efforts should be continued to improve SMOS data quality.

The clear improvement in SMOS L2 soil moisture performance from 2010 to 2011 that is shown by (dall'Amico et al., 2011a) and (dall'Amico, 2012) demonstrates that significant improvements in the performance of the SMOS satellite products are possible during the first years of such a mission. In other parts of the world, the SMOS L2 soil moisture product performs very well. (Jackson et al., 2011) e.g. state that the RMSE of the comparison between SMOS L2 soil moisture and measurements in four catchments in the US are $0.043\,\mathrm{m^3\,m^{-3}}$. This demonstrates that the SMOS soil moisture retrieval can work very reliably if there is no RFI. To study the potential origin of problems in the SMOS L2 soil moisture product, coupled land surface and radiative transfer models are helpful.

The value of coupled land surface and radiative transfer models for the validation and analysis of passive microwave remote sensing data has been shown in this study. The

Discussion Paper | Discussion Paper | Discussion Paper | Discussion Paper | Discussion Paper

HESSD

9, 1–48, 2012

Analysis of SMOS brightness temperature...

F. Schlenz et al.

Title Page

Abstract | Introduction

Conclusions | References

Tables | Figures

◄ | ►

Back | Close

Full Screen / Esc

Printer-friendly Version

Interactive Discussion

models made an extensive SMOS data analysis possible that would have been limited to a few days of distributed ground and airborne data without them. Even though an extensive field campaign was conducted, hardly any conclusions could be drawn from this without the models.

In a next step the coupled models could be used for different soil moisture retrievals from SMOS L1c data to assess the potential of improvements in the SMOS L2 soil moisture product.

References

Albergel, C., Calvet, J.-C., de Rosnay, P., Balsamo, G., Wagner, W., Hasenauer, S., Naeimi, V., Martin, E., Bazile, E., Bouyssel, F., and Mahfouf, J.-F.: Cross-evaluation of modelled and remotely sensed surface soil moisture with in situ data in southwestern France, Hydrol. Earth Syst. Sci., 14, 2177–2191, doi:10.5194/hess-14-2177-2010, 2010.

Albergel, C., Zakharova, E., Calvet, J.-C., Zribi, M., Pardé, M., Wigneron, J.-P., Novello, N., Kerr, Y., Mialon, A., and Fritz, N.-E.-D.: A first assessment of the SMOS data in Southwestern France using in situ and airborne soil moisture estimates: the CAROLS airborne campaign, Remote Sens. Environ., 115, 2718–2728, doi:10.1016/j.rse.2011.06.012, 2011.

Discussion Paper | Discussion Paper | Discussion Paper | Discussion Paper | Discussion Paper

HESSD

9, 1–48, 2012

Analysis of SMOS brightness temperature...

F. Schlenz et al.

Title Page

Abstract | Introduction

Conclusions | References

Tables | Figures

◄ | ►

Back | Close

Full Screen / Esc

Printer-friendly Version

Interactive Discussion

Albergel, C., de Rosnay, P., Gruhier, C., Muñoz-Sabater, J., Hasenauer, S., Isaksen, L., Kerr, Y., and Wagner, W.: Evaluation of remotely sensed and modelled soil moisture products using global ground-based in situ observations, Remote Sens. Environ., 118, 215–226, doi:10.1016/j.rse.2011.11.017, 2012.

Bach, H. and Mauser, W.: Methods and examples for remote sensing data assimilation in land surface process modeling, IEEE T. Geosci. Remote, 41, 1629–1637, 2003.

Bach, H., Braun, M., Lampart, G., and Mauser, W.: Use of remote sensing for hydrological parameterisation of Alpine catchments, Hydrol. Earth Syst. Sci., 7, 862–876, doi:10.5194/hess-7-862-2003, 2003.

Balling, J. E., Kristensen, S. S., Sobjaerg, S. S., and Skou, N.: Surveys and analysis of RFI in preparation for SMOS: results from airborne campaigns and first impressions from satellite data, IEEE T. Geosci. Remote, 49, 4821–4831, 2011.

Bartalis, Z., Wagner, W., Anderson, C., Bonekamp, H., Naeimi, V., and Hasenauer, S.: Validation of coarse resolution microwave soil moisture products, Int. Geosci. Remote Se., II-173–176, 2008.

Bircher, S., Balling, J. E., Skou, N., and Kerr, Y.: SMOS validation by means of an airborne campaign in the Skjern River catchment, Western Denmark, IEEE T. Geosci. Remote, 99, 1–15, doi:10.1109/TGRS.2011.2170177, 2011. TS2

Bolten, J. D., Crow, W. T., Xiwu, Z., Jackson, T. J., and Reynolds, C. A.: Evaluating the utility of remotely sensed soil moisture retrievals for operational agricultural drought monitoring, IEEE J. Sel. Top. Appl., 3, 57–66, 2010.

Brooks, R. and Corey, A.: Hydraulic properties of porous media, Tech. Rep., Hydrology Paper 3, Colorado State University, Fort Collins, Colorado, 1964.

BÜK 1000 Bodenübersichtskarte Deutschland 1 : 1 000 000: available at: http://www.bgr.bund.de/cln_006/nn_325414/DE/Themen/Boden/Produkte/Karten/BUEK_1000.html, 1997. TS3

Crow, W. T., Ryu, D., and Famiglietti, J. S.: Upscaling of field-scale soil moisture measurements using distributed land surface modeling, Adv. Water Resourc., 28, 1–14, doi:10.1016/j.advwatres.2004.10.004, 2005.

dall'Amico, J.: Multiscale analysis of soil moisture using satellite and aircraft microwave remote sensing, in situ measurements and numerical modeling, Ph.D., Department for Geography, Ludwig Maximilians University, Munich, Germany, 2012.

dall'Amico, J. T., Schlenz, F., Loew, A., and Mauser, W.: First results of SMOS soil moisture validation in the Upper Danube catchment, IEEE T. Geosci. Remote, 1–10, in press, 2011a. TS4

Please note the remarks at the end of the manuscript.

dall'Amico, J. T., Schlenz, F., Loew, A., Mauser, W., Kainulainen, J., Balling, J., and Bouzinac, C.: The SMOS Validation Campaign 2010 in the Upper Danube catchment: a data set for studies of soil moisture, brightness temperature and their spatial variability over a heterogeneous land surface, IEEE T. Geosci. Remote, accepted, 2011b. TS5

Delwart, S., Bouzinac, C., Wursteisen, P., Berger, M., Drinkwater, M., Martin-Neira, M., and Kerr, Y. H.: SMOS validation and the COSMOS campaigns, IEEE T. Geosci. Remote, 46, 695–704, 2008.

Dirmeyer, P. A.: Using a global soil wetness dataset to improve seasonal climate simulation, J. Climate, 13, 2900–2922, doi:10.1175/1520-0442(2000)013¡2900:UAGSWD¿2.0.CO;2, 2000.

Dorigo, W. A., Wagner, W., Hohensinn, R., Hahn, S., Paulik, C., Xaver, A., Gruber, A., Drusch, M., Mecklenburg, S., van Oevelen, P., Robock, A., and Jackson, T.: The International Soil Moisture Network: a data hosting facility for global in situ soil moisture measurements, Hydrol. Earth Syst. Sci., 15, 1675–1698, doi:10.5194/hess-15-1675-2011, 2011. TS6

Entekhabi, D., Asrar, G. R., Betts, A. K., Beven, K. J., Bras, R. L., Duffy, C. J., Dunne, T., Koster, R. D., Lettenmaier, D. P., Mclaughlin, D. B., Shuttleworth, W. J., Van Genuchten, M. T., Wei, M.-Y., and Wood, E. F.: An agenda for land-surface hydrology research and a call for the second international hydrological decade, B. Am. Meteorol. Soc., 80, 2043–2057, 1999.

ESA: Mission Objectives and Scientific Requirements of the Soil Moisture and Ocean Salinity (SMOS) Mission, Version 5, European Space Agency (ESA), 2002.

Grant, J. P., Wigneron, J. P., Van de Griend, A. A., Kruszewski, A., Søbjærg, S. S., and Skou, N.: A field experiment on microwave forest radiometry: L-band signal behaviour for varying conditions of surface wetness, Remote Sens. Environ., 109, 10–19, doi:10.1016/j.rse.2006.12.001, 2007.

Gruhier, C., de Rosnay, P., Hasenauer, S., Holmes, T., de Jeu, R., Kerr, Y., Mougin, E., Njoku, E., Timouk, F., Wagner, W., and Zribi, M.: Soil moisture active and passive microwave products: intercomparison and evaluation over a Sahelian site, Hydrol. Earth Syst. Sci., 14, 141–156, doi:10.5194/hess-14-141-2010, 2010.

Hank, T.: A Biophysically Based Coupled Model Approach for the Assessment of Canopy Processes under Climate Change Conditions, Phd, Department for Geography, Ludwig Maximilians University, Munich, Germany, 2008.

Hornbuckle, B. K., Rowlandson, T. L., Patton, J. C., and Bramer, L. M.: How is the angular signature of SMOS brightness temperature different in the morning and evening?, Int. Geosci. Remote Se., 3125–3128, 2011. TS7

Jackson, T. J., Bindlish, R., Cosh, M. H., Zhao, T., Starks, P. J., Bosch, D. D., Seyfried, M., Moran, M. S., Goodrich, D. C., Kerr, Y. H., and Leroux, D.: Validation of Soil Moisture and Ocean Salinity (SMOS) soil moisture over watershed networks in the US, IEEE T. Geosci. Remote, 1–14, 2011. TS8

Juglea, S., Kerr, Y., Mialon, A., Wigneron, J.-P., Lopez-Baeza, E., Cano, A., Albitar, A., Millan-Scheiding, C., Carmen Antolin, M., and Delwart, S.: Modelling soil moisture at SMOS scale by use of a SVAT model over the Valencia Anchor Station, Hydrol. Earth Syst. Sci., 14, 831–846, doi:10.5194/hess-14-831-2010, 2010.

Kerr, Y. TS9, Waldteufel, P., Richaume, P., Davenport, P., Ferrazzoli, P., and Wigneron, J.-P.: SMOS level 2 processor soil moisture algorithm theoretical basis document (ATBD) V 3.5, CBSA, UoR, TV and INRA, Toulouse, 2011.

Kerr, Y. H., Waldteufel, P., Wigneron, J. P., Delwart, S., Cabot, F., Boutin, J., Escorihuela, M. J., Font, J., Reul, N., Gruhier, C., Juglea, S. E., Drinkwater, M. R., Hahne, A., Martín-Neira, M., and Mecklenburg, S.: The SMOS mission: new tool for monitoring key elements of the global water cycle, Proc. IEEE, 98, 666–687, 2010.

Loew, A.: Impact of surface heterogeneity on surface soil moisture retrievals from passive microwave data at the regional scale: the Upper Danube case, Remote Sens. Environ., 112, 231–248, doi:10.1016/j.rse.2007.04.009, 2008.

Loew, A. and Schlenz, F.: A dynamic approach for evaluating coarse scale satellite soil moisture products, Hydrol. Earth Syst. Sci., 15, 75–90, doi:10.5194/hess-15-75-2011, 2011.

Loew, A., Ludwig, R., and Mauser, W.: Derivation of surface soil moisture from ENVISAT ASAR wide swath and image mode data in agricultural areas, IEEE T. Geosci. Remote, 44, 889–899, 2006.

Ludwig, R. and Mauser, W.: Modelling catchment hydrology within a GIS based SVAT-model framework, Hydrol. Earth Syst. Sci., 4, 239–249, doi:10.5194/hess-4-239-2000, 2000.

Ludwig, R., Mauser, W., Niemeyer, S., Colgan, A., Stolz, R., Escher-Vetter, H., Kuhn, M., Reichstein, M., Tenhunen, J., Kraus, A., Ludwig, M., Barth, M., and Hennicker, R.: Web-based modelling of energy, water and matter fluxes to support decision making in mesoscale catchments – the integrative perspective of GLOWA-Danube, Phys. Chem. Earth, 28, 621–634, 2003.

Title Page

Abstract | Introduction

Conclusions | References

Tables | Figures

◄◄ | ►►

◄ | ►

Back | Close

Full Screen / Esc

Printer-friendly Version

Interactive Discussion

Mauser, W. and Bach, H.: PROMET – Large scale distributed hydrological modelling to study the impact of climate change on the water flows of mountain watersheds, J. Hydrol., 376, 362–377, 2009.

Mauser, W. and Schädlich, S.: Modelling the spatial distribution of evapotranspiration on different scales using remote sensing data, J. Hydrol., 212–213, 250–267, doi:10.1016/s0022-1694(98)00228-5, 1998.

Miralles, D. G., Crow, W. T., and Cosh, M. H.: Estimating spatial sampling errors in coarse-scale soil moisture estimates derived from point-scale observations, J. Hydrometeorol., 11, 1423–1429, doi:10.1175/2010JHM1285.1, 2010.

Montzka, C., Bogena, H., Weihermueller, L., Jonard, F., Dimitrov, M., Bouzinac, C., Kainulainen, J., Balling, J. E., Vanderborght, J., and Vereecken, H.: Radio brightness validation on different spatial scales during the SMOS validation campaign 2010 in the Rur catchment, Germany, Int. Geosci. Remote Se., 3760–3763, 2011. TS10

Muerth, M.: A Soil Temperature and Energy Balance Model for Integrated Assessment of Global Change Impacts at the regional scale, Phd, Department for Geography, Ludwig Maximilians University, Munich, Germany, 2008.

Oliva, R., Daganzo-Eusebio, E., Kerr, Y. H., Mecklenburg, S., Nieto, S., Richaume, P., and Gruhier, C.: SMOS radio frequency interference scenario: status and actions taken to improve the RFI environment in the 1400–1427-MHz passive band, IEEE T. Geosci. Remote, 1–13, 2012. TS11

Panciera, R., Walker, J. P., and Merlin, O.: Improved understanding of soil surface roughness parameterization for L-band passive microwave soil moisture retrieval, IEEE Geosci. Remote S., 6, 625–629, 2009.

Parrens, M., Zakharova, E., Lafont, S., Calvet, J.-C., Kerr, Y., Wagner, W., and Wigneron, J.-P.: Comparing soil moisture retrievals from SMOS and ASCAT over France, Hydrol. Earth Syst. Sci., 16, 423–440, doi:10.5194/hess-16-423-2012, 2012.

Pauwels, V. R. N., Timmermans, W., and Loew, A.: Comparison of the estimated water and energy budgets of a large winter wheat field during AgriSAR 2006 by multiple sensors and models, J. Hydrol., 349, 425–440, doi:10.1016/j.jhydrol.2007.11.016, 2008.

Philip, J.: The theory of infiltration: 1. the infiltration equation and its solution, Soil Sci., 83, 345–357, 1957.

Prigent, C., Aires, F., Rossow, W. B., and Robock, A.: Sensitivity of satellite microwave and infrared observations to soil moisture at a global scale: relationship of satellite

observations to in situ soil moisture measurements, J. Geophys. Res., 110, D07110, doi:10.1029/2004jd005087, 2005.

Probeck, M., Ludwig, R., and Mauser, W.: Fusion of NOAA-AVHRR imagery and geographical information system techniques to derive subscale land cover information for the upper Danube watershed, Hydrol. Process., 19, 2407–2418, doi:10.1002/hyp.5892, 2005.

Rowlandson, T. L., Hornbuckle, B. K., Bramer, L. M., Patton, J. C., and Logsdon, S. D.: Comparisons of evening and morning SMOS passes over the Midwest United States, IEEE T. Geosci. Remote, 1–12, 2012. TS12

Saleh, K., Wigneron, J. P., Waldteufel, P., de Rosnay, P., Schwank, M., Calvet, J. C., and Kerr, Y. H.: Estimates of surface soil moisture under grass covers using L-band radiometry, Remote Sens. Environ., 109, 42–53, doi:10.1016/j.rse.2006.12.002, 2007.

Saleh, K., Kerr, Y. H., Richaume, P., Escorihuela, M. J., Panciera, R., Delwart, S., Boulet, G., Maisongrande, P., Walker, J. P., Wursteisen, P., and Wigneron, J. P.: Soil moisture retrievals at L-band using a two-step inversion approach (COSMOS/NAFE'05 experiment), Remote Sens. Environ., 113, 1304–1312, doi:10.1016/j.rse.2009.02.013, 2009.

Schlenz, F., dall'Amico, J. T., Loew, A., and Mauser, W.: Uncertainty assessment of the SMOS validation in the Upper Danube Catchment, IEEE T. Geosci. Remote, 1–13, in press, 2011. TS13

Schlenz, F., Fallmann, J., Marzahn, P., Loew, A., and Mauser, W.: Characterization of rape field microwave emission and implications to surface soil moisture retrievals, Remote Sens., 4, 247–270, 2012.

Schwank, M., Wiesmann, A., Werner, C., Mätzler, C., Weber, D., Murk, A., Völksch, I., and Wegmüller, U.: ELBARA II, an L-band radiometer system for soil moisture research, Sensors, 10, 584–612, 2009.

Skou, N., Misra, S., Balling, J. E., Kristensen, S. S., and Sobjaerg, S. S.: L-band RFI as experienced during airborne campaigns in preparation for SMOS, IEEE T. Geosci. Remote, 48, 1398–1407, 2010.

Strasser, G., Schneider, K., and Mauser, W.: The use of ERS SAR data derived soil moisture distributions for SVAT-model validation, Int. Geosci. Remote Se., 1921–1923, vol. 1924, 1999. TS14

Strasser, U. and Mauser, W.: Modelling the spatial and temporal variations of the water balance for the Weser catchment 1965–1994, J. Hydrol., 254, 199–214, doi:10.1016/s0022-1694(01)00492-9, 2001.
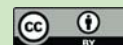
Wigneron, J. P., Kerr, Y., Waldteufel, P., Saleh, K., Escorihuela, M. J., Richaume, P., Ferraz-zoli, P., de Rosnay, P., Gurney, R., Calvet, J. C., Grant, J. P., Guglielmetti, M., Hornbuckle, B., Mätzler, C., Pellarin, T., and Schwank, M.: L-band Microwave Emission of the Biosphere (L-MEB) model: description and calibration against experimental data sets over crop fields, Remote Sens. Environ., 107, 639–655, doi:10.1016/j.rse.2006.10.014, 2007.

HESSD

9, 1–48, 2012

Analysis of SMOS brightness temperature...

F. Schlenz et al.

Title Page

Abstract | Introduction

Conclusions | References

Tables | Figures

|◄ | ►|

◄ | ►

Back | Close

Full Screen / Esc

Printer-friendly Version

Interactive Discussion

Table 1. The land cover specific L-MEB parameters used for the radiative transfer modelling.

	H_R	Q_R	NRh/NRv	tt$h$/tt$v$	ωh/ωv	b'	b''
Bare soil	0.1	0	0/–1	1/1	0/0	0	0
Crops general	0.15	0	0/–1	1/1	0/0	0.05	0
Wheat	0.1	0	0/–1	1/8	0/0	0.035	0
Corn	0.6	0	0/–1	2/1	0.05/0.05	0.05	0
Grass	1.3–1.13*SM	0	1/0	1/1	0/0.05	0.04	0.03
Coniferous	1.2	0	1.8/2	0.9/0.8	0.07/0.07	τNAD = 0.65	0
Deciduous	1.	0	1/2	0.6/0.5	0.07/0.07	τNAD = 1	0
Rape	0.93	0	0/–1	1/1	0/0	0.09	0.08

HESSD

9, 1–48, 2012

Analysis of SMOS brightness temperature...

F. Schlenz et al.

Title Page

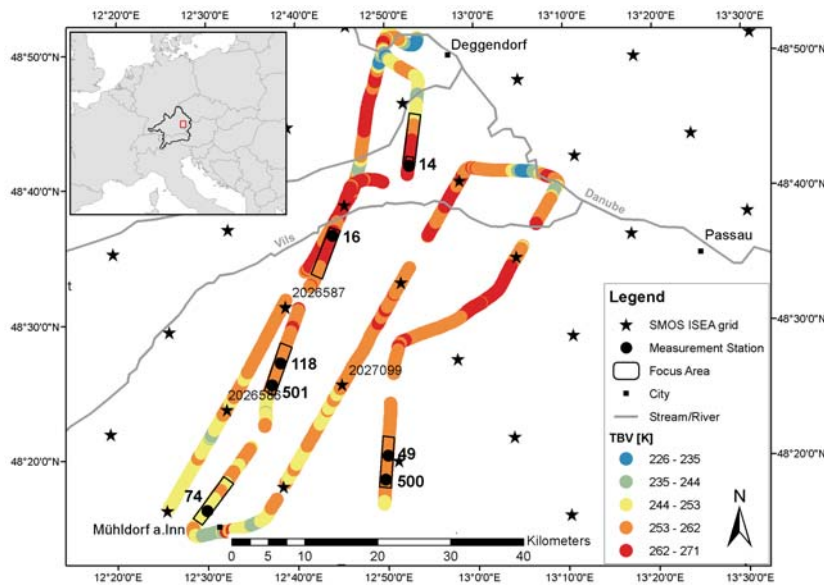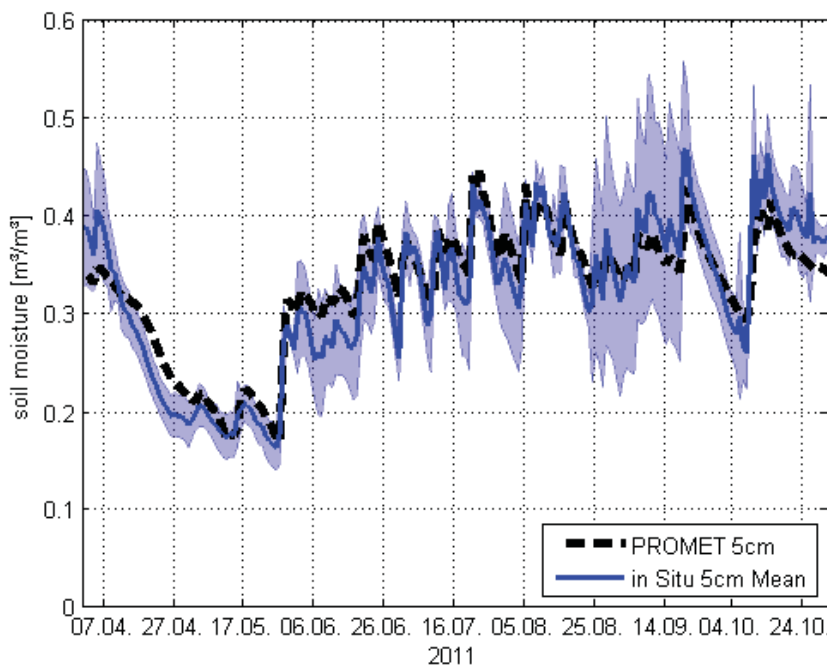Abstract | Introduction

Conclusions | References

Tables | Figures

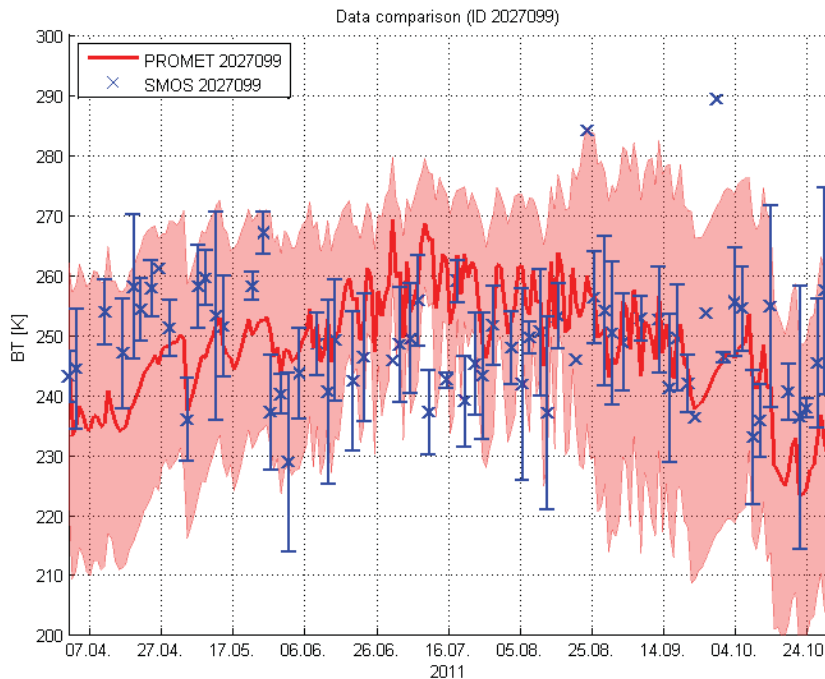|◄ | ►|

◄ | ►

Back | Close

Full Screen / Esc

Printer-friendly Version

Interactive Discussion

Table 2. The statistics for the comparison of SMOS L1c and modelled brightness temperature for different look angles for the central ISEA ID in the Vils test site (2027099) in 2011.

Look angle	R [−]	RMSE [K]	Gain [−]	Offset (SMOS-PROMET) [K]	Mean (STDV) SMOS [K]	Mean (STDV) PROMET [K]	N
TBH10	0.17	12.09	0.14	−4.13	245.24 (7.86)	249.37 (8.97)	35
TBH20	0.13	13.14	0.13	1.0	248.97 (10.24)	247.97 (9.47)	67
TBH30	0.29	12.46	0.27	4.04	249.68 (9.79)	245.64 (10.39)	99
TBH40	0.3	17.69	0.27	11.58	254.08 (10.82)	242.50 (11.91)	130
TBH50	0.41	21.82	0.33	17.94	256.85 (11.05)	238.91 (14.20)	77
TBV10	0.29	10.50	0.25	2.73	252.97 (8.21)	250.24 (8.65)	35
TBV20	0.1	12.71	0.11	2.35	255.66 (9.93)	253.31 (8.60)	67
TBV30	0.3	11.38	0.38	1.05	259.03 (10.63)	257.98 (8.40)	99
TBV40	0.39	10.99	0.56	0.94	264.69 (11.30)	263.75 (7.83)	130
TBV50	0.36	12.77	0.66	−5.52	264.57 (12.32)	270.09 (6.77)	77
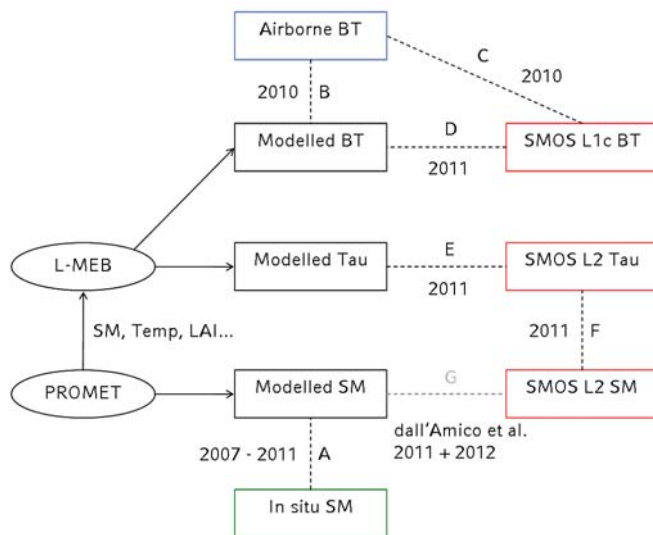
Fig. 1. A flowchart illustrating the different data sets (boxes) and comparisons (dashed lines) in this paper. Black boxes depict modelled data sets provided by the models PROMET and L-MEB, red boxes represent SMOS data, the blue box airborne data and the green box in situ data. The comparisons consist of: (A) land surface model validation with in situ soil moisture (SM) from the years 2007–2011; (B) radiative transfer model validation with airborne EMIRAD brightness temperatures (BT) during the SMOS Validation Campaign 2010; (C) analysis of SMOS L1c brightness temperatures with EMIRAD data during the SMOS Validation Campaign 2010; (D) analysis of SMOS L1c with modelled brightness temperatures throughout the vegetation period 2011; (E) analysis of SMOS L2 optical depth (Tau) with modelled optical depth Tau throughout the vegetation period 2011; (F) comparison of SMOS L2 optical depth and SMOS L2 soil moisture throughout the vegetation period 2011; The analysis of SMOS L2 soil moisture with modelled soil moisture (G) has already been performed by dall'Amico et al. (2011a) and dall'Amico (2012) and is not subject of this paper.

Fig. 2. The Vils test site with focus areas, soil moisture measuring stations, SMOS ISEA IDs and EMIRAD TBV data from 12 June 2010. The small overview map in the upper left corner shows the location of the Upper Danube Catchment (black) and the Vils test site (red) in Central Europe.

Fig. 3. A comparison of modelled and measured soil moisture in 5 cm depth from April to October 2011. Shown are the mean values of the five soil moisture stations that are within 20 km radius of the SMOS ID 2027099. ± one standard deviation are indicated for the in situ data.
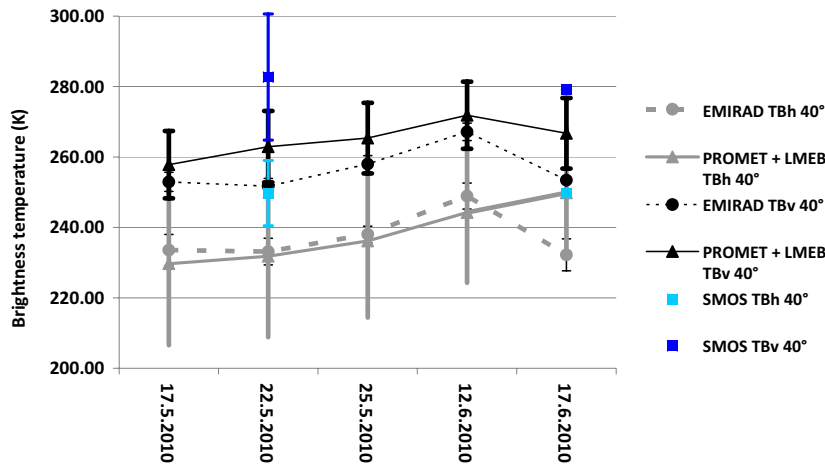
Fig. 4. A comparison of modelled (triangles) and measured (EMIRAD, circles) 40° brightness temperatures on the five campaign days of the SMOS Validation Campaign 2010 based on the central ISEA grid point in the Vils test site (2027099). For completion the SMOS L1c brightness temperatures for 40° are also plotted for the two days they are available (squares). All data sets are valid roughly for 06:00 a.m. local time.

Fig. 5. The time series of modelled and SMOS L1c brightness temperatures for April to October 2011 for the 20° look angle and horizontal polarization for the central ISEA grid point in the Vils test site. Error bars indicate ± one standard deviation for angular (SMOS) and spatial (model) averaging.

Fig. 6. The time series of modelled and SMOS L1c brightness temperatures for April to October 2011 for the 40° look angle and horizontal polarization for the central ISEA grid point in the Vils test site. Error bars indicate ± one standard deviation for angular (SMOS) and spatial (model) averaging.
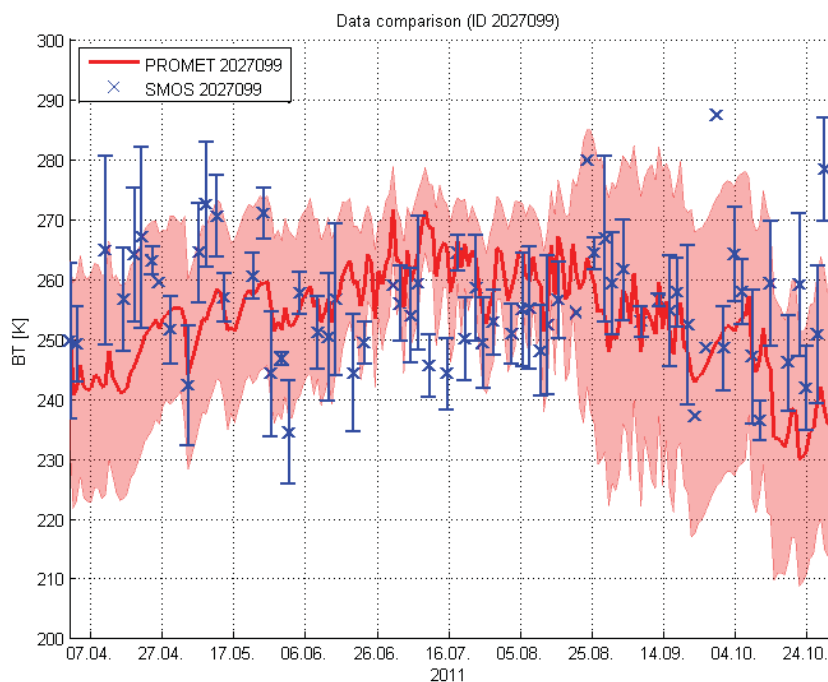
Fig. 7. The time series of modelled and SMOS L1c brightness temperatures for April to October 2011 for the 20° look angle and vertical polarization for the central ISEA grid point in the Vils test site. Error bars indicate ± one standard deviation for angular (SMOS) and spatial (model) averaging.

Fig. 8. The time series of modelled and SMOS L1c brightness temperatures for April to October 2011 for the 40° look angle and vertical polarization for the central ISEA grid point in the Vils test site. Error bars indicate ± one standard deviation for angular (SMOS) and spatial (model) averaging.
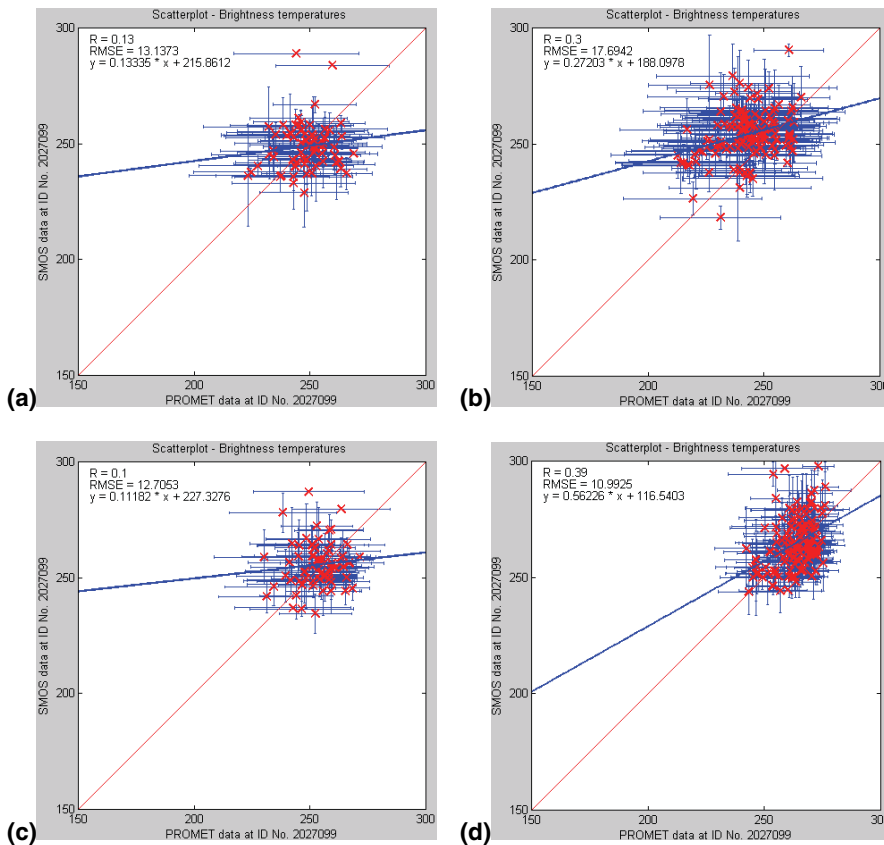
Fig. 9. Scatter plots for the comparison of modelled vs. SMOS L1c brightness temperatures for the look angles H20° **(a)**, H40° **(b)**, V20° **(c)**, V40° **(d)**.
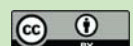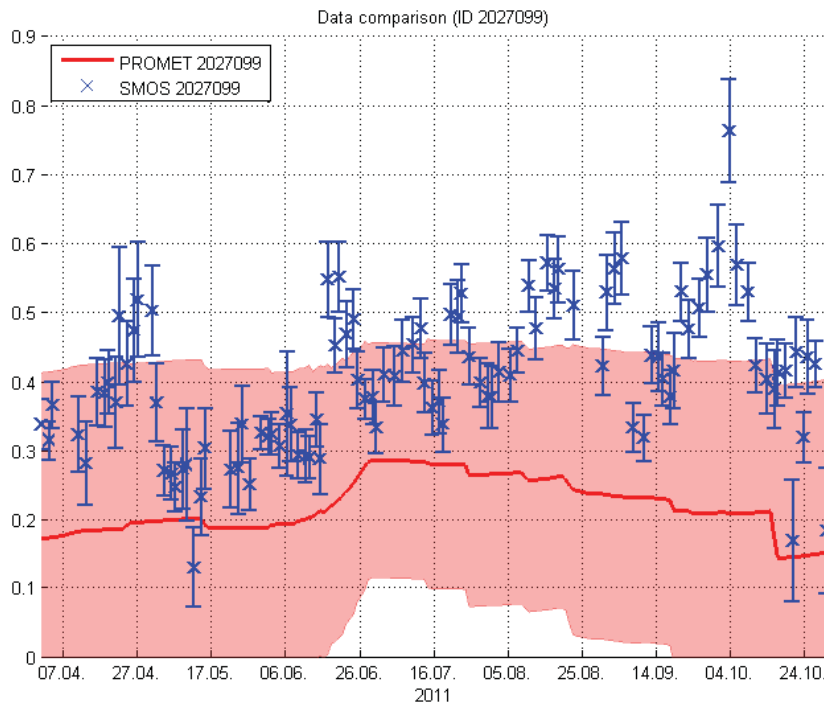
Fig. 10. A comparison between modelled (red) and SMOS L2 optical depth (blue) for the central ISEA ID in the Vils test site. Both values are valid for the nominal land use class (low vegetation). Error bars indicate ± the DQX value for SMOS and the standard deviation for the spatial averaging for PROMET.
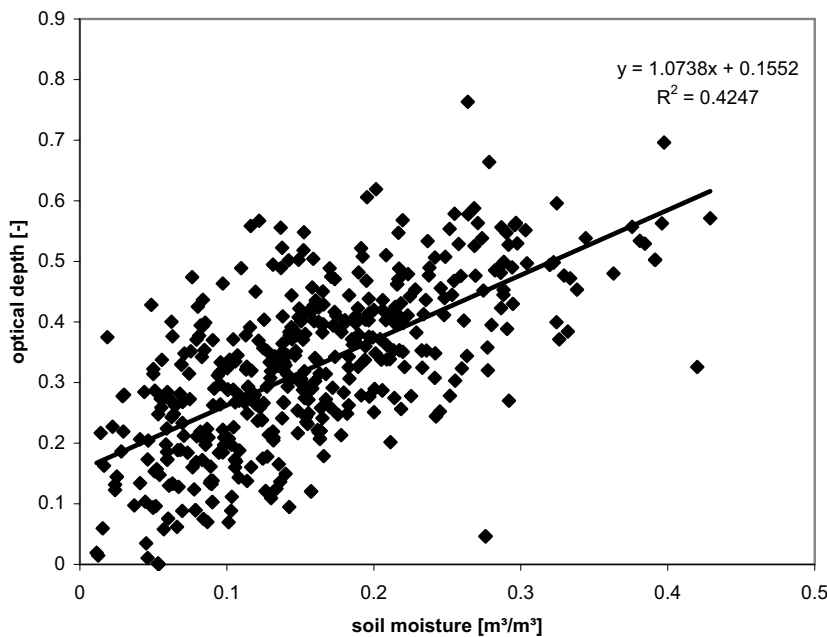
Fig. 11. Scatter plot for the comparison between SMOS L2 soil moisture and optical depth for the ID 2027099.

Appendix II

Additional paper

The following paper by dall'Amico et al. is related to the work described in this thesis and is therefore added to enable a comprehensive overview of the topic:

dall'Amico, J. T., Schlenz, F., Loew, A., and Mauser, W.: First Results of SMOS Soil Moisture Validation in the Upper Danube Catchment, Geoscience and Remote Sensing, IEEE Transactions on, PP, 1-10, 2011. (in print, published online: http://ieeexplore.ieee.org/Xplore/guesthome.jsp)

First Results of SMOS Soil Moisture Validation in the Upper Danube Catchment

Johanna T. dall'Amico, Florian Schlenz, *Member, IEEE*, Alexander Loew, and Wolfram Mauser, *Member, IEEE*

Abstract—With the Soil Moisture and Ocean Salinity (SMOS) satellite launched in 2009, global measurements of L-band microwave emissions and processed "soil moisture" products at a fine time resolution are available. They may, after validation, lead to quantitative maps of global soil moisture dynamics. This paper presents a first validation of the SMOS "soil moisture" product delivered by the European Space Agency in the upper Danube catchment (southern Germany). Processing of the SMOS "soil moisture" product and the methodology to compare it with *in situ* and model data are described. The *in situ* data were taken from May to mid-July 2010 in a small and homogeneous area within the catchment, while the modeled time series spans from April to October 2010 for the whole catchment. The comparisons exhibit a dry bias of the SMOS data of about $0.2~\mathrm{m^3 \cdot m^{-3}}$ with respect to *in situ* measurements. Throughout the catchment, the SMOS data product shows a dry bias between 0.11 and $0.3~\mathrm{m^3 \cdot m^{-3}}$ when compared to modeled soil moisture. Correlation coefficients between both data were found to be mostly below 0.3. Radio-frequency interference (RFI) over Europe appears to be the main problem in obtaining valuable information from the SMOS soil moisture product over this region. RFI is not adequately captured by current methods for filtering and flagging. Nevertheless, some improvements of these results might be achievable through refinements of the soil moisture modeling as well as through improvements to the processors used to generate the SMOS soil moisture product.

Index Terms—Passive microwave remote sensing, soil moisture.

I. INTRODUCTION

SOIL Moisture and Ocean Salinity (SMOS), the European Space Agency (ESA)'s recent satellite for the observation of soil moisture and ocean salinity, was launched on November 2, 2009. It carries an interferometric L-band radiometer (1.4 GHz) with multiangular viewing capabilities [1]. SMOS' novel technique is used to provide global near-surface soil moisture maps with a temporal resolution of about two to three days, a spatial resolution on the order of 40 km, and an accuracy target of $0.04~\mathrm{m^3 \cdot m^{-3}}$ [2], [3]. The soil moisture is obtained from multiangular L-band microwave brightness temperatures using an inverse modeling approach with the tau–omega radiative transfer model as forward model [4]. This involves uncertainties about the representation of several effects, e.g., surface roughness and vegetation opacity [5], [6]. As the microwave brightness temperature is largely affected by the spatial heterogeneity of the land surface at scales of tens of kilometers, an appropriate consideration of the subscale variability of land surface properties needs to be taken into account during the soil moisture retrieval. The spatial heterogeneity might introduce biases and uncertainties in the soil moisture product [7].

For the validation of the SMOS soil moisture product and for adjustments to the retrieval algorithms used in its processor, test sites in different climatic zones of the Earth were established [8]. These test sites should be large enough to contain at least several SMOS pixels, but they should also be well characterized in terms of meteorological and soil moisture conditions, as well as soil and vegetation properties.

Some examples of such calibration and validation (henceforth cal/val) sites for SMOS are in Antarctica [9], West Africa [10], and Australia [11]. In Europe, cal/val activities are being undertaken, among others, at the Valencia Anchor Station in Spain [12], the Surface Monitoring of Soil Reservoir Experiment (SMOSREX) site in France [13], the Hobe site in Denmark [14], [15], the Rur catchment in northwestern Germany [16], and the upper Danube catchment (UDC) in southern Germany [17]. The insights gained through the SMOS data validation at such sites can be useful feedback to adjust and calibrate the algorithms used in the data processors in order to produce more accurate data products. An overview of the cal/val activities is given in [18].

The aim of this paper is to present the validation of SMOS soil moisture data during the first Northern Hemisphere growing season after launch (April to October 2010) in the UDC by making use of *in situ* data as well as model simulations. In Section II, the test site, all data sets used, and the methodology are described. Section III contains the comparison of the SMOS soil moisture product with *in situ* and model data. In Section IV, the results are discussed, and conclusions are drawn.

II. DATA AND METHODOLOGY

The cal/val activities for SMOS in the UDC use a multiscale framework of *in situ* data and soil moisture maps produced by the hydrological land surface model called the Process Oriented

J. T. dall'Amico, F. Schlenz, and W. Mauser are with the Department of Geography, University of Munich, 80333 Munich, Germany (e-mail: j.dallamico@iggf.geo.uni-muenchen.de; f.schlenz@iggf.geo.uni-muenchen.de; w.mauser@lmu.de).

A. Loew is with the Max Planck Institute for Meteorology, 20146 Hamburg, Germany (e-mail: alexander.loew@zmaw.de).

Multiscale EvapoTranspiration (PROMET) model [19], [20]. Soil moisture data are recorded continuously at several ground stations and used to validate PROMET on the point scale [21]. In addition to these ground stations, distributed soil moisture measurements were taken during the SMOS Validation Campaign 2010 during the growing season between May and July [22]. These distributed *in situ* data can be used to validate the 2-D model output as done in [21] and also for a direct comparison with SMOS soil moisture data on selected dates in a limited area. In order to perform an area-wide comparison over a longer period of time, the time series of soil moisture maps produced by PROMET are compared to the SMOS soil moisture data product in the parts of the catchment where both data sets are available, containing about 230 grid points with SMOS soil moisture data.

A. Test Site

The UDC covers an area of about $77\,000$ km^2 and is located mostly in southern Germany. It is characterized by a temperate humid climate and, in the north and center, mostly agricultural land use. In the south of the catchment, arable crops give way to grasslands and eventually the Alps. Other features include the cities of Munich and Ingolstadt and a few lakes just North of the Alps.

The UDC has been the focus of many remote sensing and global change studies, e.g., [19], [20], and [23]–[26]. In 2007, an area of about the size of a SMOS footprint (with a diameter of roughly 50 km) was equipped with soil moisture stations. This so-called Vils area is located in the Northeast of Munich and is used for intensive agriculture on undulating terrain. In this area, SMOS retrieval errors are expected to be small due to the absence of large urban areas and water bodies [7]. The Vils area was also the focus of field campaigns in spring 2008, summer 2009, and late spring/early summer 2010. The campaigns in 2008 and 2010 were connected to airborne campaigns organized and funded by ESA. A subset of the *in situ* data collected during the campaign in 2010, which is called SMOS Validation Campaign 2010, is used in this study. Both the UDC and the Vils area are shown in Fig. 1.

B. Ground Data

During the SMOS Validation Campaign 2010 in the UDC, ground teams recorded, among other parameters, the soil moisture of the upper 6 cm in the five focus areas spread throughout the Vils area using Delta-T's Theta frequency-domain probes. In each of the focus areas, there was also a ground station where soil moisture was recorded continuously at depths ranging from 5 to 40 cm using IMKO time-domain reflectometer probes.

Each focus area was about 7 km long and 3 km wide, containing about 60 measurement points on fields with a variety of land uses, predominantly wheat, maize, and grass. The spatial distribution of the focus areas can be seen in Fig. 1. At each measurement point, five soil moisture measurements were taken. The ground teams took measurements on May 17, May 22, May 25, May 28, June 12, June 17, and July 8, 2010, aligned with SMOS morning overpasses. The decision

to use only the days with morning overpasses for ground measurements was taken due to ESA's decision to perform airborne L-band measurements only on those days. Some ground measurements were also taken on June 14 but had to be aborted due to rain before full coverage of the focus areas was achieved. They are not used in this study.

Throughout the campaign period, a detailed land cover map was prepared by ground teams not only for the focus areas but also for large parts of the flight track. A total of more than 192 km^2, corresponding to roughly 10% of an SMOS footprint, is covered by this land cover map, which is henceforth called land cover map 2010. More details on the campaign data sets are given in [22].

C. Hydrological Model: PROMET

The PROMET model is a spatially distributed physically based hydrologic land surface model. Meteorological data from about 130 stations run by the Bavarian State Research Center for Agriculture are available in near-real time. They are interpolated to the model grid by combining information on altitudinal gradients with various corrections, including information on monthly mean precipitation [20]. The interpolated precipitation fields are used to force the model. The stations are spread over the German federal state of Bavaria to which the main part of UDC belongs. No other measurements are used to force or calibrate the model, but of course, other spatially distributed input is needed. This includes a high-resolution land cover map which was composed from satellite imagery and statistical information on community level. The calculations and the model output (e.g., soil moisture and temperature, runoff, and evaporation) use a regular 1 km × 1 km grid. Fig. 1 (right panel) shows an example of a modeled soil moisture map of the entire UDC. The wetter band in the south of the catchment corresponds to the Alpine foreland with its typical orographically enhanced precipitation. The wetter band in the north of the catchment is associated with the Swabian mountains.

For the comparison with SMOS data, the southern part of the catchment and the most western corner are excluded. In the south, no SMOS soil moisture data are available due to the strong topography of the Alps, and for the most western corner, there are no meteorological data available in near-real time to force the model, as this part of the catchment lies outside of the German federal state of Bavaria.

The PROMET output has been validated on different spatial scales in different test sites with good results [19], [20], [26], [27]. The soil water model, in particular, has been validated in different test sites using *in situ* soil moisture measurements of soil moisture profiles and remote sensing observations with good results [23], [28]. For the Vils area, [21] studied the uncertainties of the soil water model on the point scale, an intermediate scale, and the scale of the grid used for SMOS data. On the point scale, modeled soil moisture was compared to the measurements of the same soil moisture stations described in the previous section for the period of 2008–2010. Reference [21] found the root-mean-square error [(rmse); including bias and random error] to vary between 0.041 and 0.153 m$^3 \cdot$ m^{-3}, the rmse of the bias-corrected model output to vary between
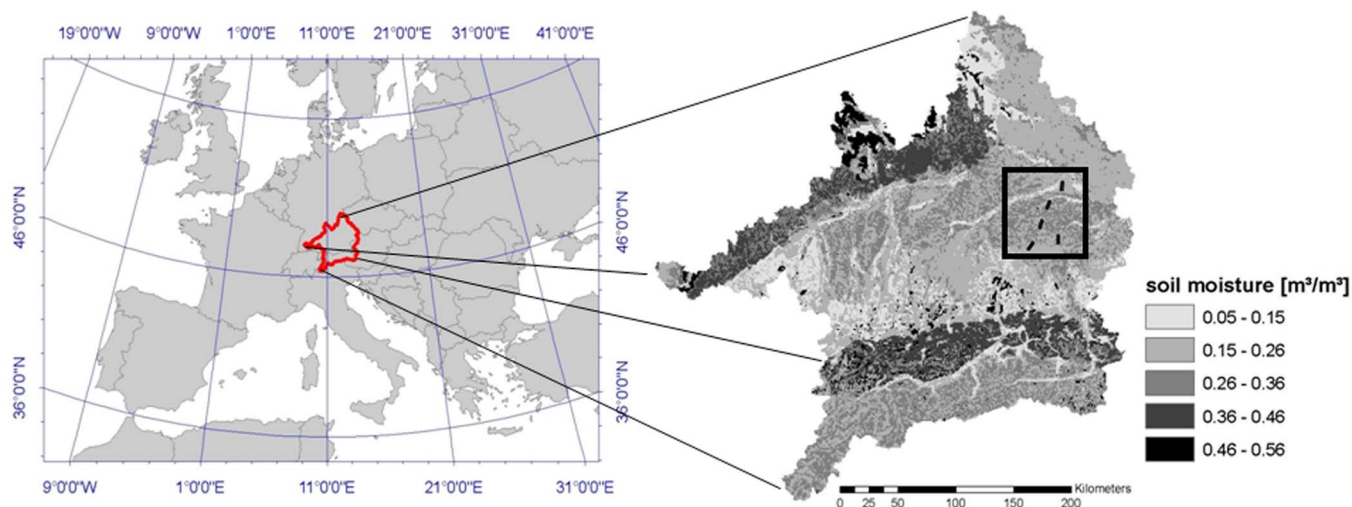
Fig. 1.   (Left panel) Location of the UDC in Europe. (Right panel) Example of a soil moisture map of the UDC as modeled by PROMET. The black box shows the Vils area containing (black patches) the five focus areas where distributed soil moisture measurements were taken during the SMOS Validation Campaign 2010.

0.033 and 0.067 $m^3 \cdot m^{-3}$, and correlation coefficients (R^2) to vary between 0.45 and 0.79. The analysis on the point scale was also conducted for two soil moisture stations outside the Vils area with slightly better results. The performance improved on the intermediate scale, for which the distributed *in situ* measurements acquired on eight days during the SMOS Validation Campaign 2010 were used. This comparison showed an rmse of 0.045 $m^3 \cdot m^{-3}$ (0.040 $m^3 \cdot m^{-3}$ for the bias-corrected data) and an R^2 of 0.75. Large-scale uncertainties are of particular importance for using PROMET simulations for a comparison with SMOS data. At the large scale, [21] averaged all modeled soil moisture values within an SMOS grid cell (195 km^2) and compared those to the mean value of all distributed *in situ* measurements per campaign day. This resulted in an rmse of 0.040 $m^3 \cdot m^{-3}$, corresponding to 13.7% of the modeled mean value of 0.2917 $m^3 \cdot m^{-3}$. The modeled soil moisture range in the considered time period was 0.22–0.32 $m^3 \cdot m^{-3}$. The rmse of the bias-corrected model output was 0.023 $m^3 \cdot m^{-3}$. This is in line with the findings in [29], which used the triple collocation method on a similar data set of the years 2008 and 2009 and showed that the large-scale random error of the PROMET simulations is better than 0.025 $m^3 \cdot m^{-3}$ at the SMOS grid scale in the Vils test site. This corresponds to 8.5% of the modeled mean value in the considered time period (May to October of the years 2008 and 2009). The modeled soil moisture range in that period was 0.25–0.39 $m^3 \cdot m^{-3}$.

D. SMOS L2 Data

For this study, SMOS data from the period April to October 2010 were used. During this period, which includes also the last part of the commissioning phase, the algorithms used in the Level 1 (L1) and Level 2 (L2) processors have been improved, so that the originally delivered time series of SMOS L2 data was not consistently processed. In early 2011, the whole data of 2010 were reprocessed using a consistent combination of L1 and L2 processors. In this study, this reprocessed data set is used. The processing of SMOS brightness temperature

data and the retrieval of soil moisture from these brightness temperatures are described in [30]. Only a few features of the used SMOS L2 data product are described here, because they are considered necessary to understand the rationale of the methodology adopted for this study.

SMOS soil moisture data are delivered on the icosahedron Snyder equal area (ISEA) grid [31], [32] with a spacing of about 12.5 km between two nodes. However, the SMOS soil moisture product is derived from multiangular brightness temperature measurements which cover an area on the order of tens of kilometers. The SMOS L2 product has a nominal spatial resolution of 43 km on average. This oversampling should be taken into account when working with SMOS data. Also, the soil moisture given in the L2 data product for a nominal retrieval configuration is only valid for the nominal land use classes, which are the classes with low vegetation (grass and crops). Hence, in the retrieval configuration of the data product used in this study, no information is given on soil moisture of other land use classes. The contributions of the fractions of nonnominal land use classes (e.g., forests and lakes) to the overall brightness temperature of the footprint are estimated and subtracted from the measured brightness temperature. Only the remaining part of the measured brightness temperature is used for the retrieval of soil moisture (and vegetation optical thickness) of the nominal land use classes. Hence, the retrieved values are only valid for the part of the footprint with nominal land use classes.

Data degradation due to radio-frequency interference (RFI) has been shown to be a major issue in the UDC cal/val site. Sources of RFI can include various emitters as radars from airports and military bases, telecommunication facilities, etc. Due to these signals traveling long distances and SMOS' large field of view and interferometric technique, RFI can be expected to be a problem not only in the UDC but also on larger scales. Some of the corrupted data are identified and eliminated in the data processing before the L2 product is delivered, but the detection and elimination of the different types of RFI are still a major research task [33]. Thus, an appropriate

prefiltering of the data is crucial before analyzing the L2 data products. The applied preprocessing steps are discussed in the following.

The SMOS User Data Product used in this study contains a number of variables. In addition to soil moisture, important information is given in the soil moisture Data Quality indeX (DQX) and in both the confidence flags and the science flags. The soil moisture DQX is the "theoretical retrieval *a posteriori* standard deviation" (see [34, p. 77] and [30, p. 92] for details) obtained during the soil moisture retrieval in unit $m^3 \cdot m^{-3}$. In this study, all data with a DQX of -999 are discarded as this means that the given soil moisture did not result from a successful retrieval. In addition to that, excluding data with a DQX value above a threshold of $0.06 \ m^3 \cdot m^{-3}$ led to the filtering of obvious outliers while still roughly 80% of the data were kept. Some of the flags have been found to be useful for filtering the data while others did not seem to be associated with poor data quality. The usefulness of the flags may depend on the study area. The confidence flag FL_NO_PROD is set whenever no product is provided for many possible reasons (e.g., retrieval failed or results out of range) and should therefore be used for filtering. Although rarely set, the confidence flags FL_RFI_Prone_H and FL_RFI_Prone_V (set when the probability of RFI is high for H and V polarizations, respectively) and the science flag FL_RAIN (set when heavy rain is expected according to auxiliary data) were also used for filtering. For more information on flags, please refer to [30] and [34]. No clear difference between morning and evening overpasses could be detected in the data over the UDC, so both of them are included in the analysis.

E. Methodology of Comparisons

The distributed *in situ* soil moisture measurements are mainly used for the validation of the PROMET model as in [21]. However, a direct comparison of *in situ* and SMOS soil moisture data has also been attempted. For each of the seven campaign days, all soil moisture measurements taken on grass or crops in all five focus areas in the Vils area were averaged. This gives one soil moisture value for each of the seven days. These mean values stem from about 1500 single soil moisture measurements for each campaign day. Thus, a comparison is made between the averaged measured distributed soil moisture and the SMOS soil moisture for seven campaign days. In order to check the soil moisture evolution with time, SMOS soil moisture data have also been compared with the soil moisture continuously measured at the five ground stations. For this comparison, the measurements at 5- and 10-cm depths of all stations were averaged to give one time series.

To compare the time series of model simulations with SMOS data throughout the catchment, each PROMET grid cell (grid size of 1 km) is assigned to the closest ISEA grid node (approximately, a spacing of 12.5 km). For each ISEA grid node, all PROMET soil moisture values assigned to it are averaged if they belong to one of the nominal land use classes for which the SMOS soil moisture is valid (see Section II-D). The PROMET soil moisture simulations used are sampled twice daily (at 5 A.M. and 5 P.M. UTC, roughly corresponding to SMOS overpass times) in the period from April 1 to October 31, 2010.

F. Representativeness of Measurements and Model Output

In the Vils area, there are three ISEA grid points on which SMOS data are delivered: ID 2027099, ID 2026586, and ID 2026587. Grid point ID 2027099 is in the center of the area, so the area contributing to most of the SMOS signal measured at this grid point lies almost entirely within the Vils area. This footprint has a diameter on the order of 50 km, so the question arises whether the *in situ* soil moisture measurements taken in that footprint are representative of the soil moisture in the whole footprint. The same needs to be considered for the modeled soil moisture. Although the model output is area wide, i.e., it does not have missing locations, the model consequently relies on area-wide input. The input data used in the model stem from a variety of sources and do not necessarily match exactly the reality as seen by SMOS at the time of the overpass. These uncertainties might degrade the model output. As for the factors influencing the modeled soil moisture distribution, in the UDC area, the main factors have been found to be precipitation and land cover (i.e., vegetation). Therefore, in the following is discussed how realistically these two factors are represented in the measurements and in the model output on the scale of the ISEA grid cells.

The five focus areas with the distributed *in situ* measurements are spread over the Vils area with a spacing of about 20 km as shown in Fig. 1. They also contain one meteorological station each, the data from which are interpolated and used to force the model PROMET. It can therefore be expected that variability due to precipitation is represented well in both *in situ* measurements and model output. Only some very local thunderstorms could lead to increased precipitation between the focus areas without affecting the focus areas themselves and, with them, the meteorological stations. However, if there were such very small thunderstorms, they would probably not lead to a significant increase of soil moisture of the whole SMOS footprint. This hypothesis is difficult to verify without area-wide precipitation measurements. Precipitation fields derived from rain radar and calibrated with gauging stations could lead to new insights on these uncertainties. Currently, such fields are being fed to PROMET, and the resulting soil moisture output will be compared to the standard case when PROMET interpolates the precipitation given by the gauging stations. However, as the spacing between the gauging stations used in this study is on the order of 20 km, i.e., well below the resolution of SMOS, the interpolation of their measurements is expected to give realistic results within Bavaria on the SMOS scale.

Similarly, the true land cover distribution of the year 2010 in the whole Vils area should be known in order to check how well it is represented in the *in situ* measurements and in the modeled soil moisture. The best available ground truth data for this are the land cover map 2010 produced during the SMOS Validation Campaign 2010 by ground teams, covering roughly 10% of the whole Vils area. Table I shows the distribution of the main land cover types for the focus areas ($\sim 105 \ km^2$), for

TABLE I
PERCENTAGE OF LAND COVER CLASSES OF THE FOCUS AREAS, OF THE WHOLE LAND COVER MAP AS MAPPED DURING THE SMOS VALIDATION
CAMPAIGN 2010, AND OF THE LAND COVER MAP USED IN THE PROMET MODEL FOR ALL 1-km PIXELS MAPPED
TO THE CENTRAL ISEA GRID POINT IN THE VILS AREA (ID 2027099)

land cover	% of all focus areas	% of land cover map 2010	% of land cover map used in PROMET
grass	13.6	22.9	15.4
maize	26.5	28.1	39.5
other crops	30.6	24.5	22.6
forest	16.9	21.9	19.5
water	0.5	0.5	0.0
other	11.9	2.6	3.1
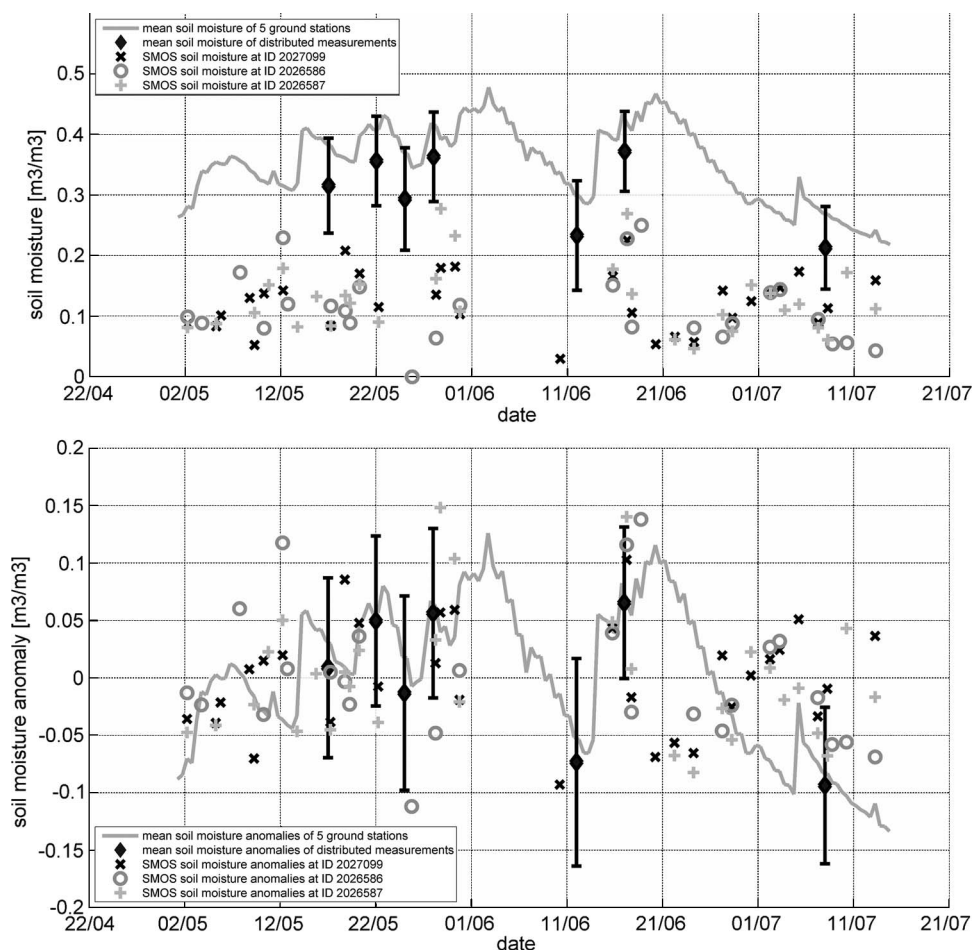
Fig. 2. (Gray line) Mean value of the soil moisture measurements taken at the five ground stations in the Vils area, (black diamonds) mean value of the distributed *in situ* soil moisture measurements taken during the SMOS Validation Campaign 2010 (with bars indicating standard deviations), and SMOS soil moisture data on ISEA grid points ID 2027099, ID 2026586, and ID 2026587. (Upper panel) Absolute values. (Lower panel) Anomalies, i.e., deviations from the mean value of each data set for the period May to mid-July 2010.

the whole land cover map 2010 (192 km^2), and for the land cover map used as input for the PROMET model for the central ISEA ID 2027099 (195 km^2). The nominal land use classes, i.e., grass and all crops, occupy roughly 75% of the area in all three cases (focus areas: 70.7%; land cover map 2010: 75.5%; PROMET land cover map: 77.5%). However, the class grass

Fig. 3.   Time series of modeled soil moisture (PROMET) and SMOS soil moisture data at the central ISEA grid point in the Vils area (ID 2027099). (Upper panel) Absolute values. (Lower panel) Anomalies, i.e., deviations from the mean value of each data set for the period April to October 2010.

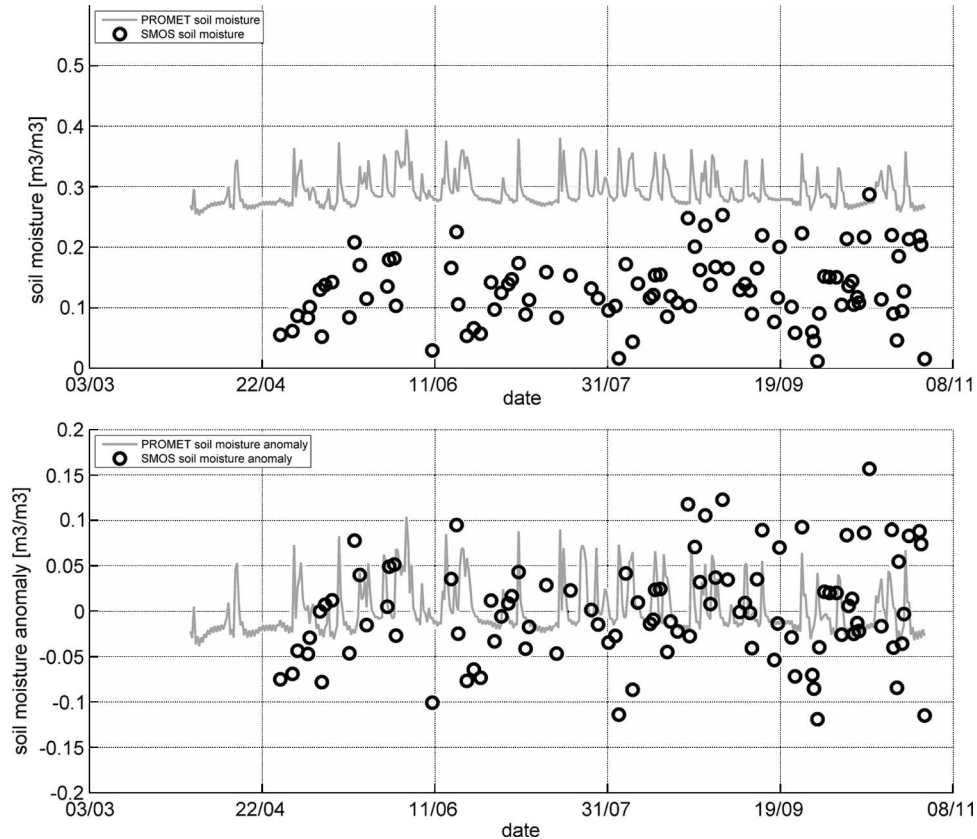is underrepresented in the focus areas and the PROMET land cover map when compared to the land cover map 2010. As in this area, soil moisture under grass has been usually found to be at least $0.06 \text{ m}^3 \cdot \text{m}^{-3}$ higher on average than that under the class "other crops"; the true mean soil moisture of the nominal land use classes within the central ISEA grid point might be slightly underestimated by the *in situ* measurements and the modeled soil moisture.

It should be noted that the comparison between PROMET and SMOS on the basis of the ISEA grid is straightforward but neglects the fact that the SMOS footprint is indeed much larger than an ISEA grid cell. As land cover fractions are not expected to change abruptly from one grid cell to the next in the UDC area, this will, in most cases, not affect the comparison. In the Vils area, the differences between PROMET simulations on the three ISEA grid points are less than $0.001 \text{ m}^3 \cdot \text{m}^{-3}$ on average, with a maximal difference on a few dates of $0.05 \text{ m}^3 \cdot \text{m}^{-3}$. However, in regions with large water bodies (e.g., some lakes in the south of Munich) or strong topography, a disturbance of the signal in neighboring ISEA grid cells can be expected.

III. Data Analysis/SMOS Validation

A. Comparison of SMOS L2 Data With In Situ Measurements

For the period of the SMOS Validation Campaign 2010, SMOS L2 data on the ISEA grid points in the Vils area (ID 2027099, ID 2026586, and ID 2026587) were compared to the mean soil moisture as measured continuously by the five ground stations and to the mean soil moisture as measured throughout the focus areas on the seven campaign days by the ground teams (Fig. 2, upper panel). It is clear that the level of soil moisture is too low in the SMOS data. Over this campaign period (May until mid-July 2010), the mean soil moisture values are $0.35 \text{ m}^3 \cdot \text{m}^{-3}$ for the automated ground stations, $0.31 \text{ m}^3 \cdot \text{m}^{-3}$ for the distributed manual measurements during the campaign, and $0.12 \text{ m}^3 \cdot \text{m}^{-3}$ for SMOS. An SMOS "soil moisture" value of around and below $0.1 \text{ m}^3 \cdot \text{m}^{-3}$ can be considered to be unrealistic for the temperate humid climate of the UDC with a rainfall event every 2.4 days, an average rainfall of 900 mm/a, and an average evapotranspiration of 500 mm/a. The Global Soil Moisture Data Bank [35] for similar conditions in Russia gives average soil water contents in the top 1 m of approximately $0.25–0.35 \text{ m}^3 \cdot \text{m}^{-3}$. Since there is no dry season in the UDC and rainfall peaks during summer, the top soil is not drying significantly, and thereby, top soil moisture is similar to root zone soil moisture in the UDC. Although the soil moisture stations overestimate soil moisture as measured by the ground teams on the campaign days, this seems to be a bias which is the same under various soil moisture conditions. This bias is due to the fact that the stations are located on grassland which is typically wetter than the surrounding cropland areas. Once the mean values are subtracted from their respective time series to obtain anomalies (Fig. 2, lower panel), the soil moisture stations agree very well with the distributed measurements.
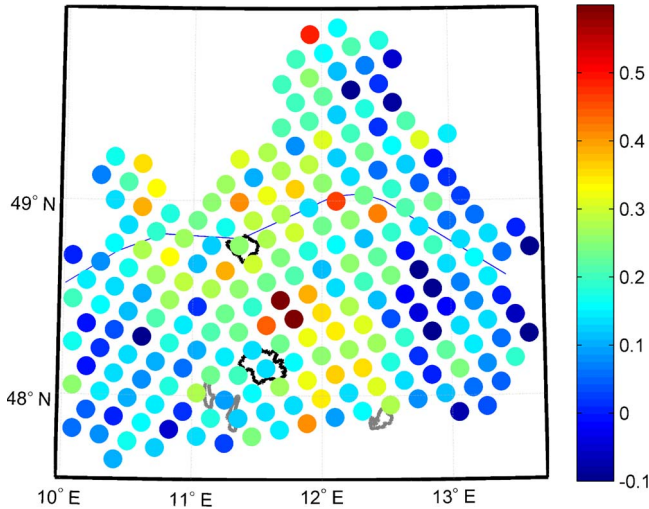
Fig. 4. Map of the correlation coefficients between modeled soil moisture (PROMET) and SMOS L2 soil moisture for the time period of April 1 to October 31, 2010 [(blue) low correlation; (red) high correlation]. The cities of Munich (south) and Ingolstadt (north) are shown as black polygons while the three gray polygons show some lakes in the Alpine foreland. The blue line shows the river Danube.

SMOS data, however, in their current state do not seem to be able to capture the soil moisture evolution over time as measured by the ground stations. The variability of the SMOS data is similar to that of the *in situ* measurements with standard deviations of 0.05 (SMOS) and 0.06 $m^3 \cdot m^{-3}$ (stations, distributed measurements).

B. Comparison of SMOS L2 Data With Model Simulations

Time Series in the Vils Area: The Vils area is a part of the UDC where soil moisture retrieval is expected to work well and is well known through ground measurements. Thus, the first step in comparing modeled soil moisture to SMOS L2 data is to consider ISEA grid point 2027099 (located in the center of the Vils area; latitude/longitude: 48.425°/12.748°). Both PROMET and SMOS time series are shown in the upper panel of Fig. 3. Again, the overall soil moisture level of the SMOS data is too low. The mean values over the shown time period are 0.29 $m^3 \cdot m^{-3}$ for PROMET and 0.13 $m^3 \cdot m^{-3}$ for SMOS. The anomalies obtained by subtracting these mean values from their respective time series are shown in the lower panel of Fig. 3. It is difficult to see a common soil moisture evolution in the two data sets, although some precipitation events and drying phases between these events as modeled by PROMET seem to be captured by SMOS as well (e.g., in August). There is also a noticeable difference in the variability of the two data sets, with the standard deviations being 0.03 $m^3 \cdot m^{-3}$ for PROMET and 0.06 $m^3 \cdot m^{-3}$ for SMOS.

Area-Wide Comparison in the UDC: For an area-wide comparison, the same comparison between SMOS and PROMET as shown in the previous section has been conducted for a total of 232 suitable ISEA grid points in the UDC. Excluded were the region of the Alps, where no SMOS L2 data are available due to strong topography, and the most western corner of the catchment, where no meteorological data are available in near-real time in order to force the model. The correlation coefficient
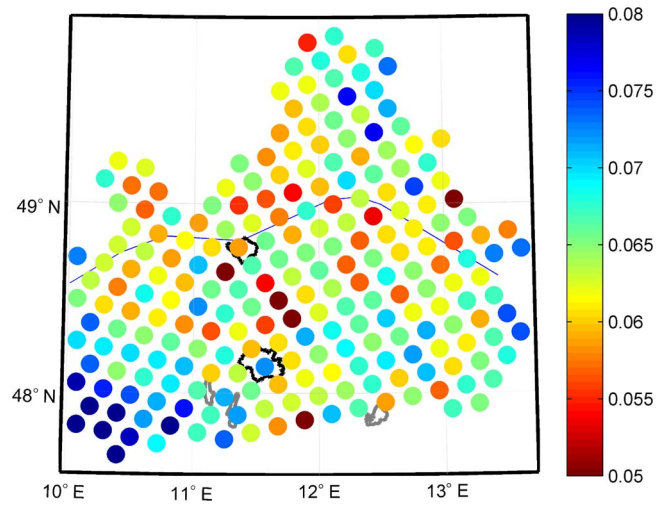

Fig. 5. Map of rmses between modeled (PROMET) and SMOS L2 soil moisture anomalies (in $m^3 \cdot m^{-3}$) for the time period of April 1 to October 31, 2010 [(red) low rmse; (blue) high rmse]. The polygons and lines are as in Fig. 4.

and the rmse of the anomalies (i.e., deviations from the mean value of the time series) have been computed for each grid point separately using the whole time series from April 1 to October 31, 2010.

The correlation coefficients are shown in Fig. 4. They have been found to be fairly low (between 0 and 0.5 and even negative at some points) with better correlations in the center of the catchment and worse correlations toward the east and the west. The rmse of the anomalies, shown in Fig. 5, varies between 0.05 and 0.08 $m^3 \cdot m^{-3}$. The largest rmse values are found in the southwest of the catchment, while some of the lowest values are found between the two cities of Munich and Ingolstadt.

In order to see whether spatial patterns of soil moisture and its variability are similar, maps of mean soil moisture and standard deviation (both for the whole time series) have been produced for both data sets, shown in Fig. 6 for SMOS and Fig. 7 for PROMET. While the mean soil moisture field simulated by PROMET exhibits an almost zonal pattern, this is not the case for SMOS. Consequently, differences can be very large. The dry bias in the SMOS data with respect to the PROMET data varies from about 0.11 to as much as 0.3 $m^3 \cdot m^{-3}$. The most striking feature in the mean soil moisture field as produced by SMOS is the very dry stripe reaching from the Alps to the north of the city of Munich. Also, standard deviations are much higher in the SMOS data than in the model simulations [note the different color scales in Figs. 6(b) and 7(b)].

IV. DISCUSSION AND CONCLUSION

In this paper, the approach and framework used to validate SMOS soil moisture data in the UDC have been presented. Modeled soil moisture is available as time series on a 1-km grid throughout the catchment. Detailed ground data on soil moisture (time series of five ground stations and distributed *in situ* data on seven days) and land cover have been collected
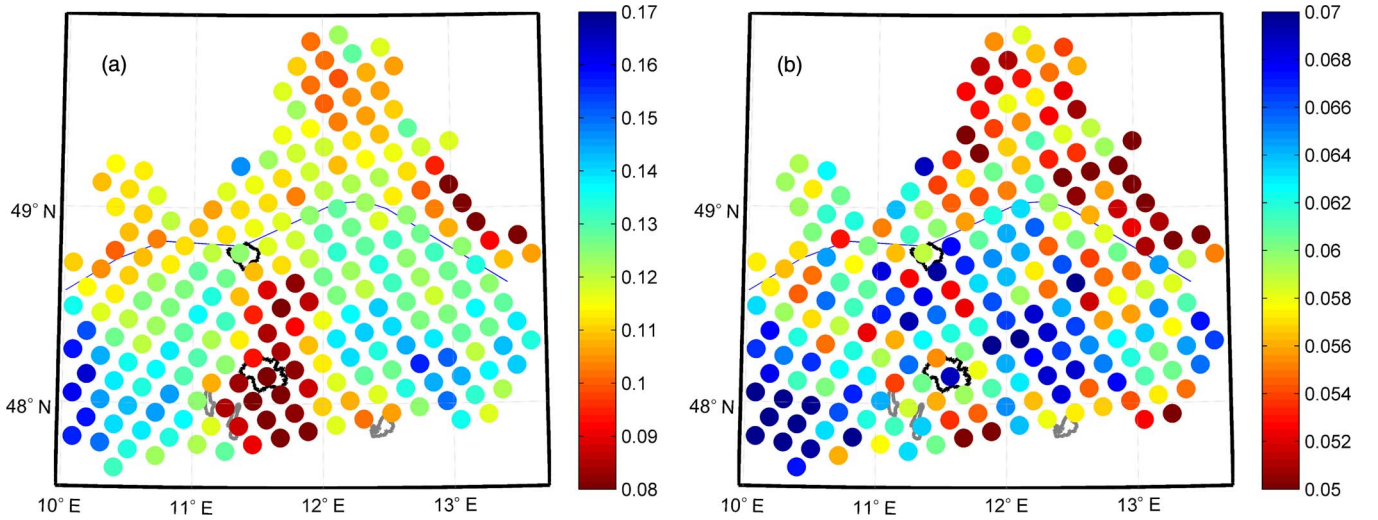
Fig. 6.   (a) Mean value of SMOS L2 data (in $m^3 \cdot m^{-3}$) for the time period of April 1 to October 31, 2010 [(red) low mean value; (blue) high mean value]. (b) Standard deviation with respect to this mean value [(red) low standard deviation; (blue) high standard deviation]. The polygons and lines are as in Fig. 4.
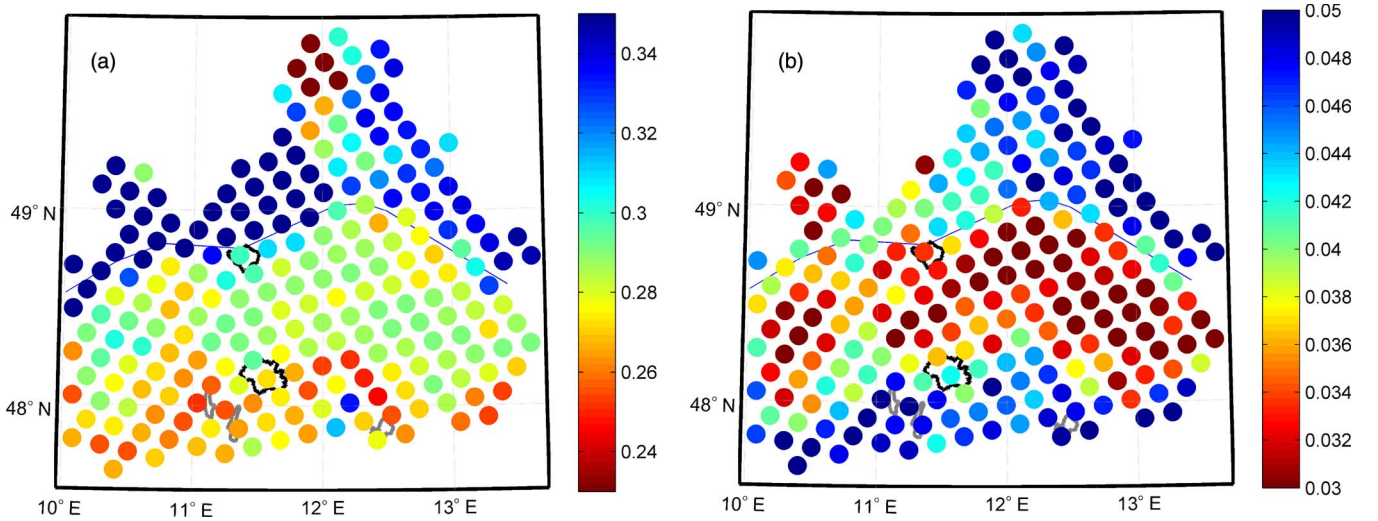
Fig. 7.   (a) Mean value of modeled (PROMET) soil moisture (in $m^3 \cdot m^{-3}$) for the time period of April 1 to October 31, 2010 [(red) low mean value; (blue) high mean value]. (b) Standard deviation with respect to this mean value [(red) low standard deviation; (blue) high standard deviation]. The polygons and lines are as in Fig. 4.

in a smaller area (called the Vils area) of about the size of an SMOS footprint. SMOS data of the first Northern Hemisphere vegetation growth period after launch have been compared with ground stations and distributed *in situ* data on three grid points in the Vils area (between May and mid-July 2010) and with model simulations for almost the whole UDC (April 1 to October 31, 2010).

The comparison with ground data shows a dry bias in the SMOS data of 0.18 $m^3 \cdot m^{-3}$ with respect to the distributed measurements (on grass and all types of crops) and of 0.23 $m^3 \cdot m^{-3}$ with respect to the mean measurements of the ground stations (on grass only). No clear agreement in the soil moisture evolution has been found between the time series of SMOS data and station measurements in the time period considered.

Despite the mismatch of resolution, the variability of the SMOS data at one grid point with time (standard deviations

on the order of 0.06 $m^3 \cdot m^{-3}$) seems to be more similar to

the temporal variability of the ground measurements (standard deviations of $0.06 \text{ m}^3 \cdot \text{m}^{-3}$) than to the temporal variability produced by the model simulations (standard deviations on the order of $0.04 \text{ m}^3 \cdot \text{m}^{-3}$). The high variability of SMOS data despite its coarse resolution could indicate that the data are affected by the interference of man-made signals (e.g., radars) or that some parameters in the algorithms used to retrieve soil moisture from the brightness temperatures need to be adjusted.

Similar to the results from the comparison with *in situ* data in the Vils area, a strong dry bias in the SMOS data with respect to the modeled soil moisture is observed in the whole catchment, varying from 0.11 to $0.3 \text{ m}^3 \cdot \text{m}^{-3}$. The correlation coefficients are mostly below 0.3, and neither the spatial pattern of the mean soil moisture fields nor that of the soil moisture variability matches for the two data sets. There are many possible reasons for this disagreement; some of them are associated with the PROMET simulations, and some of them are associated with the SMOS data.

The uncertainties of the soil moisture output of the model PROMET are not known everywhere in the catchment. The fact that the southwestern part of the area exhibits larger rmse values of the anomalies could be associated with uncertainties in the meteorological data used to force the model, as there are only two meteorological stations in that corner. Also, there could be unknown errors in the maps of soil texture and/or land cover which are used as input. However, in the regions where PROMET has been validated with *in situ* measurements, errors with an rmse of $0.2 \text{ m}^3 \cdot \text{m}^{-3}$ or correlation coefficients of 0.3 and below have never been found.

The uncertainties associated with SMOS L2 data are manifold [30, p. 101]. First, it is known that SMOS data in most of Europe are affected by RFI. Care has been taken to use flags and error estimates provided with the L2 data product in order to filter corrupted data, but most likely, more sophisticated methods for RFI mitigation and flagging are needed in the processing from the L1 to the L2 data product. Second, a lot still has to be learnt about soil moisture retrieval from brightness temperatures measured at L-band at such a large scale. Possible error sources in the retrieval mechanism include model parameters (such as roughness), static input (such as soil texture and land cover), and time-variant input (such as surface temperature fields). It is very likely that the overall observed dry bias in the SMOS L2 data in this area can be reduced through improvements to the retrieval algorithm. More research in this field is needed to gain experience and develop a more sophisticated data product, but in order to do this in areas like the UDC, the problems caused by RFI need to be tackled first.

REFERENCES

[1] K. D. McMullan, M. A. Brown, M. Martin-Neira, W. Rits, S. Ekholm, J. Marti, and J. Lemanczyk, "SMOS: The payload," *IEEE Trans. Geosci. Remote Sens.*, vol. 46, no. 3, pp. 594–605, Mar. 2008.

[2] Y. Kerr, P. Waldteufel, J.-P. Wigneron, S. Delwart, F. Cabot, J. Boutin, M. Escorihuela, J. Font, N. Reul, C. Gruhier, S. Juglea, M. Drinkwater, A. Hahne, M. Martin-Neira, and S. Mecklenburg, "The SMOS mission: New tool for monitoring key elements of the global water cycle," *Proc. IEEE*, vol. 98, no. 5, pp. 666–687, May 2010.

[3] H. M. J. Barre, B. Duesmann, and Y. H. Kerr, "SMOS: The mission and the system," *IEEE Trans. Geosci. Remote Sens.*, vol. 46, no. 3, pp. 587–593, Mar. 2008.

[4] J. P. Wigneron, Y. Kerr, P. Waldteufel, K. Saleh, M. J. Escorihuela, P. Richaume, P. Ferrazzoli, P. de Rosnay, R. Gurney, J. C. Calvet, J. P. Grant, M. Guglielmetti, B. Hornbuckle, C. Mätzler, T. Pellarin, and M. Schwank, "L-band Microwave Emission of the Biosphere (L-MEB) model: Description and calibration against experimental data sets over crop fields," *Remote Sens. Environ.*, vol. 107, no. 4, pp. 639–655, Apr. 2007.

[5] A. G. Konings, D. Entekhabi, S. K. Chan, and E. G. Njoku, "Effect of radiative transfer uncertainty on L-band radiometric soil moisture retrieval," *IEEE Trans. Geosci. Remote Sens.*, vol. 49, no. 7, pp. 2686–2698, Jul. 2011.

[6] J. P. Wigneron, A. Chanzy, Y. H. Kerr, H. Lawrence, J. Shi, M. J. Escorihuela, V. Mironov, A. Mialon, F. Demontoux, P. de Rosnay, and K. Saleh-Contell, "Evaluating an improved parameterization of the soil emission in L-MEB," *IEEE Trans. Geosci. Remote Sens.*, vol. 49, no. 4, pp. 1177–1189, Apr. 2011.

[7] A. Loew, "Impact of surface heterogeneity on surface soil moisture retrievals from passive microwave data at the regional scale: The upper Danube case," *Remote Sens. Environ.*, vol. 112, no. 1, pp. 231–248, Jan. 2008.

[8] S. Delwart, C. Bouzinac, P. Wursteisen, M. Berger, M. Drinkwater, M. Martin-Neira, and Y. H. Kerr, "SMOS validation and the COSMOS campaigns," *IEEE Trans. Geosci. Remote Sens.*, vol. 46, no. 3, pp. 695–704, Mar. 2008.

[9] G. Macelloni, M. Brogioni, and S. Vey, "Calibration of a ground based radiometer for a one-year experiment in Antarctica: A contribution to SMOS calibration," in *Proc. IEEE IGARSS*, 2007, pp. 2423–2426.

[10] P. de Rosnay, C. Gruhier, F. Timouk, E. Mougin, P. Hiernaux, L. Kergoat, and V. LeDantec, "Multi-scale soil moisture measurements at the Gourma meso-scale site in Mali," *J. Hydrol.*, vol. 375, no. 1/2, pp. 241–252, Aug. 2009.

[11] R. Panciera, J. P. Walker, J. D. Kalma, E. J. Kim, J. M. Hacker, O. Merlin, M. Berger, and N. Skou, "The NAFE'05/COSMOS data set: Toward SMOS soil moisture retrieval, downscaling, and assimilation," *IEEE Trans. Geosci. Remote Sens.*, vol. 46, no. 3, pp. 736–745, Mar. 2008.

[12] S. Juglea, Y. Kerr, A. Mialon, J.-P. Wigneron, E. Lopez-Baeza, A. Cano, A. Albitar, C. Millan-Scheiding, M. C. Antolin, and S. Delwart, "Modelling soil moisture at SMOS scale by use of a SVAT model over the Valencia Anchor Station," *Hydrol. Earth Syst. Sci.*, vol. 14, no. 5, pp. 831–846, 2010.

[13] P. de Rosnay, J.-C. Calvet, Y. H. Kerr, J.-P. Wigneron, F. Lemaître, M.-J. Escorihuela, J. M. Sabater, K. Saleh, J. Barrié, G. Bouhours, L. Coret, G. Cherel, G. Dedieu, R. Durbe, N. E. D. Fritz, F. Froissard, J. Hoedjes, A. Kruszewski, F. Lavenu, D. Suquia, and P. Waldteufel, "SMOSREX: A long term field campaign experiment for soil moisture and land surface processes remote sensing," *Remote Sens. Environ.*, vol. 102, no. 3/4, pp. 377–389, Jun. 2006.

[14] S. Bircher, J. Balling, and N. Skou, "SMOS validation activities at different scales in the Skjern River catchment, western DK," in *Proc. ESA Living Planet Symp.*, Bergen, Norway, 2010.

[15] S. Bircher, J. E. Balling, N. Skou, and Y. Kerr, "SMOS validation by means of an airborne campaign in the Skjern River catchment, western Denmark," *IEEE Trans. Geosci. Remote Sens.*, 2011, to be published, DOI: 10.1109/TGRS.2011.2170177.

[16] C. Montzka, H. Bogena, L. Weihermueller, F. Jonard, C. Bouzinac, J. Kainulainen, J. E. Balling, A. Loew, J. T. dall'Amico, E. Rouhe, J. Vanderborght, and H. Vereecken, "Brightness temperature validation at different scales during the SMOS Validation Campaign in the Rur and Erft catchments, Germany," *IEEE Trans. Geosci. Remote Sens.*, 2011, submitted for publication.

[17] J. T. Dall'Amico, F. Schlenz, A. Loew, and W. Mauser, "SMOS soil moisture validation: Status at the upper Danube cal/val site eight months after launch," in *Proc. IEEE IGARSS*, 2010, pp. 3801–3804.

[18] S. Mecklenburg, M. Drusch, Y. Kerr, J. Font, M. Martin-Neira, S. Delwart, G. Buenadicha, N. Reul, E. Daganzo-Eusebio, R. Oliva, and R. Crapolicchio, "ESA's Soil Moisture and Ocean Salinity mission: An overview after one year of operations," *IEEE Trans. Geosci. Remote Sens.*, 2011, submitted for publication.

[19] W. Mauser and S. Schädlich, "Modelling the spatial distribution of evapotranspiration on different scales using remote sensing data," *J. Hydrol.*, vol. 212/213, pp. 250–267, Dec. 1998.

[20] W. Mauser and H. Bach, "PROMET—Large scale distributed hydrological modelling to study the impact of climate change on the water flows of mountain watersheds," *J. Hydrol.*, vol. 376, no. 3/4, pp. 362–377, Oct. 2009.

[21] F. Schlenz, J. T. dall'Amico, A. Loew, and W. Mauser, "Uncertainty assessment of the SMOS validation in the upper Danube catchment," *IEEE Trans. Geosci. Remote Sens.*, 2012, accepted for publication, DOI: 10.1109/TGRS.2011.2171694.

[22] J. T. dall'Amico, F. Schlenz, A. Loew, W. Mauser, J. Kainulainen, J. Balling, and C. Bouzinac, "The SMOS Validation Campaign 2010 in the Upper Danube Catchment: A Data Set for Studies of Soil Moisture, Brightness Temperature and their Spatial Variability over a Heterogeneous Land Surface," *IEEE Trans. Geosci. Remote Sens.*, 2011, submitted for publication.

[23] A. Loew, R. Ludwig, and W. Mauser, "Derivation of surface soil moisture from Envisat ASAR wide swath and image mode data in agricultural areas," *IEEE Trans. Geosci. Remote Sens.*, vol. 44, no. 4, pp. 889–899, Apr. 2006.

[24] M. Probeck, R. Ludwig, and W. Mauser, "Fusion of NOAA-AVHRR imagery and geographical information system techniques to derive sub-scale land cover information for the upper Danube watershed," *Hydrol. Processes*, vol. 19, no. 12, pp. 2407–2418, Aug. 2005.

[25] H. Bach, M. Braun, G. Lampart, and W. Mauser, "Use of remote sensing for hydrological parameterisation of Alpine catchments," *Hydrol. Earth Syst. Sci.*, vol. 7, no. 6, pp. 862–876, 2003.

[26] R. Ludwig and W. Mauser, "Modelling catchment hydrology within a GIS based SVAT-model framework," *Hydrol. Earth Syst. Sci.*, vol. 4, no. 2, pp. 239–249, 2000.

[27] U. Strasser and W. Mauser, "Modelling the spatial and temporal variations of the water balance for the Weser catchment 1965–1994," *J. Hydrol.*, vol. 254, no. 1–4, pp. 199–214, 2001.

[28] V. R. N. Pauwels, W. Timmermans, and A. Loew, "Comparison of the estimated water and energy budgets of a large winter wheat field during AgriSAR 2006 by multiple sensors and models," *J. Hydrol.*, vol. 349, no. 3/4, pp. 425–440, Feb. 2008.

[29] A. Loew and F. Schlenz, "A dynamic approach for evaluating coarse scale satellite soil moisture products," *Hydrol. Earth Syst. Sci.*, vol. 15, no. 1, pp. 75–90, 2011.

[30] SMOS Level 2 Processor Soil Moisture ATBD for the SMOS Level 2 Soil Moisture Processor Development Continuation Project, Submitted by Array Systems Computing Inc.—Prepared by: CBSA, UoR, TV and INRA2011.

[31] D. B. Carr, R. Kahn, K. Sahr, and T. Olsen, "ISEA Discrete Global Grids," *Statistical Computing & Graphics Newsletter*, vol. 8, no. 2, pp. 31–39, 1997.

[32] K. Sahr, D. White, and A. J. Kimerling, "Geodesic Discrete Global Grid Systems," *Cartography Geograph. Inf. Sci.*, vol. 30, no. 2, pp. 121–134, 2003.

[33] N. Skou, S. Misra, J. E. Balling, S. S. Kristensen, and S. S. Søbjærg, "L-band RFI as experienced during airborne campaigns in preparation for SMOS," *IEEE Trans. Geosci. Remote Sens.*, vol. 48, no. 3, pp. 1398–1407, Mar. 2010.

[34] Indra Espacio S.A.2011 SMOS Level 2 and Auxiliary Data Products Specifications, Indra Espacio S.A.2011.

[35] A. Robock, K. Y. Vinnikov, G. Srinivasan, J. K. Entin, S. E. Hollinger, N. A. Speranskaya, S. Liu, and A. Namkhai, "The Global Soil Moisture Data Bank," *Bull. Amer. Meteorol. Soc.*, vol. 8, no. 16, pp. 1281–1299, 2000.

Johanna T. dall'Amico received the B.Sc. degree in mathematics from the University of Reading, Reading, U.K., in 2007 and the Diploma degree in geography with remote sensing and mathematics from the University of Munich, Munich, Germany, in 2008, where she is currently working toward the Ph.D. degree in the Department of Geography.

In 2005, she was a Visiting Student at the U.K. Natural Environment Research Council Environmental Systems Science Centre, Reading, working on remote sensing applications for fluvial flood mapping and modeling. Since 2007, she has been with the University of Munich, working on the project Integrative analysis of SMOS soil moisture data (SMOSHYD) which aims at the calibration and validation of Soil Moisture and Ocean Salinity data in the upper Danube catchment as well as at the study of related scaling issues. Her current research interests include airborne and satellite remote sensing of soil moisture and its spatial variability, including the analysis of ground data, model output, and ancillary remote sensing data.

Florian Schlenz (M'08) was born in Forchheim, Germany, in 1980. He received the Diploma degree in physical geography with remote sensing and computer science from the University of Munich, Munich, Germany, in 2007.

Since 2007, he has been with the Department of Geography, University of Munich, where he works as a Researcher on the project Integrative analysis of SMOS soil moisture data (SMOSHYD) which aims at the calibration and validation of Soil Moisture and Ocean Salinity data in the upper Danube catchment as well as at the study of scaling issues. His research interests include hydrological and radiative transfer modeling, as well as airborne and satellite-based remote sensing of soil moisture, including the analysis of field data and passive microwave radiometer data.

Mr. Schlenz is a member of the European Geosciences Union.

Alexander Loew (M'04) studied geography, computer science, remote sensing, and landscape ecology at the University of Munich (LMU), Munich, Germany. He received the M.S. degree in geography and the Ph.D. degree from LMU in 2001 and 2004, respectively.

From 2001 to 2008, he was a Postdoctoral Fellow with LMU, working on the retrieval of bio- and geophysical parameters from microwave remote sensing data. In 2007, he was a Visiting Scientist with the Goddard Space Flight Center, National Aeronautics and Space Administration, Greenbelt, MD. In 2009, he joined the Max Planck Institute for Meteorology, Hamburg, Germany, where he is leading a research group on terrestrial global remote sensing, focusing on global-scale remote sensing for climate studies. He is an Editor for *Hydrology and Earth System Sciences* and acts as a Reviewer for several national and international journals. His research interests include the quantitative retrieval of geophysical parameters from remote sensing data, the development of image-processing algorithms, coupling of land surface process models with microwave scattering and emission models, and the development of land surface process models and data assimilation techniques.

Wolfram Mauser (M'92) was born in Innsbruck, Austria, in 1955. He received the M.S. degrees in experimental physics and geography/hydrology and the Ph.D. degree in hydrology from the University of Freiburg, Freiburg im Breisgau, Germany, in 1979, 1981, and 1984, respectively.

In 1981, he worked with the University of Maryland, College Park, and the Goddard Space Flight Center, Greenbelt, MD, in the field of remote sensing and hydrology. From 1984 to 1991, he was an Assistant Professor with the Department of Hydrology, Institute of Physical Geography, University of Freiburg. Since 1991, he has been a Full Professor for geography and geographical remote sensing with the Department of Geography, University of Munich, Munich, Germany. From 2003 to 2009, he was the Chairman of the German National Committee on Global Change Research. He has been working in the field of remote sensing and hydrology within the major European research programs. He was appointed Principal Investigator (PI) by the European Space Agency (ESA) for its ERS-1, ERS-2, and Envisat programs and is PI for the Shuttle Radar Topography Mission and Soil Moisture and Ocean Salinity mission. He was a Member of ESA's Mission Advisory Group of the Earth Explorer Surface Processes and Ecosystem Changes Through Response Analysis mission. He took part in the Multi-Sensor Airborne Campaign (MAC Europe), the European Multisensor Airborne Campaign (EMAC) and the Digital Airborne Imaging Spectrometer Experiment (DAISEX). His special research interest is the development and validation of spatially distributed land surface process models and image processing algorithms, as well as model assimilation procedures for microwave and hyperspectral optical data.

Curriculum vitae

Florian Schlenz

Date of birth	28.9.1980
Place of birth	Forchheim
Nationality	German

PROFESSIONAL CAREER

Since 9/2007	Research associate and Phd student in the field of hydrological modelling and passive microwave remote sensing of soil moisture (DLR-funded SMOS cal/val project SMOSHYD)
at	Ludwig-Maximilians-Universität München, Department of Geography, Chair for Geography and Remote Sensing
5/2004 – 2/2007	Student research assistant in different projects (e.g. GLOWA-DANUBE) in the fields of software development, JAVA programming and field work
at	Ludwig-Maximilians-Universität München, Department of Geography, Chair for Geography and Remote Sensing
2000 - 2002	Side jobs
at	BMW AG, München; VHV Haftpflichtversicherung, München; Sixt Leasing AG, Taufkirchen

EDUCATION

10/2001 – 9/2007	Studies of Physical Geography with the side subjects Remote Sensing, Computer Science and Anorganic Chemistry (Graduate degree: Diplom Geograph (Univ.))
	Diploma thesis: Water balance modelling in New-Delhi
at	Ludwig Maximilians Universität München
1991 –2000	Secondary School Fürstenfeldbruck (degree: Abitur)
1995 – 1996	European School Culham, Oxfordshire, Great Britain
1987 – 1991	Primary School Grafrath, Landkreis Fürstenfeldbruck

LIST OF PUBLICATIONS

Peer Reviewed papers

- Schlenz, F., dall'Amico, J. T., Mauser, W., and Loew, A.: Analysis of SMOS brightness temperature and vegetation optical depth data with coupled land surface and radiative transfer models in Southern Germany, Hydrol. Earth Syst. Sci., submitted, 2012.

- dall'Amico, J. T., Mauser, W., Schlenz, F., and Bach, H.: Precipitation fields interpolated from gauge stations versus a merged radar-gauge precipitation product: influence on modelled soil moisture at local scale and at SMOS scale, Hydrol. Earth Syst. Sci. Discuss., 9, 3385-3413, 10.5194/hessd-9-3385-2012, 2012.

- dall'Amico, J. T., Schlenz, F., Loew, A., Mauser, W., Kainulainen, J., Balling, J., and Bouzinac, C.: The SMOS Validation Campaign 2010 in the Upper Danube Catchment: A Data Set for Studies of Soil Moisture, Brightness Temperature and their Spatial Variability over a Heterogeneous Land Surface, IEEE Transactions on Geoscience and Remote Sensing, accepted, 2012.

- Schlenz, F., Fallmann, J., Marzahn, P., Loew, A., and Mauser, W.: Characterization of Rape Field Microwave Emission and Implications to Surface Soil Moisture Retrievals, Remote Sensing, 4, 247-270, 2012.

- dall'Amico, J. T., Schlenz, F., Loew, A., and Mauser, W.: First Results of SMOS Soil Moisture Validation in the Upper Danube Catchment, Geoscience and Remote Sensing, IEEE Transactions on, PP, 1-10, 2011.

- Schlenz, F., dall'Amico, J. T., Loew, A., and Mauser, W.: Uncertainty Assessment of the SMOS Validation in the Upper Danube Catchment, Geoscience and Remote Sensing, IEEE Transactions on, PP, 1-13, 2011.

- Loew, A., and Schlenz, F.: A dynamic approach for evaluating coarse scale satellite soil moisture products, Hydrol. Earth Syst. Sci., 15, 75-90, 10.5194/hess-15-75-2011, 2011.

- dall'Amico, J. T., Schlenz, F., Loew, A., and Mauser, W.: SMOS soil moisture validation: Status at the Upper Danube cal/val site eight months after launch, Geoscience and Remote Sensing Symposium (IGARSS), 2010 IEEE International, Honolulu, 2010, 3801-3804, 2010.

- Kainulainen, J., Rautiainen, K., Sievinen, P., Seppanen, J., Rouhe, E., Hallikainen, M., dall'Amico, J., Schlenz, F., Loew, A., Bircher, S., and Montzka, C.: SMOS calibration and validation activities with airborne interferometric radiometer HUT-2D during spring 2010, Geoscience and Remote Sensing Symposium (IGARSS), 2010 IEEE International, Honolulu, 2010, 702-705, 2010.

- Mauser, W., Schlenz, F., dall'Amico, J., and Loew, A.: Europäischer Bodenfeuchtesatellit SMOS wird validiert - Validation of European Soil Moisture Satellite SMOS, Hydrologie und Wasserbewirtschaftung - Hydrology and Water Resources Management - Germany, 4, 252-254, 2010.

- Loew, A., Schwank, M., and Schlenz, F.: Assimilation of an L-Band Microwave Soil Moisture Proxy to Compensate for Uncertainties in Precipitation Data, Geoscience and Remote Sensing, IEEE Transactions on, 47, 2606-2616, 2009.

- Schlenz, F., Loew, A., and Mauser, W.: Soil Moisture Retrieval from Passive Microwave Data: A Sensitivity Study Using a Coupled Svat-Radiative Transfer Model at the Upper Danube Anchor Site, Geoscience and Remote Sensing Symposium (IGARSS), 2008 IEEE International, Boston, 2008, II-680-II-683, 2008.

Conference papers

- Hank, T., Marzahn, P., Schlenz, F., and Mauser, W.: Assessing Moisture Conditions of Heterogeneous Landsurfaces through Hyperspectral Analysis of Water Absorption Features, Hyperspectral 2010 Workshop, Frascati, Italy, 17 - 19 March 2010, ESA special publication SP-674, 2010.

- Schlenz, F., dall'Amico, J. T., Loew, A., and Mauser, W.: SMOS validation in the Upper Danube catchment (UDC): A status report eight months after launch, ESA Living Planet Symposium 2010, Bergen, Norway, 28 June - 2 July 2010, ESA special publication SP-686, 2010.

- Schlenz, F., Gebhardt, T., Loew, A., Marzahn, P., and Mauser, W.: L-Band Radiometer Experiment in the SMOS Test Site Upper Danube, ESA Living Planet Symposium 2010, Bergen, Norway, 28 June - 2 July 2010, ESA special publication SP-686, 2010.

- dall'Amico, J. T., Schlenz, F., Loew, A., and Mauser, W.: Airborne campaigns in the Upper Danube Catchment in the context of the calibration and validation of SMOS, ESA Living Planet Symposium 2010, Bergen, Norway, 28 June - 2 July 2010, ESA special publication SP-686, 2010.

- dall'Amico, J. T., Loew, A., Schlenz, F., and Mauser, W.: SMOS rehearsal campaign 2008: radiometer data analysis and soil moisture retrieval using the LPRM, Earth Observation and Water Cycle conference, Frascati (Rome), 18 - 20 November 2009, ESA special publication SP-674, 2009.

- Schlenz, F., Gebhardt, T., Loew, A., and Mauser, W.: L-band radiometer experiment in the SMOS test site Upper Danube, Earth Observation and Water Cycle conference, Frascati (Rome), 18 - 20 November 2009, ESA special publication SP-674, 2009.

- Loew, A., dall'Amico, J. T., Schlenz, F., and Mauser, W.: The Upper Danube soil moisture validation site: measurements and activities, Earth Observation and Water Cycle conference, Frascati (Rome), 18 - 20 November 2009, ESA special publication SP-674, 2009.

- Schlenz, F., Loew, A., dall'Amico, J. T., and Mauser, W.: SMOS rehearsal campaign 2008: Data analysis and soil moisture retrieval at the Upper Danube test site, Earth Observation and Water Cycle conference, Frascati (Rome), 18 - 20 November 2009, ESA special publication SP-674, 2009.

- Schlenz, F., Loew, A., and Mauser, W.: Sensitivity of the soil moisture retrieval from passive microwave data at the Upper Danube Catchment test site, Earth Observation and Water Cycle conference, Frascati (Rome), 18 - 20 November 2009, ESA special publication SP-674, 2009.

Conference abstracts

- Schlenz, F., dall'Amico, J. T., Loew, A., and Mauser, W.: SMOS validation results in the Upper Danube catchment, EGU General Assembly 2011, Vienna, 2011, Geophysical Research Abstracts, 13, EGU2011-1997, 2011.

- Schlenz, F., dall'Amico, J.T., Loew, A., Mauser, W. (2011): L-band radiometer experiment in the SMOS test site Upper Danube, EGU General Assembly 2011, Vienna, 2011, Geophysical Research Abstracts, 13, EGU2011-1980, 2011.

- Loew, A. and Schlenz, F. (2011): A dynamic approach for evaluating coarse scale satellite soil moisture products, EGU General Assembly 2011, Vienna, 2011, Geophysical Research Abstracts, 13, EGU2011-8875, 2011.

- Schlenz, F., Gebhardt, T., Loew, A., Marzahn, P., Mauser, W. (2010): L-band radiometer experiment in the SMOS test site Upper Danube, EGU General Assembly 2010, Vienna, 2010, Geophysical Research Abstracts, 12, EGU2010-9677, 2010.

- Loew, A., dall'Amico, J.T., Schlenz, F., Mauser, W. (2010): The Upper Danube soil moisture validation site: measurements and Activities, EGU General Assembly 2010, Vienna, 2010, Geophysical Research Abstracts, 12, EGU2010-9706, 2010.

- Muerth, M., Schlenz, F., Loew, A., Mauser, W. (2010): Coupled simulation of soil energy and water content to compare dielectric behaviour with TDR measurements in frozen soil, EGU General Assembly 2010, Vienna, 2010, Geophysical Research Abstracts, 12, EGU2010-14320, 2010.

- Schlenz, F., Loew, A., dall'Amico, J.T., Mauser, W. (2009): SMOS rehearsal campaign 2008: Data analysis and soil moisture retrieval using the L-MEB model at the Upper Danube anchor site, EGU General Assembly 2009, Vienna, 2009, Geophysical Research Abstracts, 11, EGU2009-8939, 2009.

- Schlenz, F., Loew, A., Mauser, W. (2009): Soil moisture retrieval from passive microwave data: A sensitivity study using a coupled SVAT-radiative transfer model at the Upper Danube anchor site, EGU General Assembly 2009, Vienna, 2009, Geophysical Research Abstracts, 11, EGU2009-7369, 2009.

- dall'Amico, J.T., Loew, A., Schlenz, F., Mauser, W. (2009): SMOS rehearsal campaign 2008, Upper Danube catchment: Radiometer data analysis and soil moisture retrieval using the Land Parameter Retrieval Model (LPRM), EGU General Assembly 2009, Vienna, 2009, Geophysical Research Abstracts, 11, EGU2009-3092, 2009.

- Loew, A., dall'Amico, J.T., Schlenz, F., Mauser, W. (2009): The Upper Danube soil moisture validation site: measurements and activities, EGU General Assembly 2009, Vienna, 2009, Geophysical Research Abstracts, 11, EGU2009-2924, 2009.